# Electricity Market Participation and Investment Planning Frameworks for Energy Storage Systems

by

Hisham Alharbi

A thesis
presented to the University of Waterloo
in fulfillment of the
thesis requirement for the degree of
Doctor of Philosophy
in
Electrical and Computer Engineering

Waterloo, Ontario, Canada, 2020

**Examining Committee Membership**

The following served on the Examining Committee for this thesis. The decision of the Examining Committee is by majority vote.

| | |
|---|---|
| **External Examiner:** | Miguel Anjos<br>Professor,<br>School of Mathematics,<br>University of Edinburgh, Edinburgh, Scotland |
| **Supervisor:** | Kankar Bhattacharya<br>Professor,<br>Dept. of Electrical and Computer Engineering,<br>University of Waterloo |
| **Internal Member:** | Magdy Salama<br>Professor,<br>Dept. of Electrical and Computer Engineering,<br>University of Waterloo |
| **Internal Member:** | Mohamed Ahmed<br>Adjunct Assistant Professor,<br>Dept. of Electrical and Computer Engineering,<br>University of Waterloo |
| **Internal-External Member:** | Jatin Nathwani<br>Professor,<br>Dept. of Civil and Environmental Engineering, &<br>Dept. of Management Sciences,<br>University of Waterloo |

## Author's Declaration

I hereby declare that I am the sole author of this thesis. This is a true copy of the thesis, including any required final revisions, as accepted by my examiners.

I understand that my thesis may be made electronically available to the public.

**Abstract**

The recent trend of increasing share of renewable energy sources (RES) in the generation mix has necessitated new operational and planning studies because of the high degree of uncertainty and variability of these sources. RES such as solar photovoltaic and wind generation are not dispatchable, and when there is excess energy supply during off-peak hours, RES curtailment is required to maintain the demand-supply balance. Furthermore, RES are intermittent resources which have introduced new challenges to the provision of ancillary services that are critical to maintaining the operational reliability of power systems. Energy storage systems (ESS) play a pivotal role in facilitating the integration of RES to mitigate the aforementioned issues. Therefore, there is a growing interest in recent years to examine the potential of ESS in the future electricity grids.

This research focuses on developing market participation and investment planning frameworks for ESS considering different ownership structures. First, a novel stochastic planning framework is proposed to determine the optimal battery energy storage system (BESS) capacity and year of installation in an isolated microgrid using a novel representation of the BESS energy diagram. A decomposition-based approach is proposed to solve the problem of stochastic planning of BESS under uncertainty. The optimal decisions minimize the net present value of total expected costs over a multi-year horizon considering optimal BESS operation using a novel matrix representing BESS energy capacity degradation. The proposed approach is solved in two stages as mixed integer linear programming (MILP) problems; the optimal ratings of the BESS are determined in the first stage, while the optimal installation year is determined in the second stage. Extensive studies considering four types of BESS technologies for deterministic, Monte Carlo Simulations, and stochastic cases are presented to demonstrate the effectiveness of the proposed approach.

The thesis further studies the investment decisions on BESS installations by a third-party investor in a microgrid. The optimal BESS power rating, energy capacity, and the year of installation are determined while maximizing the investor's profit and simultaneously minimizing the microgrid operational cost. The multi-objective problem is solved using a goal programming approach with a weight assigned to each objective.

The BESS is modeled to participate in energy arbitrage and provision of operating reserves to the microgrid, considering its performance parameters and capacity degradation over the planning horizon.

Finally, in the third problem addressed in the thesis in the context of electricity markets, the non-strategic and strategic participation of a pumped hydro energy storage (PHES) facility in day-ahead energy and performance-based regulation (PBR) markets, which includes regulation capacity and mileage, are examined. The PHES is modeled with the capability of operating in hydraulic short-circuit (HSC) mode with detailed representation of its operational constraints, and integrated with an energy-cum-PBR market clearing model. For its strategic participation, a bi-level market framework is proposed to determine the optimal offers and bids of the PHES that maximize its profit. The operation of PHES is modeled at the upper level, while the market clearing is modeled in the lower level problem. The bi-level problem is formulated as a mathematical programming with equilibrium constraints (MPEC) model, which is linearized and solved as an MILP problem. Several case studies are carried out to demonstrate the impact of PHES' non-strategic and strategic operations on market outcomes. Furthermore, stochastic case studies are conducted to determine the PHES strategies considering the uncertainty of the net demand and rivals' price and quantity offers.

**Acknowledgements**

First and foremost, all praises are due to Allah the Almighty for giving me strength, knowledge, patience, and opportunity to successfully accomplish completing this chapter of my life.

Then, I would like to express my gratitude to my supervisor Professor Kankar Bhattacharya for his invaluable guidance, patience, kindness, encouragement, and endless support throughout the period of my graduate studies, and thanks to him for helping me to achieve my full potential and for the enriched learning experience that enhanced my skills, not only on the academic level but also on my personal character level. I am honoured to have completed my PhD studies under his supervision, and he will continue to be my role model in his exceptional professionalism and commitment to a high standard of quality throughout my academic career.

I also would like to thank Prof. Miguel Anjos, from the University of Edinburgh, and Prof. Magdy Salama, Dr. Mohamed Ahmed, and Prof. Jatin Nathwani, from the University of Waterloo, for serving on my doctoral committee and for their insightful comments and suggestions which have helped in improving the quality of the thesis.

I wish to acknowledge the funding and support provided by Taif University to pursue my graduate studies, and the continued assistance from the Saudi Arabian Cultural Bureau in Canada. I also acknowledge the funding and support from the Natural Sciences and Engineering Council of Canada (NSERC) through the NSERC Energy Storage Technology (NEST) Network.

Many thanks to all the colleagues in the Power and Energy Systems Group at the University of Waterloo, and to the lab mates in the the Electricity Market Simulation and Optimization Laboratory (EMSOL) for their valuable discussions and creating a pleasant and friendly working environment. Also, thanks to all the NEST Network's members for enriching my knowledge about energy storage systems from different perspectives and disciplines.

My appreciation also goes to all the administrative staff at the University of Waterloo and in the Electrical and Computer Engineering Department for their assistance and cooperation throughout my PhD studies.

My sincere thanks go to my beloved parents Abdulrahman and Halima for their years of care and support. I would not have been able to get to this point in my academic career without their encouragement and prayers. I also would like to thank my brothers Hossam and Ahmed and my sister Raghad who supported me all the way.

My special thanks and gratitude to my lovely wife Mashael for her endless love, understanding, encouragement, and support. Her patience, composure, and sacrifices, even while she was also pursuing her Bachelor's degree, allowed me to focus on my studies during the hard times we have passed through. Many thanks to her and to our daughters Beesan and Layann for filling my life with happiness.

## Dedication

*This thesis is dedicated to my parents, my wife, my daughters, and all those who have supported me along the way.*

# Table of Contents

# List of Figures

# List of Tables

# List of Acronyms

| | |
|---|---|
| **ACE** | Area Control Error |
| **AESO** | Alberta Electric System Operator |
| **AGC** | Automatic Generation Control |
| **BESS** | Battery Energy Storage System |
| **CAISO** | California Independent System Operator |
| **CHP** | Combined Heating and Power |
| **DG** | Distributed Generator |
| **DOD** | Depth of Discharge |
| **DSO** | Distribution System Operator |
| **EMS** | Energy Management System |
| **E/P** | Energy to Power Ratio |
| **EPEC** | Equilibrium Problem with Equilibrium Constraints |
| **ERCOT** | The Electric Reliability Council of Texas |
| **ESS** | Energy Storage System |
| **FERC** | The US Federal Energy Regulatory Commission |
| **HSC** | Hydraulic Short-Circuit |
| **IESO** | The Independent Electricity System Operator of Ontario |
| **IRR** | Internal Rate of Return |
| **ISO** | Independent System Operator |
| **ISO-NE** | Independent System Operator of New England |
| **KKT** | Karush Kuhn Tucker |
| **LHS** | Latin Hypercube Sampling |
| **Li-ion** | Lithium-ion Batteries |

| | |
|---|---|
| **MARR** | Minimum Acceptable Rate of Return |
| **MCS** | Monte Carlo Simulations |
| **MGO** | Microgrid Operator |
| **MILP** | Mixed Integer Linear Programming |
| **MINLP** | Mixed Integer Non-linear Programming |
| **MISO** | Midcontinent Independent System Operator |
| **MPEC** | Mathematical Programming with Equilibrium Constraints |
| **NaS** | Sodium Sulfur Batteries |
| **NERC** | The North American Electric Reliability Corporation |
| **NGR** | Non-Generator Resources |
| **NPV** | Net Present Value |
| **NYISO** | New York Independent System Operator |
| **O&M** | Operations and Maintenance |
| **OPES** | Optimal Power and Energy Sizing |
| **PbA** | Lead Acid Batteries |
| **PBR** | Performance-Based Regulation |
| **PCC** | Point of Common Coupling |
| **PDF** | Probability Density Function |
| **PHES** | Pumped Hydro Energy Storage |
| **PV** | Photovoltaic |
| **REM** | Regulation Energy Management |
| **RES** | Renewable Energy Sources |
| **SOC** | State of Charge |
| **SPP** | Southwest Power Pool |
| **UC** | Unit Commitment |
| **VRB** | Vanadium Redox Flow Batteries |

# Chapter 1

# Introduction

## 1.1 Motivation

The recent trend of increasing share of renewable energy sources (RES) in the generation mix has necessitated new operational and planning studies because of the high degree of uncertainty and variability of these sources. RES such as solar photovoltaic (PV) and wind generation are not dispatchable, and when there is excess energy supply during off-peak hours, RES curtailment is required to maintain the demand-supply balance. Furthermore, RES are intermittent resources which have introduced new challenges to the provision of ancillary services that are critical to maintaining the operational reliability of power systems. Energy storage systems (ESS) play a pivotal role in facilitating the integration of RES to mitigate the aforementioned issues. Therefore, there is a growing interest in recent years to examine the potential of ESS in the future electricity grids.

The Long Term Energy Plan (2013) of Ontario, Canada [1] had set a target plan to increase the share of RES to 50% of the total generation mix of the province by 2025. As shown in Figure 1.1, as of the first quarter of 2020 [2], the Independent Electricity System Operator (IESO) of Ontario reports that the share of RES in total capacity is 37%, which includes PV and wind generation capacity of about 13% of total, hydro and biofuel accounting for 23% and 1% of the total, respectively. To accommodate these

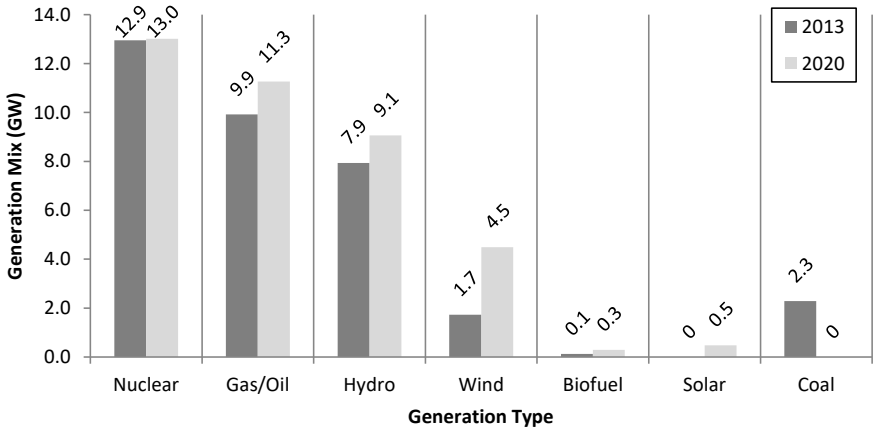


Figure 1.1: Ontario generation mix.

changes in system generation mix, new procurement contracts were put in place by the IESO in 2014 to integrate 50 MW of ESS, 32.8 MW of which has been procured in the Phase-I to provide regulation, reactive power support, and voltage control services, while in Phase-II, 16.75 MW has been procured [3]. Furthermore, in 2017, the IESO awarded contracts to two battery energy storage system (BESS) facilities (total 55 MW) to provide regulation services.

ESS have different operational and physical characteristics compared to traditional resources, thereby requiring new policies and regulations to integrate them to existing power systems. In order to facilitate effective ESS participation in electricity markets, the US Federal Energy Regulatory Commission (FERC) has issued policies to remove the barriers limiting their competitiveness with traditional resources. For example, FERC Order 755, issued in 2011 [4], outlines one of the key policies to pave the way for ESS participation in regulation markets, and FERC Order 841, issued in 2018 [5], facilitates ESS to participate side-by-side with traditional market participants by considering their physical and operational characteristics in the energy, capacity, and ancillary services markets.

In addition to the operational challenges, the high installation cost of ESS is the main barrier to their wider deployment [6]. Therefore, optimal investment decisions of ESS need be arrived at using appropriate frameworks wherein the ESS business paradigms, which

aim to accrue direct economic benefits or indirect cost savings [7,8], are taken into account. From the owner's perspective, the ESS investment frameworks can be classified, as follows:

- The ESS is owned and dispatched by the same entity: for example utility system operator such as the Independent System Operator (ISO), the Distribution System Operator (DSO) or Microgrid Operator (MGO), to minimize their operational cost and enhance the power quality; or end-users to offset their cost of energy purchased from the grid.
- The ESS is owned by third-party investor and dispatched by system operator: the investor recovers its investment through regulated cost-of-service payments based on an agreed rate of return; while the system operator seeks to minimize its operations costs taking into account charging and discharging costs.
- The ESS is owned by third-party investor and dispatched through its participation in the wholesale energy and ancillary service markets.

In the first structure when the ESS is owned and operated by a system operator, the applications can be classified into two broad areas: energy management, and power quality applications. Several ESS technologies are available for use; however, some technologies may excel over others in certain applications because of their different inherent characteristics, as shown in Figure 1.2 [9]. Furthermore, ESS applications can range from both bulk power systems, *i.e.*, at the transmission system level, managed by the ISO, as in Ontario IESO, to the distribution system level, managed by the DSO, to isolated or grid-connected microgrids, managed by MGO.

Among the various ESS technologies, BESS have received significant attention over the last decade for their role in improvement of system operations and reduction in system operation costs. They are suitable for both large power systems as well as microgrids because of their capability to be used for both energy management and power quality improvement applications. This is because of their fast response, options for different energy to power (E/P) ratios, and compact size and mobility.

The larger the installed size of the BESS, the greater is the improvement in operations, in addition to a reduction in thermal generation costs. However, as mentioned earlier, large

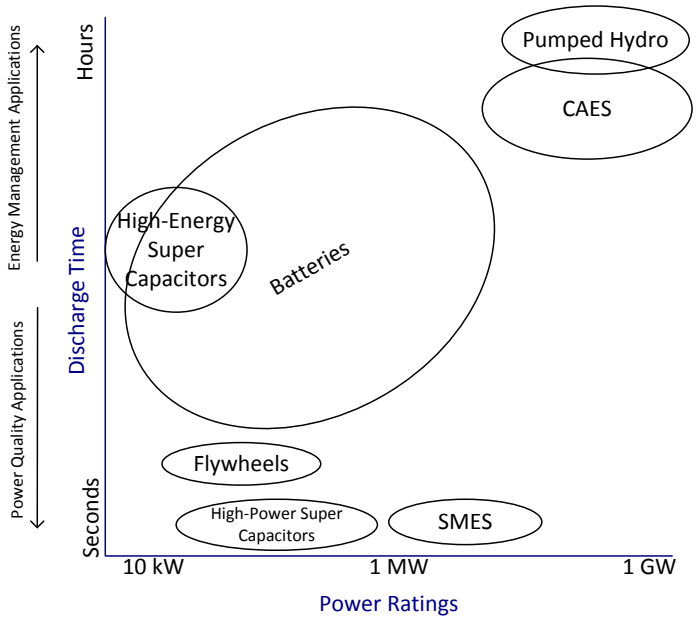


Figure 1.2: Energy storage technologies for different applications.

BESS installations require high capital cost, and therefore, the proper size of BESS need be determined in an operational-planning framework to maximize the total benefits at the lowest BESS installation cost.

Furthermore, the BESS operations are impacted by their lifecycle and degradation of energy capacity along with other BESS technology-specific and cost parameters, and hence these are crucial aspects to be considered in the BESS planning problems. To accommodate the intermittent RES and demand, it is necessary to consider their uncertainties in such operational-planning frameworks. Therefore, there is a need to develop BESS investment planning frameworks for system operators considering all the aforementioned aspects.

In the second structure, the ESS is owned by a third-party investor but operated by the system operator, considering the same range of ESS applications. The investment framework involves conflicting objectives where the system operator determines the optimal ESS schedules to minimize its operations costs, while the investor seeks to recover the total investment cost while meeting its minimum acceptable rate of return (MARR). The optimal investment decisions and the economic value for both the system operator and

ESS investors need be examined in a multi-objective investment planning framework.

In the third structure, the ESS owner submits offers and bids in the day-ahead and real-time energy markets to maximize its profit. Because of its competition with other energy resources, the main revenue stream for the ESS is typically from its participation in ancillary service markets because of their fast response time as compared to other resources. The new policies and regulations, such as FERC Order 755, provide more incentives to ESS investors to participate in the recently structured Performance-Based Regulation (PBR) markets.

Furthermore, it has been noted in [10–18] that large-scale ESS participating in the markets have the potential and the capacity to influence the market price by their strategic operational decisions and hence increase their potential profit from such price-setting behavior.

One of the large-scale ESS technologies that can strategically participate in electricity markets are the Pumped Hydro Energy Storage (PHES) facilities[1]. The ability to store a large amount of energy in hydro reservoirs, with higher conversion efficiency compared to many other technologies, makes PHES one of the most appealing large-scale ESS technologies [20]. This mature technology has been evolving, and with the recent interest in ESS, new operational aspects and technologies have been developed to improve the PHES operational flexibility such as by operating in hydraulic short-circuit (HSC) mode while participating in regulation markets [21].

Therefore, there is a need to examine the non-strategic and strategic participation of PHES systems, considering their detailed technical models and operational aspects such as HSC mode, in price-setting market frameworks for both energy and ancillary services, considering the recent implementation of FERC Order 755 that facilitates ESS market participation.

[1]Currently, more than 18 GW of PHES capacity is in operation in North America [19]. Of particular note is the Sir Adam Beck Pump Generating Station in Niagara Falls, Ontario; this 174 MW facility is the only PHES system in Canada, supplying power since 1957.

## 1.2 Literature Review

### 1.2.1 Investment Planning of Energy Storage Systems

The problem of ESS investment planning, from the perspective of system operators and third-party investors, has been addressed by several researchers in recent years, examining a range of issues; a brief review of which is presented below.

In studies considering RES and ESS, the focus is on the operation of ESS to facilitate the integration of RES by mitigating fluctuations, or by minimizing the net local load and renewable energy curtailed. Sizing BESS for wind power plants have been addressed in [22–25] to minimize the difference between predicted and actual wind generation. While in [22] the BESS cost is not considered, which may lead to oversizing; in [23] and [24] the size of BESS is determined using a cost-benefit analysis which may not yield the optimum. Energy arbitrage and peak shaving applications are examined in [25] considering a residential PV/BESS system connected to the grid; the optimal size of BESS is determined so as to minimize the cost of net power purchased during peak hours as well as minimize the cost of capacity degradation after each discharging process. However, in the above studies, the ESS only facilitates the RES integration without considering the operation of other resources in the grid, and hence its sizing may not be optimal from the grid's perspective.

In the context of a large power system, the ESS size is determined in [26] to provide auxiliary reserves required to facilitate large-scale integration of wind by considering the aggregated upward and downward gradient capabilities of the generation units in the system. However, the costs of BESS and generation units are not considered in the study, and hence the obtained BESS size may not be economically optimum. The optimal size and location of large-scale ESS in power systems with wind generation is determined in [27]. In [28], a bi-level stochastic optimization model for a large-scale ESS participating in energy market is developed. The optimal size of ESS is determined using Benders decomposition approach considering a master planning problem and several operational subproblems.

In [29], the investment planning decisions of a merchant ESS facility in transmission systems is examined using a tri-level model where the third-party investor's perspective

is considered in the upper level, the system operator's perspective in the middle level, and the day-ahead market is modeled in the lower level. In [30], simultaneous planning of transmission expansion and BESS is carried out using a stochastic multi-stage method wherein a linear BESS capacity degradation rate is considered. The upward reserves of the system are maintained by the dispatchable generating units and BESS. However, the upward reserve provisions from the BESS are assumed to be only in discharging mode, while in fact, the BESS upward reserve capacity in charging mode is double the BESS rating, since it can interrupt charging immediately.

Since the operation of resources in the grid have an impact on the energy management system (EMS), BESS sizing need to consider the unit commitment (UC) constraints appropriately. Although the operating costs of dispatchable generators and their operational constraints, *e.g.* ramp rate, are considered, the commitment decisions of generators are not considered in [26–29]. In [30], only a select set of generators are considered in the UC problem, while the others are assumed to be always committed. Moreover, the generators in the first set are assumed to start up and shut down at any time, and hence, the UC problem is modeled without binary variables. The operational aspects of RES and dispatchable generators and their optimal UC decisions have been considered in the ESS planning problem in [31], wherein a bi-level framework is proposed to maximize the third-party investor's profit by determining the optimal site and size of ESS in transmission systems. The investment planning problem is formulated in the upper level, while several representative operational days are considered in the lower level. However, the lifecycle of ESS and the impact of energy capacity degradation was not considered.

The optimal capacity of BESS for distribution system applications is determined in [32–39]. In [32], the optimal capacities of two types of redox-flow BESS are determined to maximize the net present value (NPV) of distribution cost savings, from deferral of distribution asset upgrades. The optimal sizes of distributed BESS, considered in a system with high PV penetration in [33] are determined at each bus, using a cost-benefit analysis considering voltage regulation and peak load shaving applications of the BESS. The capacity degradation of the BESS unit is also considered in [33] by modeling it as a linear function of the operation cycles. The optimal size of BESS is determined in [34]

which enhances the system reliability and peak shaving in a long-term expansion planning problem of an active distribution system. The proposed optimization framework minimizes the total cost including cost of investment, maintenance, arbitrage (*i.e.*, exchanging energy with bulk markets), and reliability costs considering the value of lost load and annual outages. In [35], the optimal size of BESS is determined to minimize wind generation curtailment and manage congestion and bus voltage profile in a distribution system, using a two-stage iterative framework. Initial planning decisions are obtained in the first stage based on hourly operation, while in the second stage the decisions are tuned to minimize wind curtailment in a smaller time resolution. However, the long-term planning constraints of BESS are not considered in this work. In [36], different BESS ownership structures such as utility and third-party are considered, and their perspectives are modeled in the context of residential feeders with high penetration of PV generation. Demand response is also considered to alleviate the need for larger sizes of BESS. The charging/discharging operation of BESS are controlled to minimize the net demand; however, the operating cost of BESS and its lifecycle are not considered in the optimization model.

In [37], a stochastic model is proposed to determine the optimal BESS ratings in distribution systems using a non-parametric chance-constrained optimization. The charging/discharging power of BESS and its relation with the state of charge (SOC) is considered using an approximate model, which reduces the computational time significantly; however, the plan decisions are affected by the inaccurate BESS operation because of the approximate model. In [38], a two-stage stochastic model is proposed for the DSO to determine the optimal siting and sizing of BESS to minimize the load shedding option and help increase distribution system reliability to a level that the customer is willing to pay for. The optimal decisions are obtained using a genetic algorithm approach. Similarly, in [39], the optimal size of BESS is determined for enhancing reliability and peak shaving in addition to voltage regulation, in the presence of high wind penetration.

The main functions of a BESS in distribution systems are to regulate the node voltages and hence reduce the losses in these radial systems, and peak shaving to defer the need for upgrading the distribution assets, and enhancing the reliability. The optimal

commitment decisions of dispatchable DG units are not considered in the reported works, since the distribution systems are mainly dependent on upstream power from the transmission system, and hence, the challenges of EMS are not present in these systems.

In the context of isolated and grid-connected microgrids, sizing of ESS is examined in [40] based on a cost-benefit analysis and UC with spinning reserve considerations. The two microgrid operational modes, grid-connected and isolated, are studied and different BESS sizes for each mode are prescribed. In [41], the BESS optimal power ratings and energy capacities are determined in isolated and grid-connected microgrids focusing on the challenges of modeling the Vanadium Redox flow batteries (VRB). The optimal size of flywheel energy storage is determined in [42] by integrating the microgrid EMS in a bi-level optimization framework. In [43], an approach based on discrete Fourier transform is proposed to optimize the size of BESS and diesel generators in isolated microgrids. The mismatch between the forecasted RES and the load is decomposed into different frequency components. BESS are assigned to balance the high-frequency band component, whereas diesel generators are assigned to balance the power in the low frequency component. The uncertainties in the microgrid resources are not considered in these works.

In [44], the optimal BESS sizing, siting, and technology selection, considering their capacity degradation, are determined in an isolated grid with high penetration of wind, using a deterministic multi-stage optimization model. The uncertainty is managed by implementing a model predictive control technique. In community microgrids, the optimal sizes of distributed energy resources and BESS are co-optimized in [45] to maximize the fuel cost savings considering environmental and regulatory constraints. In [46], the optimal size of BESS and reserve capacities are jointly determined to enhance microgrid reliability with high penetration of RES. In [47], the RES and BESS sizes are determined in residential microgrids considering degradation of BESS capacity and the stochastic nature of RES and load. Although the uncertainties in microgrid resources are considered in [44–47], the optimization models in these works are solved as deterministic ones, considering separate scenarios, which may not yield a robust plan.

Stochastic approaches have been used to determine optimum BESS sizes in microgrids [48–53]. For instance, BESS sizing in isolated microgrids is carried out in the presence of wind and solar based RES in [48] using a joint optimization model wherein the large

number of stochastic scenarios are handled using a distributed optimization approach, which divides the problem into several sub-problems. BESS sizing is proposed in [49] using a stochastic approach wherein the scenarios are generated using Monte Carlo Simulation (MCS) followed by a scenario reduction technique. The optimization model is based on the UC formulation and solved as a mixed integer linear programming (MILP) problem. In [50], the optimal BESS size is determined in isolated and grid-connected microgrids using an UC formulation considering a probabilistic constraint to account for the uncertainty of wind generation, the probability of generation maintained at a predetermined threshold of load shedding. In [49] and [50], demand growth is not considered, hence only one year of planning is assumed, to size the BESS.

In a wind-diesel isolated microgrid [51], the optimal BESS size is determined so as to minimize the fuel and operating costs of the system over a 20-year planning period, while facilitating wind generation penetration. A two-stage stochastic approach is used to capture the wind variability and load uncertainty. Several scenarios are considered corresponding to different profiles of wind and load. The first stage determines the BESS size that satisfies all scenarios while the second stage identifies the optimal operation, given the optimal size determined in the first stage. In [52], stochastic optimization is used for sizing of BESS in remote microgrids with the option of expanding its energy capacity to extend the BESS lifetime in the long-term horizon. Although BESS life cycle is modeled using the Ah-throughput model, its energy capacity degradation and its consequent impact on the optimum sizing and operation, are not considered. In [53], the optimal investment decisions on RES, ESS and demand response are determined jointly in a microgrid using a two-stage stochastic optimization. In the first stage, the optimal investment plan is determined, while in the second, the microgrid operation is optimized in an iterative framework. A low depth of discharge (DOD) setting is used to reduce the impact of capacity degradation; however, this results in oversizing the BESS since the effective usable capacity is reduced with low DOD.

Table 1.1 presents a summary of the literature review. Several aspects are examined which impose a challenge to the ESS planning problems. The BESS capacity degradation is a non-trivial factor affecting its operation in long-term planning problems, yet only few studies have considered its impact on the optimal plan of BESS. Also, the uncertainty

Table 1.1: Summary of Literature Review

| Ref | System Considered | Commitment of Dispatchable DG | RES | Uncertainty | Stochastic Optimization | BESS Capacity Degradation | Energy Storage Technologies |
|---|---|---|---|---|---|---|---|
| [22] | Wind/BESS Power Station | N/A | Wind | N/A | N/A | N/A | Zinc-bromine |
| [23] | Wind/BESS Power Station | N/A | Wind | Considered | N/A | N/A | Not specified |
| [24] | Wind/BESS Power Station | N/A | Wind | Considered | N/A | N/A | PbA |
| [25] | Residential PV/BESS | N/A | PV | N/A | N/A | Considered | PbA |
| [26] | Large Power System | N/A | Wind | N/A | N/A | N/A | Not specified |
| [27] | Large Power System | N/A | Wind | Considered | Considered | N/A | CAES |
| [28] | Energy Market | N/A | N/A | Considered | Considered | N/A | Pumped hydro |
| [29] | Transmission System | N/A | General | N/A | N/A | N/A | Not specified |
| [30] | Transmission System | N/A | Wind | Considered | Considered | Considered | Not specified |
| [31] | Transmission System | Considered | Wind | N/A | N/A | N/A | Not specified |
| [32] | Distribution System | N/A | N/A | N/A | N/A | N/A | Polysulfide-bromine, VRB |
| [33] | Distribution System | N/A | PV | N/A | N/A | Considered | Li-ion |
| [34] | Distribution System | N/A | N/A | N/A | N/A | N/A | Li-ion |
| [35] | Distribution System | N/A | Wind | N/A | N/A | N/A | Li-ion |
| [36] | Distribution System | N/A | PV | N/A | N/A | N/A | Not specified |
| [37] | Distribution System | N/A | PV | Considered | Considered | N/A | Li-ion |
| [38] | Distribution System | N/A | Wind | Considered | Considered | N/A | NaS, PbA, VRB, CAES |
| [39] | Distribution System | N/A | Wind | Considered | Considered | N/A | Zinc-bromine |
| [40] | Connected/Isolated Microgrid | Considered | PV, Wind | N/A | N/A | N/A | Li-ion |
| [41] | Connected/Isolated Microgrid | Considered | PV | N/A | N/A | N/A | VRB |
| [42] | Connected Microgrid | N/A | PV | N/A | N/A | N/A | Flywheel |
| [43] | Isolated Microgrid | N/A | PV, Wind | N/A | N/A | N/A | Not specified |
| [44] | Isolated Grid | Considered | Wind | Considered | N/A | Considered | NaS, PbA, Li-ion |
| [45] | Isolated Microgrid | N/A | PV, Wind | Considered | N/A | N/A | NaS |
| [46] | Connected Microgrid | N/A | General | Considered | N/A | N/A | Li-ion |
| [47] | Connected Microgrid | N/A | PV, Wind | Considered | N/A | Considered | PbA |
| [48] | Isolated Microgrid | N/A | PV, Wind | Considered | Considered | N/A | PbA, Li-ion, Pumped hydro |
| [49] | Connected Microgrid | Considered | Wind | Considered | Considered | N/A | Not specified |
| [50] | Connected/Isolated Microgrid | Considered | PV, Wind | Considered | Considered | N/A | Li-ion |
| [51] | Isolated Microgrid | Considered | Wind | Considered | Considered | N/A | Not specified |
| [52] | Isolated Microgrid | Considered | Wind | Considered | Considered | N/A | NaS, PbA, Zinc-bromine |
| [53] | Connected Microgrid | N/A | PV, Wind | Considered | Considered | N/A | Not specified |

(NaS): Sodium Sulfur BESS, (VRB): Vanadium Redox Flow BESS, (PbA): Lead Acid BESS, (Li-ion): Lithium-ion BESS, (CAES): Compressed Air Energy Storage.

in RES and load has to be considered which adds another challenge in solving planning problems. Although some papers handled the uncertainty by generating several scenarios and solving the problem as deterministic optimization model, such as in [44] and [47], stochastic models should be considered to obtain more robust results by including all the scenarios simultaneously in determining the optimal decisions. Furthermore, the optimal operation of dispatchable generating units needs to be integrated in the EMS models. The challenge of these models is because of the presence of binary variables to model the generators' commitment decisions properly, as well as the other operational constraints of dispatchable generating units in the UC problem.

From the aforementioned review of literature, it is noted that none of these studies have proposed a stochastic optimization approach to determine the BESS optimal plan, considering its capacity degradation, alongside determining the optimal UC and dispatch decisions of generating units in conjunction with RES. Furthermore, these aspects have not been studied, in the very few proposed investment-planning frameworks, in the literature, when the BESS is installed by a third-party investor.

### 1.2.2 Market Participation of Energy Storage Systems

The participation of ESS in electricity markets has been reported in the literature and can be divided into two main threads- those where the ESS have been considered as price-takers and those where the ESS bidding strategies can impact market outcomes.

In the first, wherein ESS facilities have been considered as price-taker entities, it is assumed that their bids and offers do not affect the market clearing prices, and hence their optimal participation are determined based on forecasted market prices. In [54], a generation utility comprising ESS and wind farm is considered to maximize its profit in energy market participation. The uncertainties in forecasted market prices and wind generation are considered and the problem is solved using a two-stage stochastic optimization approach. In [21] and [55], the simultaneous participation of a price-taker PHES, considering its flexibility in pumping mode, in the Spanish energy and secondary reserve markets is studied; it is noted that the PHES optimal operation and its consequent revenue stream are significantly dependent on its participation in the

regulation market. The flexibility of variable-speed PHES when participating in the Swiss secondary and tertiary reserve markets is reported in [56] wherein the impact of upgrading and improving the operational aspects of the PHES on increasing the revenue from ancillary service provisions has been examined.

In the aforementioned studies, the market prices are not affected by the bidding decisions of the ESS. In the second thread on ESS participation in markets, their potential to influence the market price by their strategic operational decisions have been studied. In [10], the optimal bidding strategy of a price-maker ESS, specifically a PHES facility, is studied considering only the energy market; the uncertainties of hydro inflows, demand, and rivals' offers are considered in a medium-term (one year) stochastic optimization model, which is solved as an MILP problem. In [11] and [12], the impact of uncertainty on the PHES market decisions is examined, considering the PHES as a price-taker in the Iberian energy market but as a price-maker in the secondary reserve market; the uncertainty in real-time reserve activation is considered in the proposed models, and the economical impact of forecasting the market clearing price is studied. In [10–12], the strategic ESS decisions are modeled using residual demand and reserve curves, in which the strategic operation of an entity is determined based on forecasting the expected market outcomes from the historical supply and demand curves of the other market participants.

In [13], a mixed complementarity problem is proposed to design a special pricing mechanism for ESS, based on the highest locational marginal price in the system, to promote its participation in the market. The impact of ESS operations and its location and size, on the market clearing outcomes have been studied. In [14], the ESS is considered as a price-maker in the energy market, but as a price-taker in the reserve and PBR markets, using a bi-level optimization model. In the upper level, the profit of several entities including the ESS is maximized, while the market clearing process in the lower level is solved as a Nash-Cournot equilibrium model, which does not consider the social welfare maximization objective. It is noted that the strategic offer/bid prices of ESS, and other market participants, were not determined in the Cournot model used in [14].

The strategic offer/bid prices and quantities can be determined using a bi-level optimization framework formulated as a Mathematical Programming with Equilibrium

Constraints (MPEC) model. The MPEC problems are based on the Stackelberg gaming competition, to determine the optimal strategy for one agent, maximizing its profit (the upper level) and constrained by the market equilibrium (the lower level), assuming that the rival agents' strategies can be anticipated and do not change with the determined strategy at the upper level [57]. The bi-level MPEC approach to determine the strategic bidding of a single firm in wholesale electricity markets was first proposed in [58].

Several works [15–18], have examined the ESS strategic participation in electricity markets using a bi-level MPEC model, and linearized and solved thereafter as an MILP problem. In [15], the optimal bidding strategy is determined to maximize the ESS profit in day-ahead energy market. A risk-constrained approach with extended look-ahead period, considering 48 hours, is proposed to solve the bi-level MPEC problem, in which the SOC level at the end of the first day is determined to maximize the profit for the two considered days. In [16], the ESS strategic decisions in joint day-ahead energy and reserve markets, as well as the real-time balancing markets are determined in a bi-level problem. The day-ahead and real-time markets are represented by two lower level problems, whereas the ESS profit maximization is developed in the upper level problem. In [17], a stochastic bi-level optimization model is proposed to maximize the profit of ESS participating in the energy market, considering ramp rate limits of conventional generators in the presence of wind generation. The impact of strategic ESS on the flexibility of the system and social welfare in energy markets is evaluated in [18] considering the bi-level ESS profit maximization approach.

In [15–18], generic ESS models have been used in the strategic price-setting studies without considering detailed technical models of any particular technology, which has a significant bearing and impact on the decisions, and hence on the ESS capability of bidding and offering in different electricity markets. For instance, a PHES operations model and technical characteristics will be significantly different from a compressed air energy storage system, and generic models are not sufficient to capture the details.

Apart from ESS participation strategies, the electricity markets are being redesigned to integrate the progressive penetration of ESS in bulk power systems in recent years. Therefore, some studies have proposed novel market frameworks and developed bidding mechanisms for ESS considering their important parameters to comply with the new

policies [59].

The new structure of regulation markets, after implementing FERC Order 755, has included an additional component to the regulation capacity payment, based on actual performance of the facility in following the regulation signal. Since the PBR market provides more incentives for fast response resources, some studies have highlighted the benefits that may be accrued by ESS from participation in such markets. The optimal scheduling and bidding policy for participation in energy and PBR markets is reported in [60–62]. In [60], the optimal price-taker bidding policy in PBR markets is determined for a BESS considering its degradation. In the proposed optimization model, the BESS seeks to maximize its profit, while the PBR market requirements are considered as chance-constraints. In [61], a price-taker participation model in energy and PBR market is proposed considering the non-linear characteristics of PbA, VRB, and Li-ion BESS. The problem is formulated as a dynamic programming based approach and solved using forward search algorithm. In [62], a bi-level MPEC approach is proposed to maximize the profit of a provider, considering a generic model, in the regulation capacity and mileage markets. However, this work did not consider energy market settlement or the operational and physical aspects of ESS.

It is noted that all these studies on PBR markets are limited to BESS or consider generic ESS models. However, other ESS technologies, such as PHES, are efficient and perform well in frequency regulation provisions and can benefit from participating in PBR markets.

The PHES units have been providing frequency regulation services, but only when operating in the generation mode. Typically, PHES do not have the ability to participate in frequency regulation markets while they are in the pumping mode, because of their fixed power consumption in this mode. To this effect, operational methods and technologies have been proposed to alleviate this limitation and maximize the potential revenue for PHES facilities participating in ancillary services markets, such as by operating in HSC mode [21], equipping PHES with variable speed drives [55], or by controlling the power generated during the switching time between the different PHES modes [63].

The uncertainty in demand and RES generation typically impacts the market

clearing, and hence these aspects should be considered in determining the strategic bidding. Furthermore, the uncertainty in rivals' price and quantity offers have major impact on the market outcomes and hence need be considered in the strategic bidding framework [64], [65].

In view of the above discussions, it is noted that none of the works have studied the strategic participation of PHES simultaneously in joint energy-PBR markets, considering regulation capacity and mileage markets. Furthermore, no work has studied the flexibility aspects of PHES participating in regulation markets while pumping, as a strategic participant.

## 1.3 Research Objectives

The main goals of the research presented in this thesis are to develop investment planning and market participation frameworks for ESS considering different ownership structures. The specific objectives of the thesis are stated as follows:

- Develop a planning framework from the utility's perspective to determine the optimal power and energy size of BESS and its optimal year of installation over a planning horizon considering different BESS technologies and their inherent characteristics including energy capacity degradation and cost parameters.
- Extend the utility-centric proposed planning framework to a stochastic optimization model for BESS planning to capture the uncertainties of solar radiation, wind speed, and power demand. Propose a two-stage decomposition-based approach to solve the stochastic optimization model where, in the first stage, the power rating and final degraded energy capacity of BESS will be determined, while in the second stage, the optimal year of installation will be obtained.
- Develop an optimal BESS investment planning framework wherein a third-party investor installs the BESS while the utility operator controls its operations. Determine the optimal BESS power rating, energy capacity, and year of installation

to simultaneously maximize the investor's profit and minimize utility's operations cost.

- Develop a market participation model from the investor's perspective, specifically considering PHES systems, to determine their optimal bidding strategies in joint energy-PBR markets. The PBR market formulation will be in line with FERC Order 755 to facilitate PHES participation in regulation markets. Hence, develop a bi-level MPEC framework to determine, at the upper level, the PHES bids and offers maximizing its profit while considering its HSC mode of operation. At the lower level, the joint energy-PBR market clearing process will be modeled considering the optimal offers and bids.

- Study stochastic scenarios of demand, RES generation, and rival generators' price and quantity offers and their impact on PHES operation and its market participation. Also, examine the non-strategic participation of PHES in the above markets as compared to its strategic operations for conventional and HSC PHES facilities.

## 1.4 Thesis Outline

The rest of the thesis is organized as follows: Chapter 2 presents the essential background on ESS, participation of ESS in ancillary services provision, ancillary services markets in North America, investment planning aspects for microgrids, and different techniques of uncertainty management in power system operational and planning models. In Chapter 3, the stochastic model for optimal BESS planning and the decomposition based approach to solve the stochastic optimization problem are discussed. In Chapter 4, the proposed goal programming approach to determine the optimal BESS investment plan by a third-party investor is studied. Chapter 5 presents the bi-level framework of energy and PBR market participation of PHES and the proposed MPEC problem. Finally, Chapter 6 presents the main conclusions and contributions of this thesis, and identifies some directions for future research work.

# Chapter 2

# Background[1]

In this chapter, a brief background to the topics relevant to the thesis is presented. Various aspects, parameters, and technologies of existing ESS and their participation in ancillary services provision are discussed, followed by a discussion of the North American ancillary services markets focusing on the integration of ESS. Then, an overview of the investment planning aspects for microgrids and their operational challenges are discussed. Finally, different techniques of uncertainty management in power system operational and planning models are outlined.

## 2.1 Nomenclature

***Indices***

| | |
|---|---|
| $h$ | Index for hours, $h = 1, 2, .., H$ |
| $i$ | Index for dispatchable DG units, $i = 1, 2, .., I$ |
| $y$ | Index for years, $y = 1, 2, .., Y_T$ |

[1]Parts of this chapter have been published in:
H. Alharbi, and K. Bhattacharya, "Energy Storage and Ancillary Services Markets in North America," in *Proc. CIGRE Canada Conference*, Montreal, QC, 2019, pp. 1-5.

***Parameters***

| | |
|---|---|
| $G_i, L_i$ | Initial up-time and down-time required of DG unit $i$ [h] |
| $Min_i^{DW}$ | Minimum down-time of DG unit $i$ [h] |
| $Min_i^{UP}$ | Minimum up-time of DG unit $i$ h] |
| $\overline{P}_i$ | Maximum output power of DG unit $i$ [kW] |
| $\underline{P}_i$ | Minimum output power of DG unit $i$ [kW] |
| $R$ | Total required reserve capacity [kW] |
| $Ramp_i^{DW}$ | Ramp down limit of DG unit $i$ [kW] |
| $Ramp_i^{UP}$ | Ramp up limit of DG unit $i$ [kW] |
| $SD_i$, $SU_i$ | Shut-down and start-up cost of DG unit $i$ [$] |
| $Pd$ | Forecasted demand [kW] |

***Variables***

| | |
|---|---|
| $P$ | DG output [kW] |
| $U, V, W$ | Binary start-up, shut-down, and commitment decision of DG units |

## 2.2 Energy Storage Systems

In order to address the differences between the various ESS technologies and their applications, their basic characteristic parameters need be understood.

### 2.2.1 Energy Storage System Characteristic Parameters

#### 2.2.1.1 Power and Energy Size, E/P Ratio

Unlike electrical generators, ESS are specified by their energy storage capacity in addition to their power rating or size. The power size of an ESS is defined as the rate at which the ESS is capable of discharging/charging power continually. In normal operation, the maximum injected/drawn power is the nameplate rating of the ESS, although, some types

of ESS have the ability to discharge more power than their rated value for a short period during contingency situations [66]. The energy size represents the maximum amount of energy that can be stored, the capacity is usually expressed in kWh or MWh.

The relationship between the power and energy size for a certain ESS technology is known as the E/P ratio, and is defined as follows:

$$E/P = \frac{Energy\ Capacity\ [kWh]}{Power\ Rating\ [kW]} \tag{2.1}$$

For example, in ESS used for power quality applications, the E/P ratio is usually less than unity since the maximum discharge/charge power is more important than the energy capacity. On the other hand, ESS used in energy management applications have an E/P ratio more than unity due to the need for large energy capacity [66].

#### 2.2.1.2 Discharge Time

Discharge time is the maximum duration for which the ESS can discharge at rated power [9], and is expressed as follows:

$$Discharge\ Time = \frac{Available\ Energy\ [kWh]}{Power\ Rating\ [kW]} \tag{2.2}$$

It is noted that while discharge time depends on the available energy and the DOD, the E/P ratio considers the entire energy capacity.

The discharge time and E/P ratio of different ESS technologies vary over a range, as shown in Figure 1.2, and accordingly the nature of applications of the ESS are determined. The ESS with low discharge times of seconds to few minutes, such as flywheels and super capacitors, are more suitable for power quality applications, while ESS with large discharge times of several minutes to hours are preferred for energy management applications [9]. It is worth mentioning that some technologies, such as batteries, have a wider range of E/P ratio than others, which make them better suited for both power quality and energy management applications.

#### 2.2.1.3 Lifetime

Most ESS suffer from degradation which affects their performance and reduces their lifetime. Three major factors affect the lifetime [67], and whenever one of them reaches its limit, the ESS should be replaced.

(a) *The calendar lifetime (years):* depending on the technology, certain number of years after installation, the ESS may not operate efficiently, although it may not have been operated frequently.

(b) *Number of cycles (cycles):* when the number of charging/discharging cycles reaches a maximum, as specified by the manufacturer, the ESS should be replaced.

(c) *Total discharged energy (kWh or MWh):* in applications that require deep charging and discharging cycles, the total discharged energy determines the lifetime of ESS.

#### 2.2.1.4 Depth of Discharge (DOD)

To reduce the impact of degradation, the ESS operation should be in a controlled manner so as to extend its usage over a longer period [66]. For example, the ESS may not be allowed to discharge beyond a certain level of its energy capacity. The maximum discharge limit is expressed as the DOD of energy storage (%). It is noted that the level of energy to which the ESS is charged is known as SOC. Accordingly, the DOD of ESS is defined as follows:

$$DOD[\%] = \frac{Energy\ Capacity\ [kWh] - Minimum\ SOC\ Level\ [kWh]}{Energy\ Capacity\ [kWh]} \times 100 \qquad (2.3)$$

Reducing the DOD has a significant impact on prolonging the lifetime of the ESS [66]. However, a low value of DOD requires installing a larger size of ESS. Therefore, balancing the two factors is important to reduce the total ESS cost.

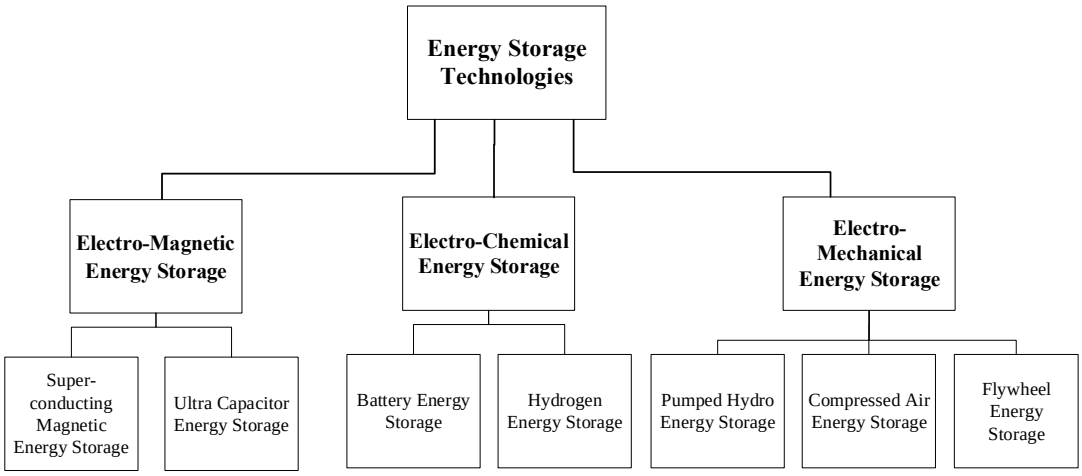


Figure 2.1: Classification of energy storage technologies.

#### 2.2.1.5 Round-Trip Efficiency

The energy loss taking place during the discharging and charging process of an ESS is represented by the round-trip efficiency. It is the net energy discharged from the ESS for a given amount of energy charged [67]. In some cases, the charging efficiency associated with energy conversion during charging process is different from the discharging efficiency. The round-trip efficiency is the multiplication of both these efficiencies. Energy storage technologies have different ranges of round-trip efficiencies, higher efficiency ESS of a certain technology might be available but at higher costs.

### 2.2.2 Energy Storage Technologies

A wide range of energy storage technologies exist today. In general, energy storage technologies are classified into three categories based on the form of the stored energy [68], as shown in Figure 2.1. The first category of technologies store energy in electro-magnetic form, for example, super conductors and ultra capacitors. The second category encompasses electro-chemical ESS technologies, comprising the battery technologies including flow batteries, and the recent development of hydrogen energy

storage. The third category of electro-mechanical ESS technologies store the energy in the form of kinetic energy or potential energy, for example, PHES, compressed air energy storage and flywheel energy storage.

In the following sub-sections, BESS and PHES technologies are discussed in detail, because these are considered for the subsequent research problems presented in this thesis.

#### 2.2.2.1 Battery Energy Storage Systems (BESS)

They are based on the principle of energy conversion from chemical energy to electrical energy. The four main BESS technologies are discussed here, along with their technical characteristics.

*Sodium Sulfur Batteries (NaS):*

Several studies have been conducted to develop this technology, especially in Japan. At the current time, NaS BESS is only available at E/P ratios ranging from 6 to 7 [67]. Therefore, it has the capability to discharge for more than 6 hours at rated power. In addition, the relatively high round-trip efficiency and their long cycle life make them more valuable in energy management applications. Moreover, NaS BESS have the capability to discharge at 5 times its rated power for a few minutes to meet transient fluctuations in power, which is a significant feature of these batteries in power system applications [67].

NaS BESS also have high energy and power density [9] and does not suffer from self-discharge effect [69]. Consequently, because of all these advantages, it is considered a mature technology and has been used in several grid-scale applications. However, because NaS BESS operation requires high temperature, there are some concerns about their safety [69].

*Vanadium Redox Flow Batteries (VRB):*

VRB BESS is a battery from the family of *flow batteries*, first introduced in the 1970s [66]. Since the power rating of these batteries depend on the size of the cell stack, while the volume of the electrolyte determines the energy capacity, VRB BESS has no E/P ratio constraints [69].

The cycle life of VRB BESS is significantly high and does not depend on the DOD [9];

hence, their lifetime is usually measured by calendar life. One of the features of VRB BESS is that the power stack can be adjusted to the desired level, and the power rating can be changed to suit the application, either power quality application such as voltage regulation or energy management application such as energy arbitrage [66]. Researchers are working on increasing the low power density of these batteries, which is one of their drawbacks.

*Lead Acid Batteries (PbA):*

PbA BESS are one of the most developed and mature batteries in the world, and widely used in several applications since they were introduced in the early 1860s [67]. The limitations of PbA BESS include their low power and energy density, and reliability. Also, PbA BESS have low cycle life as compared to other batteries. Despite these limitations, PbA BESS can be used in power system applications because of their noticeable low cost and high efficiency [69].

*Lithium-ion Batteries (Li-ion):*

The research on Li-ion BESS was started in the 1960s [70]. They have been used in small-scale energy storage applications for several decades and recently found a place in large-scale applications, especially in the automotive sector.

The advantages of Li-ion BESS include their very high efficiency, high cycle life and fast response time. However, these are expensive compared to the other types of batteries because of their protection and insulation requirements [71].

In recent times, these ESS have found significant applications in power systems.

#### 2.2.2.2 Pumped Hydro Energy Storage (PHES)

This is one of the earliest large-scale energy storage technologies. The first PHES system was installed in the Alpine region of Europe in 1890s, and comprised pump impellers and separate turbine generator [72]. The design of PHES has evolved since the 1950s to the single reversible pump/turbine units [72], as shown in Figure 2.2.

During low demand periods, the energy is drawn from the grid by motors to pump water to a higher level reservoir, which essentially is the charging process of the PHES system. When energy is required to be discharged, the stored water is released to a lower level

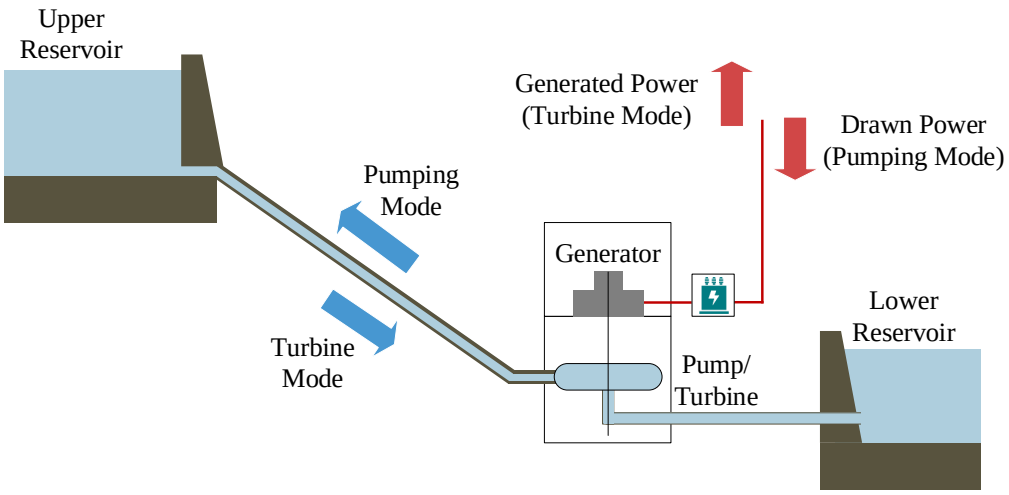


Figure 2.2: Typical pumped hydro energy storage plant.

reservoir, and the potential energy of the released water is used to operate a hydroelectric turbine and generate electrical energy. The difference between the PHES and a traditional hydroelectric power station is that the former consumes more energy than it generates because of the conversion losses mainly during the process of pumping water to the upper reservoir [73]. Nevertheless, PHES systems are used for energy management applications because of their high energy capacity and low energy cost, by virtue of an optimally scheduled PHES with appropriate charging and discharging operation, which can reduce the system costs significantly. However, the geographic and environmental restrictions limit the instalation of PHES. Also, despite the low cost of energy, the fixed installation cost of PHES is very high and requires longer time for cost recovery as compared to other technologies [9].

Most of the existing PHES plants are equipped with fixed-speed pumps which allow them to provide frequency regulation during the generation cycle only. However, PHES systems equipped with variable speed pumps or operating in the HSC mode can also provide frequency regulation while pumping [20]. There are two configurations allowing PHES to operate in HSC mode. First, PHES can be equipped with ternary units, each comprising a generator/motor coupled with Francis or Pelton turbine connected through

a lock-up clutch to a pump. Individual units can operate either as a pump and/or a turbine simultaneously because of the presence of the clutch. Although the pumps still operate at fixed speed, the overall operation of the PHES unit can be controlled in order to provide frequency regulation services. The second HSC configuration comprises reversible Francis pump-turbine units, same as conventional PHES, but with at least two units- one generating and the other pumping, where the generating unit is controlled to offset the fixed pumping power.

Figure 2.3 presents the operation of conventional and HSC PHES systems. In pumping mode, fixed-speed pumps move the water from the lower to the upper reservoir to store the energy, Figure 2.3(a), whereas in generating mode, the water is discharged from the upper to the lower reservoir to generate power, Figure 2.3(b). The units of a conventional PHES can only operate in either the generating or the pumping mode, as shown in Figure 2.3(a) and 2.3(b). Hence, if a unit is in pumping mode, then all the other units have to operate in pumping mode, or remain idle. Since a PHES unit can only operate at a fixed speed while pumping, the participation of the PHES facility in regulation provisions is not possible in pumping mode.

On the other hand, the HSC PHES system has more flexibility to operate its units in any mode, regardless of the operation mode of the other units, as shown in Figure 2.3(c). Although the pumps still operate at fixed speed, the PHES units can operate also in generation mode to control the overall pumping energy. This is an important feature that allows the PHES system to pump water from its lower reservoir to the upper, *i.e.* increasing its water volume, while it can also participate in regulation provisions.

## 2.3 Ancillary Service Provisions

The North American Electric Reliability Corporation (NERC) has defined ancillary services as "elementary *reliability building blocks* from generation (and sometimes load) necessary to maintain bulk electric system reliability". These services are: (1) regulation, (2) load following, (3) contingency reserve (spinning and supplemental reserve), (4) reactive power supply from generation sources, (5) frequency response, and (6) system

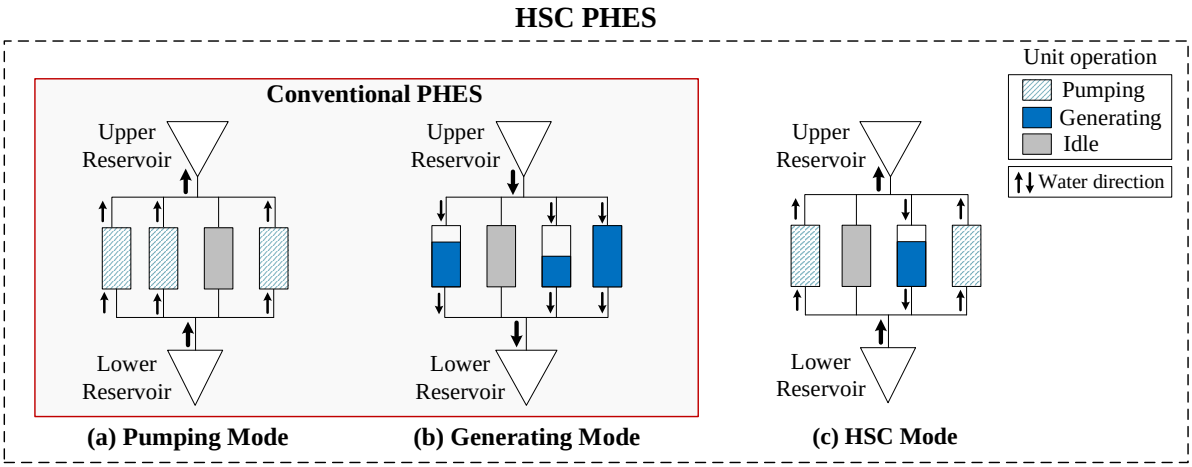


Figure 2.3: Schematic representation of conventional and HSC PHES.

black start capability [74].

While frequency regulation, spinning and non-spinning reserves are procured through a competitive market, the other services are procured on a cost basis and contractual agreements. ESS have the potential to improve the efficiency of ancillary service provisions and enhance system reliability. This section presents a review of the reserves and regulation markets, and the key advantages and limitations of ESS in the provision of these ancillary services.

### 2.3.1 Market-based Ancillary Services

It is noted that regulation and reserves are interchangeable terms across different markets, and hence it is important to distinguish these services and their definitions. Both of these services are crucial to maintain the supply-demand balance activated in different time frames to ensure the frequency of the system to be within the acceptable limits.

In power systems, the frequency control hierarchical structure comprises three levels: primary, secondary, and tertiary frequency control [75]. Primary frequency control is the local automatic control which adjusts the active power automatically within few seconds following a sudden and large generation or load outage. The main objective of primary

control is to stabilize the frequency, without seeking to restore it to the nominal. Secondary frequency control is to maintain the balance in a time frame ranging from seconds to a few minutes by injecting/drawing active power following the automatic generation control (AGC) signal. The main goal of secondary control is to restore the frequency to its nominal value. The third level is tertiary frequency control which is activated within 10-30 minutes to manually change the unit commitment dispatch.

In North America, primary frequency control services are procured through contracts, while secondary and tertiary control services are procured mostly through a market based mechanism. Although some of the markets refer to frequency regulation as operating reserve, in this thesis, the term operating reserve will be used for contingency reserves which can be classified as spinning, non-spinning and replacement/supplemental reserves.

### 2.3.2 Energy Storage as Ancillary Service Providers

The ancillary service markets have been more active with the recent trend of increasing share of RES in the generation mix. ESS play a pivotal role in facilitating the integration of RES and the provision of ancillary services because they are characterized by their fast response time and high ramping capability, which are critical features in ancillary service provisions, in order to maintain the demand-supply balance effectively. Furthermore, ESS can operate as a generator and a demand, allowing them to provide regulation and reserves in both directions.

However, ESS have different operational and physical characteristics compared to the traditional ancillary service providers, as discussed in Section 2.2.1. Because of these characteristics, it is challenging for ESS to compete in ancillary service markets that have been designed considering conventional resources. Furthermore, the high capital cost of ESS is another factor limiting the investments in ESS. Therefore, new regulation and policies have been initiated by regulatory authorities to integrate ESS to existing market clearing models such as the FERC Order 755 and Order 841 [4], [5].

FERC Order 841 facilitates the participation of ESS by considering their physical and operational characteristics in the capacity, energy, and ancillary services markets. One

of the most important changes introduced in US electricity markets under FERC, is to consider bidding parameters in market settlement representing the ESS characteristics, such as SOC, SOC limits, charge and discharge time, charge and discharge limits, charge and discharge ramp rates, and run time limits. Furthermore, ESS with a capacity of 100 kW or more, can now participate in all the markets, whereas prior to FERC Order 841, most markets required at least 1 MW of capacity, in order to participate. Also, after implementing FERC Order 841, ESS are now able to set the market prices as both wholesale buyer and seller, and ESS facilities have been allowed to bid/offer their de-rated capacity in the capacity market, based on their energy capacity available for continuous discharge that meets the minimum run-time requirements.

FERC Order 755 was issued to improve the performance of regulation market participants, including ESS. The price formation in PBR markets, as per FERC Order 755, considers the speed of response and accuracy of following the operator signal by the provider. Therefore, a participant in the PBR market receives a two-part payment: the traditional regulation capacity payment, and a new performance payment for the actual quantity of regulation power provision, referred to as "*mileage*" [76], which are explained in the following sub-sections.

#### 2.3.2.1 Regulation Capacity

It can be defined as the reserved capacity of a unit to provide regulation power during a determined period of time. The market operator compensates the regulation provider for the reserved capacity, regardless of its deployment in real-time operation.

#### 2.3.2.2 Regulation Mileage

It is an index to measure the performance of a regulation provider, and can be defined as the sum of absolute movements towards the set point of the regulation signal. Figure 2.4 shows an example of the set point of the regulation signal and the mileage scored by a resource.

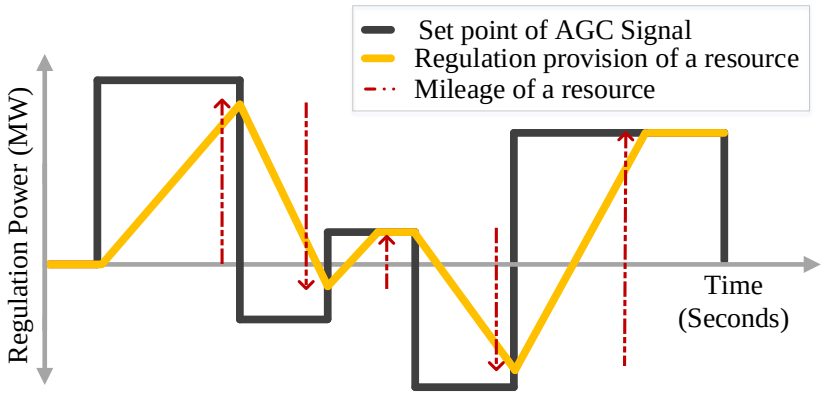


Figure 2.4: Regulation mileage definition.

It is noted that the performance payment differs from one market to another, but generally is computed after real-time operations, as follows:

$$Performance\ Payment[\$] = Mileage\ Offer[\$/MW] \times Mileage[MW] \times Performance\ Score[\%] \tag{2.4}$$

where the Performance Score is an index computed by the ISO to measure the accuracy of injected/drawn regulation power in response to the AGC signal [76]. It is noted that the regulation capacity and mileage settlements take place simultaneously in the day-ahead and/or in the real-time market.

### 2.3.3 Ancillary Services Markets in North America

An overview of ancillary services in the electricity markets in North America (USA and Canada) and the practices pertaining to ESS participation, is discussed in the following sub-sections. These markets are operated by six ISOs in USA under FERC jurisdiction, the Electric Reliability Council of Texas (ERCOT), USA (outside FERC jurisdiction), and for the two electricity markets in Canada, the IESO of Ontario and the Alberta Electric System Operator (AESO).

#### 2.3.3.1 PJM

The electricity market operated by PJM is one of the US markets under FERC jurisdictions. In PJM, the installed capacity of ESS is more than 278 MW/269 MWh, mostly from battery storage systems, which is considered as one of the largest ESS market capacities in North America [77]. PJM has two categories of ESS: energy storage resources which include batteries and flywheels, and capacity storage resources, which in addition to energy storage resources includes hydroelectric plants. Both operating reserves and frequency regulation are procured through a market-based system.

The operating reserves in PJM are defined as the amount of power that can be received within a specific time from synchronized or offline generators and certain loads. The operating reserves are categorized into: primary reserve, which can be received within 10 minutes, and supplemental reserve which can be available within 30 minutes. The primary reserve is divided into synchronized and quick start reserves based on the status of the resource. Currently, ESS are not eligible to participate in non-synchronized reserve provision. Although ESS are allowed to participate in synchronized reserve provision, allocating ESS capacities to participate in regulation markets is more profitable for ESS investors.

In the PJM regulation market, the providers are instructed to adjust their generation or demand in response to an automated signal to maintain the area control error (ACE) within its limit. To comply with FERC Order 755, PJM generates two types of signals: RegA and RegD, and the regulation providers can choose to follow either one. RegA is a low-pass filtered signal to recover large and long fluctuations, and designed for slow resources, whereas RegD is a high-pass filtered signal requiring instantaneous response from fast resources. Furthermore, RegD signal is designed to be zero-mean energy within 15 minutes period, which allows ESS to maintain their SOC level after the regulation provisions.

The regulation providers are required to submit two-part offers, capacity (capability) offer in ($/MW) and performance offer in ($/$\Delta$MW). The mileage is defined in PJM as "the summation of movement requested by the regulation control signal a resource is

following" [78], and is formulated as follows:

$$Mileage_{RegA} = \sum_{t=0}^{T} \left| RegA_t - RegA_{t-1} \right| \quad , \quad Mileage_{RegD} = \sum_{t=0}^{T} \left| RegD_t - RegD_{t-1} \right| \tag{2.5}$$

The regulation market clearing process is based on the adjusted costs [78], as follows:

$$Adjusted\ Regulating\ Capability\ Cost\ [\$] = \frac{\alpha[\frac{\$}{MW}]\ C[MW]}{\pi\rho} \tag{2.6}$$

$$Adjusted\ Performance\ Cost\ [\$] = \frac{\beta[\frac{\$}{\Delta MW}]\ M[\frac{\Delta MW}{MW}]\ C[MW]}{\pi\rho} \tag{2.7}$$

$$Adjusted\ Lost\ Opportunity\ Cost\ [\$] = \frac{\gamma[\frac{\$}{MW}]\ C[MW]}{\pi\rho} \tag{2.8}$$

where $\alpha$ and $\beta$ are the capability and performance offers, respectively, while $C$ and $M$ are the capability and mileage quantities, respectively. The estimated lost opportunity cost ($\gamma$) is based on the energy locational marginal prices. The historic performance score ($\rho$) is a factor averaged over 30 days denoting the performance in following one type of regulation signals by a resource. The benefit factor ($\pi$) of RegD ranges between $10^{-5}$ and 2.9, while it is fixed at unity for RegA.

#### 2.3.3.2 California Independent System Operator (CAISO)

CAISO is the first system operator in North America that procured ancillary services through competitive market settlements, and has one of the largest ESS market with capacity of about 130 MW/381 MWh [77]. ESS can offer and bid as non-generator resources (NGR) in day-ahead energy, reserve, and regulation markets.

The regulation market in CAISO is split into regulation-up and regulation-down, and procured in day-ahead and real-time markets. The required hourly quantities from the day-ahead market and the 15 minute quantities from the real-time markets are determined based on CAISO's demand forecast for these services. CAISO co-optimizes the energy and ancillary services markets to determine the market clearing prices and the regulation

capacity awards. A selected regulation provider receives regulation capacity payment, which includes the opportunity cost and payment for net energy, and mileage payment considering accuracy adjustment. The mileage is defined as: "the absolute change in AGC set points between 4 second intervals" [79].

It is noted that ESS participating as NGR can benefit from regulation energy management (REM), designed by CAISO for energy limited resources [79]. While traditional non-REM units require 60 minutes continuous energy, REM units require only 15 minutes of continuous energy, and hence allows the ESS to offer higher regulation capacities. For example, an ESS of 20 MW/5 MWh, participating under REM, allows it to offer 20 MW of capacity for the 15 minutes duration, while it can only offer 5 MW of capacity for 60 minutes because of the limited SOC.

#### 2.3.3.3 New York Independent System Operator (NYISO)

The ancillary services procured through market-based mechanisms are regulation, operating reserve, and energy imbalance. ESS can participate in the NYISO markets under one of the following categories: energy limited resources, limited energy storage resources, demand side ancillary service, and special case resource [80].

ESS can participate in operating reserve market as energy limited resources, however it must be able to provide at least 1 MW of continuous power for 4 consecutive hours without aggregating with other units. ESS can also participate in reserve provisions under the demand side ancillary service program and as a special case resource with the possibility of aggregating the required minimum capacity with other units.

The NYISO regulation markets operate on PBR basis, where a participant submits a capacity bid and regulation movement (mileage) bid, both in ($/MW). The regulation provision is procured through day-ahead and real-time markets. ESS participating in the regulation market under limited energy storage resources are managed by real-time dispatching of NYISO, and the offered regulation capacity may be reduced if the available SOC in one of the directions, either charging or discharging, is less than the cleared offer. The real-time dispatching manages the SOC to maintain its level every 5-minute interval.

#### 2.3.3.4 Electric Reliability Council of Texas (ERCOT)

The electricity markets operated by ERCOT are the only markets in USA not regulated by FERC. The ancillary services, including responsive reserves, non-spinning reserve, replacement reserve, regulation-up, and regulation-down, are procured in a day-ahead market. Since ERCOT is not under FERC, there is no performance payment considered, however the performance of resources are monitored in the regulation markets.

The total installed capacity of ESS is about 83 MW/41 MWh [77], and ESS can participate in energy or ancillary services markets as generators with a minimum capacity of 1 MW.

#### 2.3.3.5 The Independent Electricity System Operator (IESO) of Ontario

The electricity market operated by the IESO is one of the two markets in Canada. Four of the ancillary services namely: certified black start facilities, regulation service, reactive power support and voltage control service, and reliability must-run are contracted, while only the operating reserves are procured through market-based system [81].

The operating reserve is defined as "stand-by power or demand reduction that can be called on with short notice to deal with an unexpected mismatch between generation and load". There are three classes of reserves in IESO: 10-minute synchronized (spinning) reserve, 10-minute non-synchronized (non-spinning) reserve, and 30-minute reserve (non-synchronized). The scheduling of operating reserve and energy in the real-time energy markets are co-optimized, and the reserve prices are determined every 5 minutes.

Currently, the IESO regulation market is based on contractual agreements, and regulation payments comprise fixed and variable components. The regulation capacity requirements are fixed for all intervals. IESO requires ±100 MW of AGC scheduled at all times, with a minimum overall ramp rate requirement of 50 MW/minute. However, the IESO has plans to increase the scheduled regulation capacity to 200 MW and additional "as-needed" regulation capacity, to maintain a total regulation capacity of up to 300 MW.

The participation of ESS including flywheels and battery storage systems in regulation provisions was launched in 2012 as part of the Alternate Technologies for Regulation Pilot Program. In 2013, the Ontario Long-Term Energy Plan proposed initiatives to understand the value of ESS in Ontario, which resulted in the procurement of 50 MW of different types of ESS in two phases [1].

In Phase I of ESS procurement (2014), 33.54 MW of capacity was contracted to provide regulation, reactive power support, and voltage control services which included 8 BESS (25.8 MW), one flywheel (5 MW), one thermal storage (0.74 MW), and a hydrogen-gas storage (2 MW). In 2017, the IESO awarded contracts to two BESS facilities (55 MW) to provide regulation services. Phase II of ESS procurement has contracted 16.75 MW of capacity (8 facilities, including 15 MW of BESS, and one 1.75 MW of compressed air ESS). As of now, ESS participation is limited to contractual agreements, and hence they cannot submit offers or bids in any of the IESO markets.

#### 2.3.3.6 The Alberta Electric System Operator (AESO)

The ancillary services in AESO are classified into: operating reserve, transmission must-run, black start, and load shedding services for imports. The operating reserves are categorized as regulating, spinning and supplemental reserves. The regulating reserves instantaneously provide the power difference between supply and demand required during that lag period. Spinning and supplemental reserves, known as contingency reserves, are used to maintain the balance of supply and demand when an unexpected system event occurs.

ESS participation in AESO is still under consideration; a cost/benefit analysis was carried out to assess the need of two main types of storage systems [82]. First, Li-ion battery representing short-duration and low-energy ESS was considered, and second, a pumped hydro storage was considered representing long-duration and high-energy ESS. It is seen that only Li-ion storage might be cost-effective in AESO because of the revenue from ancillary services markets. However, the ancillary services market in AESO is small, and hence, the market is able to support only a small amount of ESS before it saturates.

## 2.4 Investment Planning Aspects for Microgrids

The basic planning concepts and investment valuation in power systems are discussed in this section. While the planning problems at the distribution system level essentially deal with substation and feeder planning, the planning problem in microgrids mainly concern the optimal integration of DG, RES and ESS. As ESS is the main focus of this thesis, and play an integral part in microgrids, their operational and planning issues in the context of microgrids are discussed.

### 2.4.1 Investment Planning in Power Systems

The annual growth in electricity demand necessitates frequent upgrades to power system infrastructure and replacement of assets that have reached their end of life. Large investments are needed to maintain system reliability and meet the demand growth; for example, in Canada, the projected total investment required to maintain the current state of power system infrastructure is about $293.8 billion from year 2010 to 2030 [83]. Therefore, planning studies are needed to examine the economic value of such investments and their timing need be coordinated considering a long-term horizon to achieve the required level of reliability at acceptable cost.

The planning process in power systems comprises five main stages which starts with defining the problem and the plan horizon [84]. The main goals of the planning study are determined thereafter to meet the long-term system requirements. Next, all possible solutions, resources, and approaches are examined in the third stage which are evaluated based on cost benefit analysis to select the optimal solution that meets the goals of the planning problem. Although, planning studies are typically conducted by the system planner or a central authority, in recent years there have been increasing participation of third parties if there is an economical value.

The economical value in long-term planning problems are quantified using several measures based on discounted cash flow, such as the NPV of profits and the internal rate

of return (IRR) [85]. The NPV of the profit is formulated as follows:

$$\Omega = \sum_{y=1}^{Y_T} \frac{Revenue_y - Cost_y}{(1+\alpha)^y} \tag{2.9}$$

where $\alpha$ is the discount rate. The IRR on the other hand is used to estimate the profitability of investments, and hence is often used to assess third-party investment feasibility. The IRR is the investment rate of return at which the NPV of the net cash flow is zero, *i.e.* the cost of investment is just recovered, and is given as follows:

$$\sum_{y=1}^{Y_T} \frac{Revenue_y}{(1+\beta)^y} = \sum_{y=1}^{Y_T} \frac{Cost_y}{(1+\beta)^y} \tag{2.10}$$

where $\beta$ is the IRR on the investment. To determine that the profit in an investment worth the risk, a Minimum Acceptable Rate of Return is set by the investor, known as MARR, and the investment is considered profitable when the IRR is greater than or equal to MARR. In vertically integrated power systems, planning studies are carried out by a single entity considering the entire system from generation, transmission, to distribution levels. However, with the transformation of power systems to deregulated competitive markets in the 1990s', planning studies are now being undertaken separately by each entity considering their costs and benefits from such investments at their system boundaries.

### 2.4.2 Microgrid Concept and Design

The microgrid comprises a group of loads and small-scale energy resources that operate as a single entity [86]. Each microgrid controls its resources, to meet its demand, which includes dispatchable DG units such as microturbines, fuel cells, and combined heat and power (CHP) units, and RES such as hydro, PV and wind generation. In addition to these components, ESS are essential elements in microgrids. Microgrids can operate as isolated systems and balance their demand via the available resources or can be connected to the main grid at the point of common coupling (PCC) for bidirectional exchange of energy. A general microgrid layout is shown in Figure 2.5.

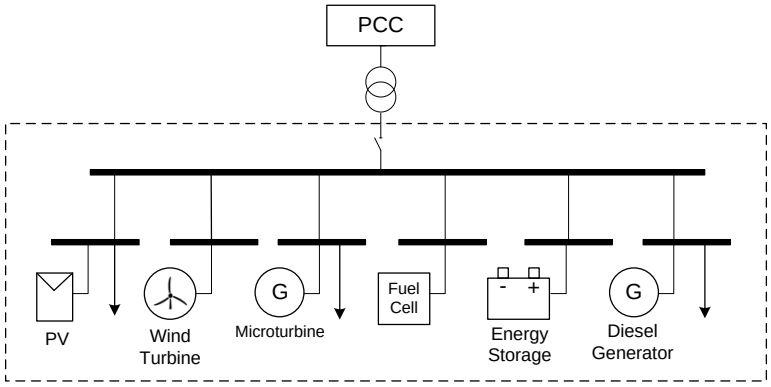


Figure 2.5: General microgrid layout.

The characteristics of microgrids are different from the conventional power systems mainly because of their low inertia, because the capacity of dispatchable DG units are relatively small. Furthermore, microgrids are also exposed to the rapid changes in demand and production fluctuations from RES [87]. Consequently, planning and designing microgrids need to consider equipping the system with state-of-art power electronics, protection devices and reinforced by two-way communication systems in order to accommodate the generation resources and maintain reliability in the presence of bi-directional power flows. Controlling these components is performed by the microgrid's EMS which optimizes its operation while ensuring reliability at least cost.

Although microgrids enhance the overall system efficiency, some operational challenges may face the MGO from the integration of RES. The fluctuations in output power from these RES have to be mitigated to ensure power quality and reliability standards in both grid-connected and isolated mode of operation. Some of the challenges in microgrids and the control strategies to overcome these issues are discussed in [86], [87].

Microgrid planning problems need to consider the challenges in different modes of operation. In isolated microgrids, ensuring sufficient generation and scheduling resources based on the forecasted demand and availability of RES are the important issues [40], [88]. The high uncertainty of RES adds a degree of complexity in maintaining their reliability. Moreover, the lack of rotational inertia from dispatchable generators require additional sources and strategies to ensure microgrid stability. On the other hand,

the main aim of grid-connected mode of operation is to maximize the microgrid's benefit from exchanging energy with the main grid [89].

Furthermore, modeling the operational aspects of all the resources are important in microgrid planning frameworks. For example, although the UC problem is a classical operational problem, because of the inter-temporal constraints of the ESS, these are included in the microgrid planning problem to capture the interactions between ESS and dispatchable generators and their impact on the NPV of profit and IRR.

### 2.4.3 Microgrid Operational Problem

The main objective of the microgrid operational problem, which is very similar to the classical UC problem, is to find the optimal commitment schedule of the available generators over a period of time to meet the demand, taking into account the characteristics of generating units and other power system constraints. Several optimization techniques and algorithms for solving the UC problem have been discussed in [90]. The objective function of the generic UC model is given as follows:

$$J = \sum_{h=1}^{H} \sum_{i=1}^{I} \left( F_i(P_{h,i}) W_{h,i} + SU_i \; U_{h,i} + SD_i \; V_{h,i} \right) \tag{2.11}$$

A linear cost function of the thermal generators is generally considered, as follows:

$$F_i(P_i) = a_i P_i + b_i \quad \forall i \tag{2.12}$$

where $a$ and $b$ are the cost coefficients of each generating unit in \$/kWh and \$/h, respectively. The associated constraints of the UC problem are discussed next.

*Demand Supply Balance:* This constraint ensures sufficient generation is available to meet the demand at each hour.

$$\sum_{i=1}^{I} P_{h,i} = Pd_h \quad \forall h \tag{2.13}$$

*Reserve Requirements:* The total capacity available from committed generators should

meet certain system reserve requirements, as follows:

$$\sum_{i=1}^{I}(\overline{P_i}W_{h,i} - P_{h,i}) \geq R_h \quad \forall h \tag{2.14}$$

*Generating Unit Limits:* Each generating unit has upper and lower bounds on its power production, as follows:

$$\underline{P_i}W_{h,i} \leq P_{h,i} \leq \overline{P_i}W_{h,i} \quad \forall i, \forall h \tag{2.15}$$

*Ramp Up/Down Constraints of Generating Units:* The inter-hour increase/decrease in generation should satisfy the ramp rate limits of generating units, as follows:

$$P_{h,i} - P_{h-1,i} - U_{h,i}\ \overline{P_i} \leq Ramp_i^{UP} \qquad \forall i, \forall h; h \neq 1 \tag{2.16}$$

$$P_{h-1,i} - P_{h,i} - V_{h,i}\ \overline{P_i} \leq Ramp_i^{DW} \qquad \forall i, \forall h; h \neq 1 \tag{2.17}$$

*Minimum Up Time Constraints of Generating Units:* When a generating unit is turned on, it must not be de-committed before satisfying its minimum up time. These constraints are formulated as in [91].

$$\sum_{h=1}^{G_i}(1 - W_{h,i}) = 0 \quad \forall i \tag{2.18}$$

$$\sum_{q=h}^{h+Min_i^{UP}-1} W_{q,i} \geq Min_i^{UP}[W_{h,i} - W_{h-1,i}] \quad \forall i, h = G_i + 1, ....H - Min_i^{UP} + 1 \tag{2.19}$$

$$\sum_{q=h}^{H}\left[W_{q,i} - (W_{h,i} - W_{h-1,i})\right] \geq 0 \quad \forall i, h = H - Min_i^{UP} + 2, ....H \tag{2.20}$$

*Minimum Down Time Constraints of Generating Units:* When a generating unit is turned off, the minimum down time should be satisfied before committing it again. The constraints are formulated as follows [91]:

$$\sum_{h=1}^{L_i} W_{h,i} = 0 \quad \forall i \tag{2.21}$$

$$\sum_{q=h}^{h+Min_i^{DW}-1} (1-W_{q,i}) \geq Min_i^{DW}[W_{h-1,i}-W_{h,i}] \quad \forall i, h = L_i+1, ....H - Min_i^{DW}+1 \quad (2.22)$$

$$\sum_{q=h}^{H} \left[1 - W_{q,i} - (W_{h-1,i} - W_{h,i})\right] \geq 0 \quad \forall i, h = H - Min_i^{DW} + 2, ....H \quad (2.23)$$

*Coordination of UC Decisions:* To ensure proper coordination between the generator status and the start-up/shut down variables, the following constraint is formulated, as below:

$$U_{h,i} - V_{h,i} = W_{h,i} - W_{h-1,i} \quad \forall i, \forall h \quad (2.24)$$

## 2.5 Uncertainty Management in Operational and Planning Models in Power Systems

Power system operational and planning studies involve several uncertainties in parameters such as RES generation, loads, and offers/bids submitted by market participants and hence the market clearing prices. Deterministic solutions for operations and planning are typically obtained in most studies using forecasted data and parameters. However, such solutions are subject to the accuracy of the forecast and the tool/ technique used, the assumptions made, and the goodness of data. Some of the alternative approaches used by researchers to take into account uncertainties in power system planning and operations studies include MCS and stochastic optimization, which are discussed briefly in the following sub-sections.

### 2.5.1 Monte Carlo Simulations

In MCS, scenarios are generated randomly for each parameter considering its probability density function (pdf). Simple random sampling may require large number of simulations to represent the pdf accurately. Therefore, stratified sampling methods, such as the Latin Hypercube Sampling (LHS) technique, have been proposed to improve the MCS convergence within only few number of simulations [92], [93]. The LHS technique ensures covering the entire pdf by dividing the cumulative distribution function into equal

intervals, in which the number of intervals is equal to the required number of scenarios, and selects a random scenario from each interval.

When MCS is applied to operational and planning problems, the expected solutions can be obtained by convergence after sufficient number of simulations, based on the statistical characteristics of the samples such as minimum, maximum, mean, median and variance of the results. The computational time mainly depends on the number of simulations required to converge to the expected solution. However, it is to be noted that the MCS solutions cannot always be obtained by statistical convergence. For example, the uncertainty in offers/bids submitted by market participants yields significantly different profiles of market clearing prices, rendering the investment decisions based on statistical characteristics less effective. In such problems, MCS is used to generate a large number of scenarios for each random parameter. Thereafter, a suitable scenario reduction technique is used to select a representative set of scenarios, which then can be employed in the stochastic optimization models [94].

### 2.5.2 Scenario-based Stochastic Optimization

The stochastic optimization model considers a set of scenarios and determines the optimal solution based on the expected objective function, in one execution run. Considering the recourse action of the uncertain parameters, the variables in stochastic optimization problems can be divided into *here-and-now* and *wait-and-see* variables. The optimal solutions of *here-and-now* variables need to be determined prior to the uncertainties being resolved. Furthermore, the *here-and-now* variables should ensure the feasibility of the *wait-and-see* variables, which are determined when the uncertainties are revealed.

The stochastic operational problems have been widely solved using a two-stage framework [95]. In the first stage, the decisions to be determined ahead of time are obtained, such as the UC status, SOC levels of ESS, and operating reserves. In the second stage, the *here-and-now* variables are considered fixed, while the *wait-and see* variables, such as the generation dispatch, power flows, and charging/discharging operations of ESS, are determined considering smaller time steps than in the first stage,

since more information of uncertain parameters are now available. On the other hand, in stochastic planning problems, all the planning variables are considered *here-and-now* variables, while all the operational variables are considered as the *wait-and-see* variables or the recourse variables.

It is noted that considering multiple scenarios in a stochastic optimization problem increases the computational time. Planning problems and day-ahead market clearing problems are less restricted by the computational time and obtaining a more reliable result is important, whereas computational efficiency is more critical in operational problems and real-time market clearing problems, hence the stochastic optimization models should be efficient to be solved within a limited time frame.

## 2.6 Summary

The chapter introduced some essential background topics required for this research. The state-of-art energy storage technologies, systems, and their important properties and parameters were presented. An overview of ancillary service provisions and markets in North America (USA and Canada) was presented, followed by a brief discussion of some investment planning aspects for microgrids. Finally, uncertainty management techniques in power systems were presented.

# Chapter 3

# Stochastic Optimal Planning of Battery Energy Storage Systems[1]

In this chapter, a stochastic planning framework is proposed to determine the optimal BESS capacity and year of installation from the perspective of the system operator in an isolated microgrid. A decomposition-based approach is proposed to solve the problem of stochastic planning of BESS under uncertainty, and is solved in two stages as MILP problems to ensure the convergence. The optimal ratings of the BESS are determined in the first stage, while the optimal installation year is determined in the second stage. Furthermore, a novel matrix representing BESS energy capacity degradation is included within the planning model. Extensive studies considering four types of BESS technologies for deterministic, MCS, and stochastic cases are presented.

[1]This chapter has been published in:
H. Alharbi, and K. Bhattacharya, "Stochastic Optimal Planning of Battery Energy Storage Systems for Isolated Microgrids," *IEEE Transactions on Sustainable Energy*, vol. 9, no. 1, pp. 211-227, Jan. 2018.

## 3.1 Nomenclature

### *Indices*

| | |
|---|---|
| $h$ | Index for hours, $h = 1, 2, .., H$ |
| $i$ | Index for dispatchable DG units, $i = 1, 2, .., I$ |
| $k$ | Index for BESS operation cycle, $k = 1, 2, .., K$ |
| $s$ | Index for scenarios, $s = 1, 2, .., S$ |
| $y$ | Index for years, $y = 1, 2, .., Y_T$ |

### *Parameters*

#### *1) Dynamic Iteration-based Parameters*

| | |
|---|---|
| $BS_{ITR}$ | NPV of budget allocation in iteration $ITR$ to determine BESS size at $Y_T$ [$] |
| $C_0$ | Total microgrid operational cost with no BESS installed [$] |
| $C_{ITR}$ | Total cost for the decisions in iteration $ITR$ [$] |
| $C^{min}$ | Minimum cost associated with the optimal solution [$] |
| $E^*_{BESS}$ | BESS energy capacity determined in Stage-I for $Y_T$ [kWh] |
| $P^*_{BESS}$ | BESS power rating determined in Stage-I for $Y_T$ [kW] |

#### *2) BESS and DG Technical Parameters*

| | |
|---|---|
| $C^f$ | Fixed installation cost of BESS [$] |
| $C^g_i$ | Marginal cost of generating unit $i$ [$/kWh] |
| $Ce^v$ | Variable installation cost of BESS associated with energy capacity [$/kWh] |
| $Cp^v$ | Variable installation cost of BESS associated with power rating [$/kW] |
| $\overline{DOD}$ | Maximum depth of discharge [%] |
| $\overline{EPR}$,$\underline{EPR}$ | Maximum/minimum energy to power ratio |
| $G_i, L_i$ | Initial up-time and down-time required of DG unit $i$ [h] |

| | |
|---|---|
| $Min_i^{DW}$ | Minimum down-time of DG unit $i$ [h] |
| $Min_i^{UP}$ | Minimum up-time of DG unit $i$ [h] |
| $OMC^f$ | Yearly fixed O&M cost of BESS [$/kW-year] |
| $OMC^v$ | Variable O&M cost of BESS [$/kWh] |
| $\overline{P}_i$ | Maximum output power of DG unit $i$ [kW] |
| $\underline{P}_i$ | Minimum output power of DG unit $i$ [kW] |
| $Ramp_i^{DW}$ | Ramp down limit of DG unit $i$ [kW] |
| $Ramp_i^{UP}$ | Ramp up limit of DG unit $i$ [kW] |
| $RC$ | Replacement cost of BESS [$/kW] |
| $R_Y$ | Replacement year of BESS |
| $SD_i$, $SU_i$ | Shut-down and start-up cost of DG unit $i$ [$] |
| $\eta_c$, $\eta_d$ | BESS charging/discharging efficiency [%] |
| $\sigma$ | BESS energy capacity degradation factor [%] |

***3) Operational and Planning Parameters***

| | |
|---|---|
| $B_0$ | NPV of budget allocation [$] |
| $C^{SHED}$ | Cost of load shedding [$/kWh] |
| $M$ | Large number (assumed 10,000) |
| $ND$ | Number of seasonal representative days |
| $Pd$ | Forecasted demand of isolated microgrid [kW] |
| $PV$ | Forecasted PV generation [kW] |
| $Pw$ | Forecasted wind generation [kW] |
| $\alpha$ | Discount rate [%] |
| $\beta$ | Fuel cost escalation rate [%] |
| $\gamma$ | Minimum reserve as percentage of demand [%] |
| $\delta_D$,$\delta_{PV}$,$\delta_W$ | Error in forecasted demand, PV and wind [%] |
| $\lambda$ | Load growth rate [%] |
| $\varepsilon$ | Small number (assumed 1) |
| $\rho_s$ | Probability of scenario $s$ |

## *Variables*

### *1) BESS Planning Variables*

| | |
|---|---|
| $E_{BESS}$ | Energy capacity of BESS [kWh] |
| $INS$ | NPV of installation cost of BESS [$] |
| $NE_{BESS}$ | Nominal BESS energy capacity at year of installation [kWh] |
| $P_{BESS}$ | Power rating of BESS [kW] |
| $Z$ | Binary BESS installation decision |
| $Zp$ | Binary BESS presence indicator |

### *2) BESS and DG Operational Variables*

| | |
|---|---|
| $E_A$ | Energy drawn from the microgrid by BESS during charging [kWh] |
| $E_B$ | Energy received by BESS during charging, net of charging losses [kWh] |
| $E_C$ | Energy discharged from BESS [kWh] |
| $E_D$ | Energy injected to the microgrid by BESS during discharging [kWh] |
| $E_L$ | Total BESS energy losses over a daily cycle [kWh] |
| $E_{CL}$, $E_{DL}$ | Energy losses during BESS charging and discharging [kWh] |
| $E_{SL}$ | Energy losses during BESS standby mode [kWh] |
| $MGOC$ | NPV of microgrid operational cost [$] |
| $OM$ | NPV of O&M cost of BESS [$] |
| $P$ | DG output [kW] |
| $PB$ | BESS power; negative when charging, and positive when discharging [kW] |
| $Pd^{SHED}$ | Load shedding [kWh] |
| $PV^{CURT}$ | PV generation curtailment [kW] |
| $Pw^{CURT}$ | Wind generation curtailment [kW] |
| $R$ | Total required reserve capacity [kW] |
| $RB^{DW}$ | Downward reserve capacity from BESS [kW] |
| $RB^{UP}$ | Upward reserve capacity from BESS [kW] |

| | |
|---|---|
| $RG^{DW}$ | Downward reserve capacity from DG [kW] |
| $RG^{UP}$ | Upward reserve capacity from DG [kW] |
| $SOC$ | BESS state of charge [kWh] |
| $TE_C$ | Total energy discharged form BESS [kWh] |
| $U, V, W$ | Binary start-up, shut-down, and commitment decision of DG units |
| $Zc, Zd$ | Binary BESS charging/discharging decision |

## 3.2 Stochastic Optimal Planning of BESS: Mathematical Models

### 3.2.1 Charging and Discharging Operation Model of BESS

The focus of this chapter is on BESS energy applications in isolated microgrids, and hence BESS is required to charge and discharge deep cycles to help other microgrid resources in meeting the demand. Therefore, detailed insight into the BESS charging and discharging cycle is necessary, and the need for an appropriate model arises. In the following discussions, a new representation of the energy diagram of the BESS is developed, along with the associated mathematical relationships.

Figure 3.1 shows the energy diagram of a BESS for one charging and discharging cycle. The BESS draws $E_A$ amount of energy from the microgrid during charging. Because of the energy losses in the charging process, denoted by the charging efficiency $\eta_c$, $E_B$ amount of energy is actually stored. There are standby losses when the BESS is idle, and the energy level drops to $E_C$. Finally, when the BESS discharges energy to the microgrid, the discharging efficiency ($\eta_d$) comes into play and the final energy supplied to the microgrid is $E_D$. Discharged energy $E_C$ quantifies the actual usage of BESS and is used in computing the variable O&M cost. It can be expressed using one variable: the BESS power ($PB$) when standby losses are negligible. Accordingly, from Figure 3.1 we have:

$$E_{Ak} = \frac{E_{Bk}}{\eta_c} = \frac{E_{Ck} + E_{SL_k}}{\eta_c} \tag{3.1}$$

$$E_{Dk} = E_{Ck}\ \eta_d \tag{3.2}$$

Assuming that the initial and final SOC of the BESS are at the same level in one operation day, the total BESS energy loss $E_L$ in that day, considering several charging/discharging cycles, is given as follows:

$$E_L = \sum_{k=1}^{K}(E_{Ak} - E_{Dk}) = \sum_{k=1}^{K}\Big[\frac{E_{SL_k}}{\eta_c} + (\frac{1-\eta_c\eta_d}{\eta_c}\ E_{Ck})\Big] = \frac{TE_{SL}}{\eta_c} + \frac{1-\eta_c\eta_d}{\eta_c}\ TE_C \tag{3.3}$$

Since $PB$ in charging mode is negative, and the total charging energy is greater than the total discharging energy because of BESS efficiencies, the total energy loss $E_{\mathrm{L}}$ in the BESS can also be given in terms of $PB$, as follows:

$$E_{\mathrm{L}} = \sum_{h=1}^{H}\big(-PB_h\ \Delta h\big) \tag{3.4}$$

Hence, the total energy discharged from BESS in one day can be expressed as follows:

$$TE_C = \frac{-\eta_c}{1-\eta_c\eta_d}\ \Big[\frac{TE_{SL}}{\eta_c} + \sum_{h=1}^{H}\big(PB_h\ \Delta h\big)\Big] \tag{3.5}$$

where $\Delta h$ is assumed to be one hour. Note that in (3.5), it is inherently assumed that the efficiencies of charging and discharging are always less than 100%.

### 3.2.2 Optimal Power and Energy Sizing (OPES) Model

#### 3.2.2.1 Objective Function

The objective is to minimize the sum of expected NPV of the BESS installation cost $E[INS]$, O&M cost $E[OM]$, and microgrid operational cost $E[MGOC]$, as given by:

$$J = E[INS] + E[OM] + E[MGOC] \tag{3.6}$$

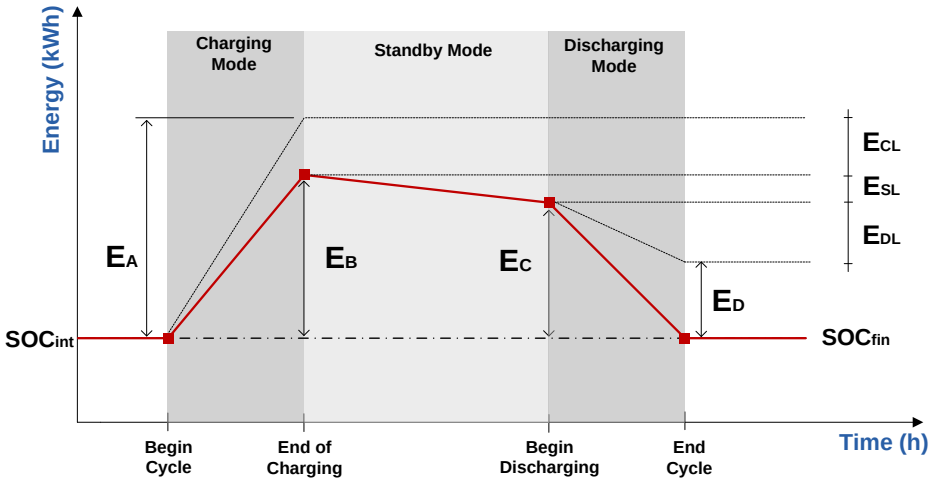


Figure 3.1: Energy diagram of BESS.

The NPV of the BESS installation cost is:

$$E[INS] = \sum_{y=1}^{Y_T} \left[ \frac{1}{(1+\alpha)^y} Z_y \left( Cp^v P_{BESS} + Ce^v N E_{BESS} + C^f \right) \right] \tag{3.7}$$

The NPV of the expected O&M cost of the BESS is:

$$\begin{aligned} E[OM] = & \sum_{y=1}^{Y_T} \left[ \frac{1}{(1+\alpha)^y} \; OMC^f \; P_{BESS} \; Zp_y \right] + \frac{365}{ND} \sum_{s=1}^{S} \rho_s \sum_{y=1}^{Y_T} \left[ \frac{1}{(1+\alpha)^y} \; OMC^v \; TE_{C\,s,y} \right] \\ & + \sum_{y=R_Y}^{Y_T} \left[ \left( \frac{1}{(1+\alpha)^y} + \frac{1}{(1+\alpha)^{y+R_Y}} + \ldots \right) \; RC \; P_{BESS} \; Z_{y-R_Y+1} \right] \end{aligned} \tag{3.8}$$

The binary variable $Zp_y$ in (3.8), denoting the presence of BESS in the system from year $y$ onwards, is determined from the binary variable $Z_y$ which denotes the BESS installation decision at year $y$. Accordingly, $Zp_y$ is given as:

$$Zp_y = \sum_{n=1}^{y} Z_n \qquad \forall y \tag{3.9}$$

In the second term of (3.8), the total energy discharged $TE_{C\ s,y}$ is computed from (3.5) considering the scenario and year indices in $PB_{s,y,h}$. Since the model considers $ND$ representative days per year, the variable cost is extrapolated to one year using a factor of $365/ND$. The third term of (3.8) denotes the replacement cost of BESS which may apply several times if the BESS life is reached more than once over the planning horizon.

By considering the BESS O&M cost, the life cycle is implicitly included in the planning objective; when this objective is minimized, the optimal charging/discharging cycles are so obtained that unnecessary cycling operations of the BESS are minimized. Furthermore, BESS life of "$R_Y$" years is considered in the model along with a replacement cost added when the operating years exceed $R_Y$. The above two features ensure optimal life cycle utilization and cycling operation of the BESS.

The NPV of $MGOC$ given below, represents the operational cost of dispatchable DG units including their start-up and shut-down cost, taking into account the annual fuel cost escalation, as well as, load shedding cost. This component is also extrapolated to one year using the factor $365/ND$.

$$E[MGOC] = \frac{365}{ND}\sum_{s=1}^{S}\rho_s\sum_{y=1}^{Y_T}\sum_{h=1}^{ND\times H}\frac{1}{(1+\alpha)^y}\Bigg[\Big[C^{SHED}Pd_{s,y,h}^{SHED}\Big] + \sum_{i=1}^{I}\Big[\big(1+\beta\big)^{y-1}F_i\big(P_{s,y,h,i}\big)W_{s,y,h,i} + SU_iU_{s,y,h,i} + SD_iV_{s,y,h,i}\Big]\Bigg] \tag{3.10}$$

where $F_i(\cdot)$ is the operational cost function of a DG.

It is to be noted that some of the variables in $E[OM]$ and $E[MGOC]$ have an index denoting the scenario. This is to capture the uncertainty in various parameters which are modeled in this work using pdf. Each scenario has an associated probability $\rho_s$ and the optimal decisions are determined for every scenario, year, and hour while minimizing the expected costs. However, the optimal BESS size is selected taking into account all the considered scenarios, and hence the variables in $E[INS]$ does not include the scenario index.

#### 3.2.2.2 Model Constraints

*Demand-Supply Balance:* These constraints ensure sufficient generation from DG and RES to meet the microgrid demand:

$$\sum_{i=1}^{I} P_{s,y,h,i} + PB_{s,y,h} + PV_{s,y,h} + Pw_{s,y,h} = Pd_{s,y,h} - Pd^{SHED}_{s,y,h} + PV^{CURT}_{s,y,h} + Pw^{CURT}_{s,y,h} \quad \forall s, \forall y, \forall h \tag{3.11}$$

where the RES curtailment and load shedding limits, assuming 30% of the load is critical or uncurtailable, are given as follows:

$$0 \leq PV^{CURT}_{s,y,h} \leq PV_{s,y,h} \quad \forall s, \forall y, \forall h \tag{3.12}$$

$$0 \leq Pw^{CURT}_{s,y,h} \leq Pw_{s,y,h} \quad \forall s, \forall y, \forall h \tag{3.13}$$

$$0 \leq Pd^{SHED}_{s,y,h} \leq 0.7Pd_{s,y,h} \quad \forall s, \forall y, \forall h \tag{3.14}$$

*Dispatchable DG Unit Constraints:* These constraints are as per standard UC models [91], considering all the probabilistic scenarios, and over each year of the planning horizon, as follows:

$$\underline{P_i} W_{s,y,h,i} \leq P_{s,y,h,i} \leq \overline{P_i} W_{s,y,h,i} \quad \forall s, \forall y, \forall h, \forall i \tag{3.15}$$

$$P_{s,y,h,i} - P_{s,y,h-1,i} - U_{s,y,h,i}\ \overline{P_i} \leq Ramp^{UP}_i \quad \forall s, \forall y, \forall i, \forall h; h \neq 1 \tag{3.16}$$

$$P_{s,y,h-1,i} - P_{s,y,h,i} - V_{s,y,h,i}\ \overline{P_i} \leq Ramp^{DW}_i \quad \forall s, \forall y, \forall i, \forall h; h \neq 1 \tag{3.17}$$

$$\sum_{h=1}^{G_i} (1 - W_{s,y,h,i}) = 0 \quad \forall s, \forall y, \forall i \tag{3.18}$$

$$\sum_{q=h}^{h+Min^{UP}_i-1} W_{s,y,q,i} \geq Min^{UP}_i [W_{s,y,h,i} - W_{s,y,h-1,i}] \quad \forall s, \forall y, \forall i, h = G_i + 1, ....H - Min^{UP}_i + 1 \tag{3.19}$$

$$\sum_{q=h}^{H} \left[ W_{s,y,q,i} - (W_{s,y,h,i} - W_{s,y,h-1,i}) \right] \geq 0 \qquad \forall s, \forall y, \forall i, h = H - Min_i^{UP} + 2, ....H \tag{3.20}$$

$$\sum_{h=1}^{L_i} W_{s,y,h,i} = 0 \qquad \forall s, \forall y, \forall i \tag{3.21}$$

$$\sum_{q=h}^{h+Min_i^{DW}-1} (1 - W_{s,y,q,i}) \geq Min_i^{DW} [W_{s,y,h-1,i} - W_{s,y,h,i}] \qquad \forall s, \forall y, \forall i, h = L_i + 1, ....H - Min_i^{DW} + 1 \tag{3.22}$$

$$\sum_{q=h}^{H} \left[ 1 - W_{s,y,q,i} - (W_{s,y,h-1,i} - W_{s,y,h,i}) \right] \geq 0 \qquad \forall s, \forall y, \forall i, h = H - Min_i^{DW} + 2, ....H \tag{3.23}$$

$$U_{s,y,h,i} - V_{s,y,h,i} = W_{s,y,h,i} - W_{s,y,h-1,i} \qquad \forall s, \forall y, \forall h, \forall i \tag{3.24}$$

It is noted that the constraints: output power limits (3.15), ramp up (3.16), ramp down (3.17), minimum up time (3.18)-(3.20), minimum down time (3.21)-(3.23), and DG coordination constraints (3.24), are general for all the types of dispatchable DG units considered in this work. These constraints have been relaxed in some microgrid EMS models to reduce the computational time in operational problems, given that dispatchable DG units have fast ramping capability and fewer restrictions on minimum-up and -down times. However, in practice, these constraints indeed impact microgrid operations [96], and since planning problems are less restricted by the computational time, these are considered in the present study, for the sake of accuracy.

*Microgrid Reserve Requirements:* The MGO ensures a minimum reserve level ($\gamma$) to take into account the operating margin, plus factors accounting for uncertainty in demand and

RES forecasting errors [40], as follows:

$$R_{s,y,h} = \big(\gamma + \delta_D\big)(Pd_{s,y,h} - Pd^{SHED}_{s,y,h}) + \delta_{PV}(PV_{s,y,h} - PV^{CURT}_{s,y,h}) + \delta_W(Pw_{s,y,h} - Pw^{CURT}_{s,y,h}) \quad \forall s, \forall y, \forall h \tag{3.25}$$

$$RG^{UP}_{s,y,h} + RB^{UP}_{s,y,h} \geq R_{s,y,h} \quad \forall s, \forall y, \forall h \tag{3.26}$$

$$RG^{UP}_{s,y,h} \leq \sum_{i=1}^{I} \big(\overline{P_i} W_{s,y,h,i} - P_{s,y,h,i}\big) \quad \forall s, \forall y, \forall h \tag{3.27}$$

$$RB^{UP}_{s,y,h} \leq -PB_{s,y,h} + \min\Big\{\big[SOC_{s,y,h} - Zp_y \ E_{BESS_y}(1 - \overline{DOD})\big]\eta_d, P_{BESS}\Big\} \quad \forall s, \forall y, \forall h \tag{3.28}$$

$$RG^{DW}_{s,y,h} + RB^{DW}_{s,y,h} \geq R_{s,y,h} \quad \forall s, \forall y, \forall h \tag{3.29}$$

$$RG^{DW}_{s,y,h} \leq \sum_{i=1}^{I} \big(P_{s,y,h,i} - \underline{P_i} W_{s,y,h,i}\big) \quad \forall s, \forall y, \forall h \tag{3.30}$$

$$RB^{DW}_{s,y,h} \leq PB_{s,y,h} + \min\Big\{\big[Zp_y \ E_{BESS_y} - SOC_{s,y,h}\big]/\eta_c, P_{BESS}\Big\} \quad \forall s, \forall y, \forall h \tag{3.31}$$

As shown in (3.26), $RB$ is the upward reserve from BESS that supports the spinning reserve from DG units; denoted by $RG$, and is given by (3.27). In (3.28), the BESS upward reserve contribution is defined either by its SOC, accounting for discharging efficiency, or its power rating. The lower value of the two, determines the maximum upward reserve power that can be provided by the BESS. Similarly, the downward reserve constraints are formulated in (3.29)-(3.31).

*BESS Operational Constraints:* The relationship between the charging and discharging power of the BESS and its SOC can be described as follows [97]:

$$-PB_{s,y,h} \ \eta_c - M \ Zd_{s,y,h} \leq SOC_{s,y,h+1} - SOC_{s,y,h} \quad \forall s, \forall y, \forall h; h \neq H \tag{3.32}$$

$$SOC_{s,y,h+1} - SOC_{s,y,h} \leq -PB_{s,y,h} \ \eta_c + M \ Zd_{s,y,h} \quad \forall s, \forall y, \forall h; h \neq H \tag{3.33}$$

$$\frac{-PB_{s,y,h}}{\eta_d} - M\big(Zc_{s,y,h} - Zd_{s,y,h} + 1\big) \leq SOC_{s,y,h+1} - SOC_{s,y,h} \qquad \forall s, \forall y, \forall h; h \neq H \tag{3.34}$$

$$SOC_{s,y,h+1} - SOC_{s,y,h} \leq \frac{-PB_{s,y,h}}{\eta_d} + M\big(Zc_{s,y,h} - Zd_{s,y,h} + 1\big) \qquad \forall s, \forall y, \forall h; h \neq H \tag{3.35}$$

The initial SOC of the BESS is assumed to be 50% of the installed energy capacity, as follows:

$$SOC_{s,y,h} = 0.5 \; E_{BESS_y} \qquad \forall s, \forall y, h = 1 \tag{3.36}$$

The final status of SOC is implemented in the constraints (3.32)-(3.35) by replacing $SOC_{s,y,h+1}$ to the desired level, *i.e.*,

$$SOC_{s,y,h+1} = 0.5 \; E_{BESS_y} \qquad \forall s, \forall y, h = H \tag{3.37}$$

In order to force the binary variables $Zc$ and $Zd$ to be activated during the charging and discharging process in (3.32)-(3.35), and to prevent simultaneous charging and discharging, the following constraints are considered:

$$-M \; Zc_{s,y,h} \leq PB_{s,y,h} \qquad \forall s, \forall y, \forall h \tag{3.38}$$

$$M \; Zd_{s,y,h} \geq PB_{s,y,h} \qquad \forall s, \forall y, \forall h \tag{3.39}$$

$$Zc_{s,y,h} + Zd_{s,y,h} \leq Zp_y \qquad \forall s, \forall y, \forall h \tag{3.40}$$

The BESS power and SOC limits are formulated as follows:

$$(1 - \overline{DOD}) E_{BESS_y} \leq SOC_{s,y,h} \leq E_{BESS_y} \qquad \forall s, \forall y, \forall h \tag{3.41}$$

$$-P_{BESS} \; Zp_y \leq PB_{s,y,h} \leq P_{BESS} \; Zp_y \qquad \forall s, \forall y, \forall h \tag{3.42}$$

*BESS Sizing Constraints:* These constraints ensure that $Z_y$ is only activated once during

the planning horizon, denoting the year of installation, and are given as follows:

$$\sum_{y=1}^{Y_T} Z_y \leq 1 \tag{3.43}$$

To activate $Z_y$ when BESS is installed, the following constraint is considered:

$$P_{BESS} \leq M \sum_{y=1}^{Y_T} Z_y \tag{3.44}$$

The energy capacity of the BESS for a certain power rating, is determined based on its energy to power ratio, as follows:

$$\underline{EPR}\ P_{BESS} \leq NE_{BESS} \leq \overline{EPR}\ P_{BESS} \tag{3.45}$$

*Budget Constraint:* The NPV of the installation cost should not exceed the NPV of the allocated budget for the year,

$$INS \leq B_0 \tag{3.46}$$

The planning problem formulated in (3.6)-(3.46) is a stochastic mixed integer non-linear programming (MINLP) model, and is referred to as Optimal Power and Energy Sizing (OPES) model in the subsequent sections.

## 3.3 Proposed Decomposition Approach

The MINLP model presented in Section 3.2.2 is computationally challenging, because the presence of probabilistic scenarios increases the model dimensionality. In this work, a novel decomposition based approach is proposed, which is demonstrated to provide an optimal solution. The proposed approach comprises two stages, as shown in Figure 3.2, Stage-I determines the BESS power and energy ratings ($P^*_{BESS}$, $E^*_{BESS}$) at the terminal year $Y_T$ by fixing the binary variable $Z_{y=Y_T}$ at unity. In Stage-II, the OPES model is solved with fixed $P^*_{BESS}$, $NE_{BESS_y}$, and $E_{BESS_y}$; the values of $NE_{BESS_y}$, and $E_{BESS_y}$ are obtained from

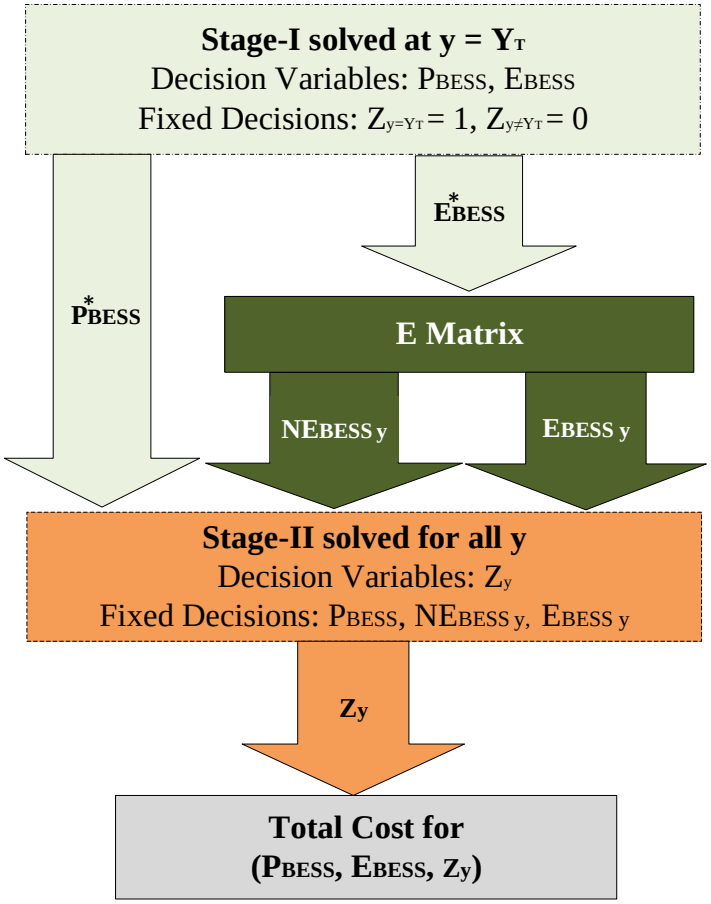


Figure 3.2: Information exchange between the steps in the proposed decomposition approach.

the computation of an $\boldsymbol{E}$ matrix considering BESS energy capacity degradation over its life; to determine the optimal year of installation of the BESS. By fixing certain variables in each of these stages, *i.e.* the BESS ratings and the installation binary variable, the OPES model becomes an MILP model and is computationally much simpler, which can be solved using commercial solvers.

### 3.3.1 Solution Algorithm

The detailed steps of the proposed decomposition approach are shown in Figure 3.3. First, the OPES model determines $P^*_{BESS}$ and $E^*_{BESS}$ at $y = Y_T$. Note that, for a given $B_0$ and $\alpha$, this will result in the installation of a BESS with larger power and energy ratings since the installation cost is discounted to the terminal year. However, although the budget is adequate for a large BESS at $y = Y_T$, its size is optimized considering the BESS effect on microgrid operations.

The $\boldsymbol{E}$ matrix, which will be discussed in Section 3.3.2, is constructed based on the optimal energy capacity determined in Stage-I for the terminal year ($E^*_{BESS}$). This $\boldsymbol{E}$ matrix will be used as input to Stage-II.

Stage-II solves the OPES model considering the entire planning horizon and fixing $P^*_{BESS}$, $NE_{BESS_y}$, and $E_{BESS_y}$. The BESS can either be installed at an earlier year of the planning horizon to incur higher benefits or can be deferred to reduce the NPV of the installation cost. The OPES model in Stage-II determines the optimal year of installation that yields the minimum cost ($C_{ITR}$). If $C_{ITR}$ is less than $C_0$, which is the microgrid's base case cost without any BESS installation, an improved solution is achieved and $C_{ITR}$ is the new $C^{min}$. The budget $BS_{ITR}$ is decremented in the next iteration from the installation cost obtained with $P^*_{BESS}$ and $E^*_{BESS}$ at $y = Y_T$, to achieve lower BESS ratings, with earlier installation times which can result in further reduction in microgrid cost.

Note that the budget limit works as a control for moving the year of installation of the BESS. If budget is not sufficient for BESS installation of a given size, the OPES model defers the year of installation to reduce its NPV and hence meet the budget constraint. Although deferring BESS installation to the end of the planning horizon may

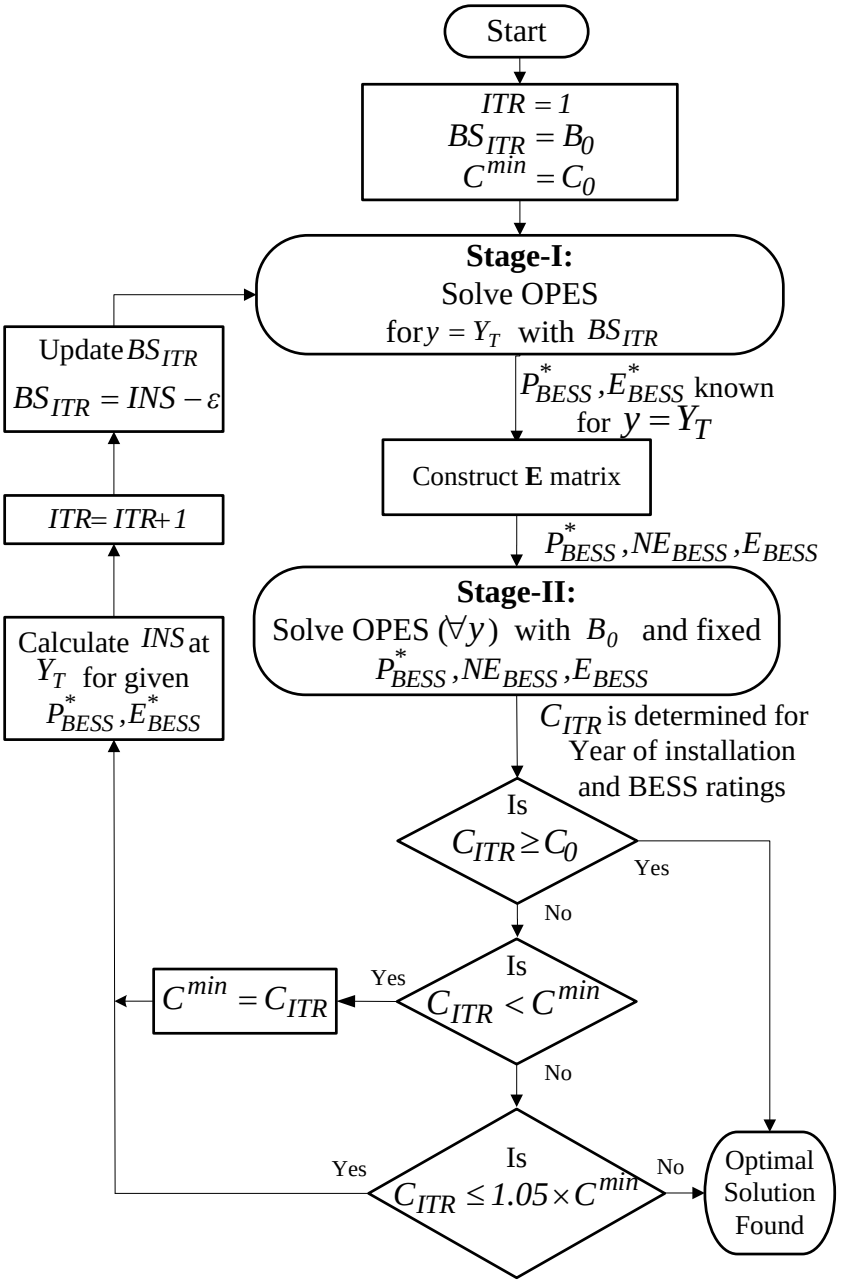


Figure 3.3: Schematic for the decomposition based approach.

allow installing a large BESS, the benefit of installing smaller BESS size earlier might yield a better solution.

Therefore, the BESS size is reduced by tightening the budget constraint to allow installing the BESS at an earlier year. This is performed iteratively by limiting the budget ($BS_{ITR}$) based on the installation cost of the BESS determined in the terminal year minus a small number ($\varepsilon$).

Figure 3.4 demonstrates the functioning of the iterative process as it converges to the optimal solution. The BESS size is determined in iteration $i$, Stage-I at $y = Y_T$, and the $\boldsymbol{E}$ matrix is constructed to ensure the size at the terminal year is the one determined in Stage-I. In Stage-II, the nominal capacity of BESS in a year can only be installed if $INS \leq B_0$. Stage-II determines the optimal year of these possible decisions, and the total cost $C_{ITR}$ for the iteration. In the next iteration, the BESS size in Stage-I is reduced, and the new nominal capacities are obtained from the $\boldsymbol{E}$ matrix which results in a reduction in $INS$, allowing the BESS to be installed at an earlier year.

After each iteration, $C_{ITR}$ is compared with $C^{min}$, the total cost is compared with the previous iteration to update the optimal solution. When the BESS size is reduced beyond the optimal ratings, the total cost in Stage-II again starts increasing, and the optimal size and year can be determined from the plot of $C^{min}$, where it attains a minimum.

The iterative process is terminated when the ratings reach zero, *i.e.* $C_{ITR} = C_0$. Since the total cost increases significantly beyond the optimal point, and to reduce the computation time, the iterative process is terminated when $C_{ITR}$ exceeds a certain percentage of $C^{min}$, *i.e.* 5% of $C^{min}$.

Finding global optimum solution in non-convex and non-linear programming problems cannot be guaranteed. However, the optimal integer solutions in each of the two MILP problems can be determined within acceptable tolerances. To ensure that the optimal solution of the main problem is obtained, the optimal BESS size is determined at the terminal year in Stage-I. Considering the demand growth over the planning horizon, and irrespective of the installation year and the BESS nominal capacities, the terminal year size of BESS should not be greater than the one determined in the first iteration, since a larger size would increase the NPV of BESS installation cost, with less impact on microgrid

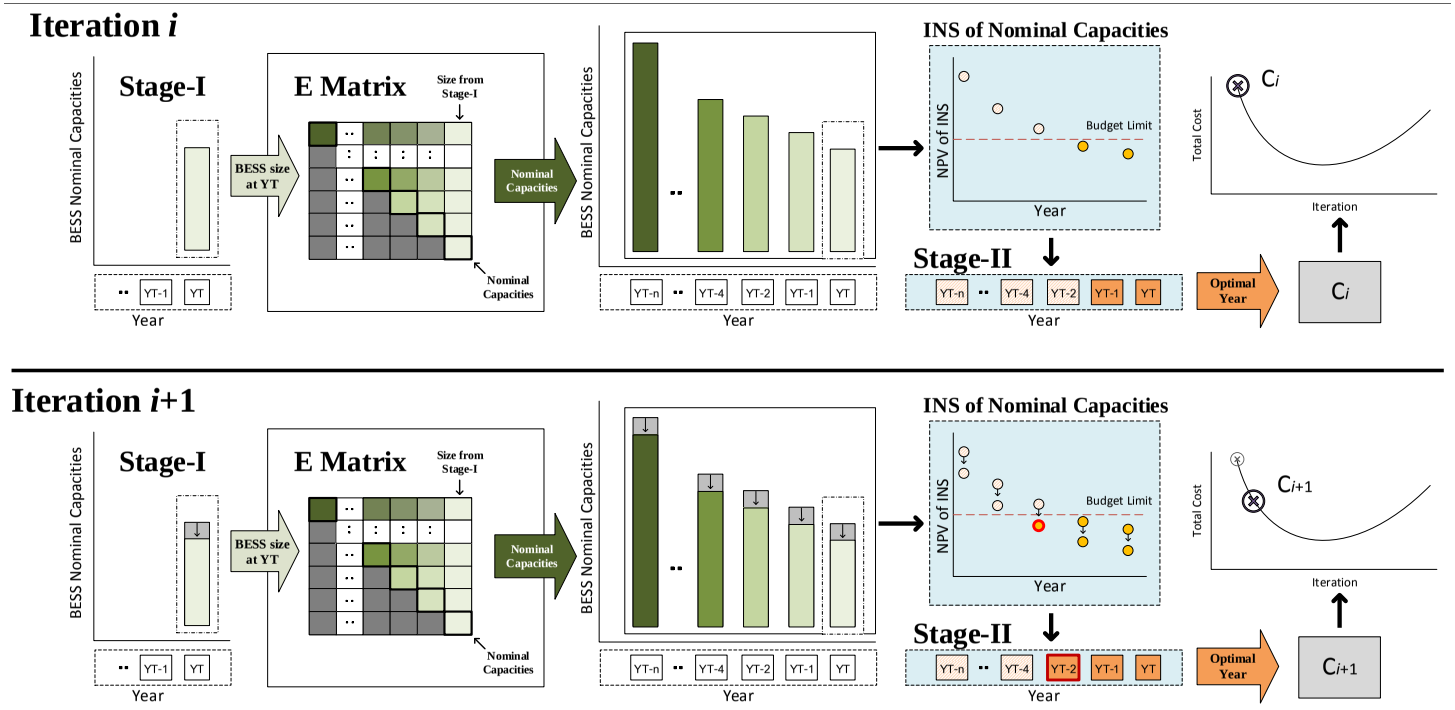


Figure 3.4: Overview of the iterative process in the proposed decomposition based approach.

operation. However, since the ratings determined in the first iteration may not be installed in the initial years because of its high $INS$, hence the optimal solution of the problem might be obtained with lower ratings, but at earlier years. Therefore, the algorithm reduces the BESS size iteratively, and finds the optimal installation year for each size, and stops only when the total cost increases significantly indicating that the solution is beyond the optimal point. It is noted that multiple optima may exist, but the framework is successful in finding these solutions, as will be seen in the results, leaving the choice to the decision maker to select either one.

Consequently, in the proposed approach, the computational burden of the problem is reduced significantly. Since the ratings are fixed in Stage-II, the computational burden is within reasonable limits; however, since the operation of the entire planning horizon is considered, this stage requires more computational time than Stage-I.

### 3.3.2 Energy Capacity Matrix

The energy capacity of BESS determined from the OPES model in Stage-I ($E^*_{BESS}$) for the terminal year is effectively the final degraded capacity at the end of the planning horizon. The BESS energy capacity at preceding years can be determined using the degradation factor and the year of installation. Therefore, a matrix of BESS energy capacities is constructed which ensures the minimum energy capacity at terminal year as the size determined in Stage-I. The energy capacity matrix $\boldsymbol{E}$ is an upper triangular matrix of dimension $Y_T \times Y_T$, and constructed using the following algorithm:

STEP 1: Initiate $\boldsymbol{E} = 0$

STEP 2: Calculate the diagonal elements of $\boldsymbol{E}$ denoting the nominal BESS capacities for different years of installation, as follows:

$$\boldsymbol{E}_{y,y} = \begin{cases} \dfrac{E^*_{BESS}}{1-\sigma(Y_T - R_Y - y)} & ; y = 1, ..., Y_T - R_Y \\ \dfrac{E^*_{BESS}}{1-\sigma(Y_T - y)} & ; y = Y_T - R_Y + 1, ..., Y_T \end{cases} \tag{3.47}$$

STEP 3: Round up the $\boldsymbol{E}_{y,y}$ elements to the next standard BESS size.

STEP 4: Calculate the off-diagonal elements $\boldsymbol{E}_{y,y'}$. For a given year in the $\boldsymbol{E}$ matrix, *i.e.*, for a given value of $y$, the elements of the row denote the degraded energy capacities over the time horizon,

$$\boldsymbol{E}_{y,y'} = \begin{cases} \boldsymbol{E}_{y,y}\big[1-\sigma(y'-y)\big] & ;y' = y,...,y+R_Y-1 \\ \\ \boldsymbol{E}_{y,y}\big[1-\sigma(y'-y-R_Y)\big] & ;y' = y+R_Y,...,Y_T \end{cases} \tag{3.48}$$

where $y = 1,...,Y_T - R_Y$.

$$\boldsymbol{E}_{y,y'} = \boldsymbol{E}_{y,y}\big[1-\sigma(y'-y)\big] \quad ;y' = y,...,Y_T \tag{3.49}$$

where $y = Y_T - R_Y + 1,...,Y_T$. It is noted that when $R_Y$ is larger than $Y_T$, the second part of (3.47) in addition to (3.49), are used to obtain the elements of the $\boldsymbol{E}$ matrix for all $y$.

After constructing the $\boldsymbol{E}$ matrix, a year index is added to $NE_{BESS}$ in the OPES model in Stage-II and $NE_{BESS_y}$ is obtained from $\boldsymbol{E}$, as follows:

$$NE_{BESS_y} = \boldsymbol{E}_{y,y} \qquad ;\forall y \tag{3.50}$$

And the BESS energy capacity at a given year, considering its degradation, is given as follows:

$$E_{BESS_y} = \sum_{y'=1}^{Y_T} (Z_{y'}\ \boldsymbol{E}_{y',y}) \qquad ;\forall y \tag{3.51}$$

## 3.4 Uncertainty Modeling

The proposed framework considers the uncertainty of load, PV, and wind generation using the MCS and scenario-based stochastic optimization, discussed in Section 2.5. The random parameters are modeled at each hour considering a normal pdf. The mean of the normal pdf at each hour can be obtained using a suitable forecasting technique based on the

microgrid historical data. The seasonality impact can also be considered by dividing the data into different seasons and obtain the hourly average of each representative day.

### 3.4.1 Monte Carlo Simulations

The MCS with LHS technique, discussed in Section 2.5.1, is implemented in both stages of the proposed approach, and in each iteration. In Stage-I, after the scenarios are generated, the optimal BESS ratings are determined by solving the OPES model for each scenario at $Y_T$. Thereafter, one value each of $P^*_{BESS}$ and $E^*_{BESS}$ is selected in the given iteration, based on the size that has the highest probability across all the scenarios, and the $\boldsymbol{E}$ matrix is constructed based on that size. The MCS is implemented again and new scenarios are generated in Stage-II to determine the optimal year for each scenario. Similarly, the optimal year of installation is the year that has the highest probability across the scenarios. The proposed framework continues to the next iteration and in each stage and iteration new scenarios are generated.

### 3.4.2 Scenario-based Stochastic Optimization

In the scenario-based stochastic optimization, several scenarios of load, PV, and wind generation are considered at each hour. In contrast to the MCS method discussed above, the stochastic optimization model considers a set of scenarios and determines the optimal plan based on the expected objective function in one run.

The uncertainty model used in [38] and [98] are considered in this work to generate the scenarios of load, PV, and wind generation at each hour. Each of these random parameters is represented using several discrete states of uncertainty, selected considering the normal pdf of these parameters; the forecasted value is the mean with with the highest probability and the other states representing the deviation from the mean with smaller probabilities. It is assumed that hourly variation of the parameters are independent, and hence the total number of scenarios at an hour is the combination of all parameters with their states, while the probability of a given scenario can be obtained by multiplying the probability of each state. Increasing the number of states of each random parameter improves the

Table 3.1: PDF of the Uncertain States

| | Demand | Probability | Wind | Probability | PV | Probability |
|---|---|---|---|---|---|---|
| High State | +6% | 0.2 | +6% | 0.25 | +4% | 0.15 |
| Forecasted Value | Nominal | 0.6 | Nominal | 0.5 | Nominal | 0.7 |
| Low State | -6% | 0.2 | -6% | 0.25 | -4% | 0.15 |

accuracy; however, the total number of scenarios at each hour increases exponentially with the number of states.

In the present work, the load, PV, and wind generation are each represented by three states each, their hourly forecasted values are shown in Table 3.1. Therefore, there are a total of 27 scenarios at each hour. The 24-hour profile of each parameter is constructed assuming that a given scenario remains fixed over 24 hours. Therefore, a total of 27 daily profiles of load, PV, and wind generation are constructed, which comprises various combinations of their scenarios.

The operational variables of BESS and other microgrid resources for a simulated day are obtained sequentially on an hour-by-hour basis, and are independent for each scenario. However, the optimal plan decisions in the stochastic optimization model are unique over the entire range of scenarios of uncertainty, and not scenario dependent unlike MCS.

## 3.5 Results and Discussions

### 3.5.1 Test System

The CIGRE microgrid benchmark test system in [88] is used to determine the optimal BESS plan using the proposed decomposition based approach. The dispatchable DG units in the microgrid are three diesel generators, one CHP diesel, and one CHP microturbine with capacities of 2,500 kW, 1,400 kW, 800 kW, 310 kW, and 500 kW, respectively, and hence a total capacity of 5,510 kW. The total installed PV capacity is 840 kW, and wind capacity is 1,450 kW.

The planning period in the case studies is 10 years. Forecasted demand and RES generation profiles, that includes wind and solar PV, for three days representing Summer,

Table 3.2: BESS Performance and Cost Parameters

| BESS Type | $Cp^v$ ($/kW) | $Ce^v$ ($/kWh) | $OMC^f$ ($/kW-y) | $OMC^v$ ($/Wh) | $RC$ ($/kW) | $R_Y$ ($y$) | $\sigma$ | $\eta_c$,$\eta_d$ | $\overline{DOD}$ | $EPR$ |
|---|---|---|---|---|---|---|---|---|---|---|
| NaS | 757 | 372 | 9.2 | 0.8 | 0 | 15 | 1.3% | 87% | 80% | 6-8 |
| VRB | 2133 | 880 | 16.5 | 1.6 | 720 | 8 | 2.5% | 83% | 100% | N/A |
| PbA | 1407 | 275 | 26.8 | 1.1 | 375 | 8 | 2.5% | 95% | 80% | 1-5 |
| Li-ion | 1859 | 901 | 13.2 | 1.4 | 1560 | 5 | 4% | 95% | 100% | 1-4 |

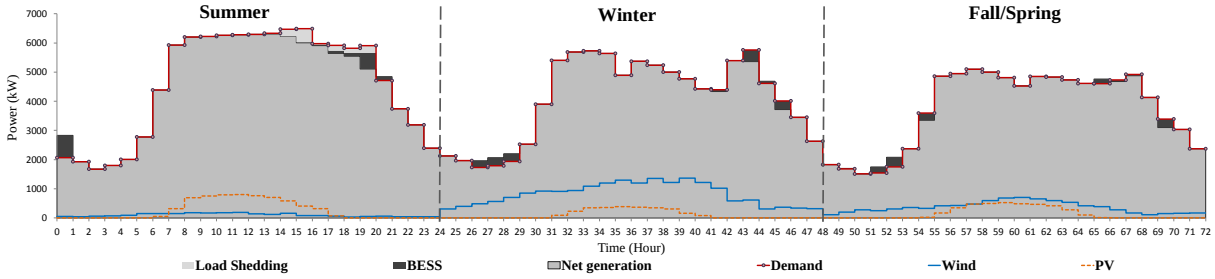


Figure 3.5: Supply and demand mix in year-10, in deterministic case (PbA BESS).

Winter and Fall/Spring seasons, are inputs to the model. The peak demand of the microgrid in the first year is 5,430 kW, and is assumed to increase annually by 2%. The fuel cost is considered to increase by 3% every year. The discount rate considered in the planning is 8%.

The microgrid is required to maintain an operating reserve equivalent to 10% of its hourly demand plus a certain fraction of the forecasted RES generation and demand, to account for forecasting errors. The forecasting error parameters $\delta_D$, $\delta_{PV}$, and $\delta_W$ are assumed to be 3%, 9%, 13%, respectively [40].

Four BESS technologies are examined, NaS, VRB, PbA, and Li-ion BESS. The performance and cost parameters of different BESS technologies, shown in Table 3.2, are taken from [9]. The fixed installation cost, applicable to all technologies, is assumed to be $20,000. The maximum $P_{BESS}$ and $E_{BESS}$ is assumed as 6,500 kW and 6,500 kWh, respectively, and the options are considered to be available in multiples of 50 kW and 50 kWh, respectively. A budget limit of $B_0$ = $1.4 million is considered to demonstrate the functioning of the proposed decomposition algorithm.

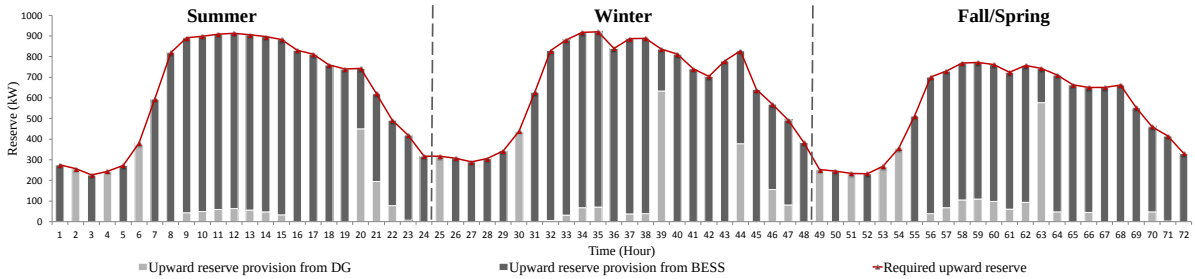


Figure 3.6: Reserve provisions in year-10, in deterministic case (PbA BESS).

### 3.5.2 Deterministic Case Study

A deterministic case study is carried out considering the forecasted profiles of demand, solar, and wind generation, as shown in Figure 3.5 for year-10, for Summer, Winter and Fall/Spring. From the optimal BESS decisions presented in Table 3.3, it is noted that PbA BESS yields the lowest cost, and its optimal design is $P_{BESS} = 850$ kW and $E_{BESS} = 1{,}450$ kWh, and installation in year-2. Note also that, there is always a reduction in the total cost with BESS installation from the case with no BESS, when the cost $C_0$ is \$56,166,054.

The overall operation of the BESS and its impact on microgrid operation follows almost the same pattern, irrespective of the technologies. Therefore, for the sake of conciseness, the operation of PbA BESS is highlighted in Figure 3.5, which presents the supply-demand balance, and Figure 3.6 shows the reserve requirements. The net generation represents the demand supplied by dispatchable DG units and RES, *i.e.*, the power drawn to charge the BESS is excluded.

### 3.5.3 MCS Case Study

The optimal BESS decisions are obtained using the MCS method discussed in Section 3.4.1. At each stage, the decisions are obtained for 100 scenarios generated randomly.

It is noted that the decisions in this case are exactly the same as the deterministic case. However, the cost presented in Table 3.3 for the MCS case is the expected cost, and hence, the small differences of costs in both cases are because of the several scenarios used to determine the expected cost in the MCS case.

Table 3.3: BESS Optimal Plan Decisions

| | BESS Type | Year | $P_{BESS}$ (kW) | $E_{BESS}$ (kWh) | $INS$ ($) | $OM$ ($) | $MGOC$ ($) | Total Costs ($) |
|---|---|---|---|---|---|---|---|---|
| **Deterministic** | NaS | 4 | 550 | 3300 | $1,305,082 | $21,660 | $54,421,319 | $55,748,061 |
| | VRB | 4 | 550 | 650 | $1,394,462 | $38,625 | $54,475,280 | $55,908,367 |
| | PbA | 2 | 850 | 1450 | $1,384,345 | $293,394 | $51,317,375 | $52,995,114 |
| | Li-ion | 4 | 650 | 700 | $1,399,570 | $584,375 | $53,573,638 | $55,557,583 |
| **MCS** | NaS | 4 | 550 | 3300 | $1,305,082 | $22,431 | $54,427,185 | $55,754,698 |
| | VRB | 4 | 550 | 650 | $1,394,462 | $38,091 | $54,492,645 | $55,925,198 |
| | PbA | 2 | 850 | 1450 | $1,384,345 | $293,353 | $51,376,317 | $53,054,015 |
| | Li-ion | 4 | 650 | 700 | $1,399,570 | $584,289 | $53,619,161 | $55,603,020 |
| **Stochastic** | NaS | 3 | 500 | 3000 | $1,305,616 | $23,529 | $55,918,075 | $57,247,220 |
| | VRB | 4 | 550 | 650 | $1,394,462 | $38,630 | $55,960,639 | $57,393,731 |
| | PbA | 1 | 800 | 1200 | $1,379,028 | $308,203 | $52,082,974 | $53,770,205 |
| | Li-ion | 2 | 550 | 550 | $1,395,833 | $584,129 | $54,788,552 | $56,768,514 |

The optimal decisions at each stage are selected based on the solution that has the highest probability across all scenarios. For example, Figure 3.7 shows a histogram of the BESS energy capacities determined for the 100 scenarios in iteration 7, when the least cost ($C^{min}$) ia attained for PbA BESS, while Figure 3.8 shows the power ratings for the same iteration. The energy capacity of 1,450 kWh is selected as the optimal solution for 64% of the scenarios, whereas the next highest probability is only 0.18 for the capacity of 1,200 kWh. Similarly, since 850 kW is selected in 90% of the scenarios, it is considered the optimal solution in this iteration. In Stage-II, the same method is used to select the optimal year. It is found that the optimal year of installation, for the ratings of 850 kW and 1,450 kWh, is year 2 for all the generated scenarios. The expected total cost is $53,054,015.

It is worth mentioning that in Figure 3.7 and Figure 3.8, the solutions are clearly concentrated in specific values for a major share of the scenarios, and hence, the number of scenarios are sufficient to determine the optimal solution.

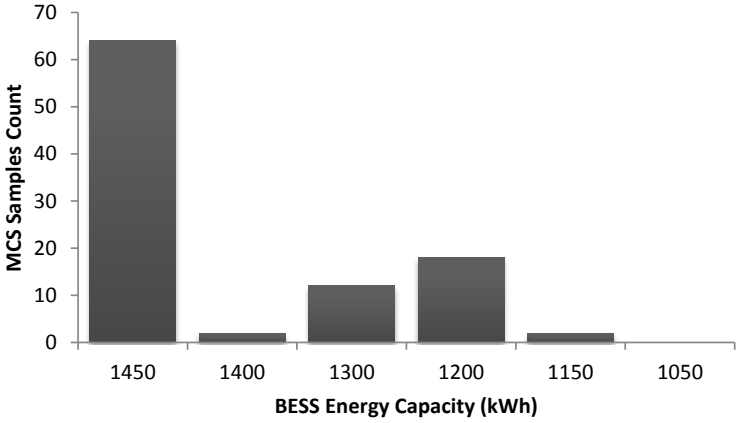


Figure 3.7: Histogram of the optimal PbA BESS energy capacities in iteration 7 for MCS.

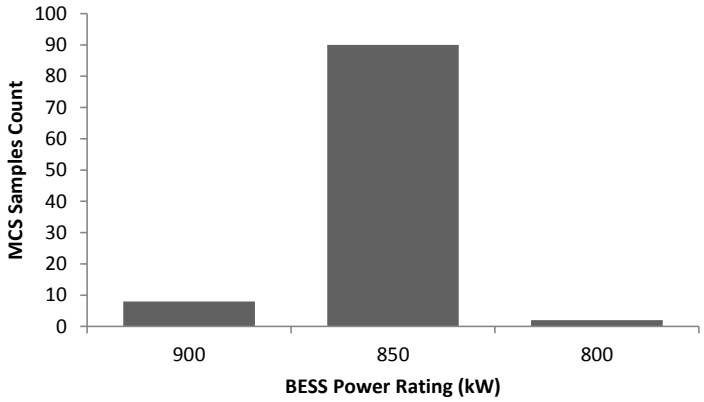


Figure 3.8: Histogram of the optimal PbA BESS power ratings in iteration 7 for MCS.

### 3.5.4 Stochastic Case Study

The stochastic optimal BESS decisions considering the set of probabilistic scenarios are presented in Table 3.3. It is noted that here too, PbA BESS accrues the least cost, and is the BESS technology of choice, with optimal $P_{BESS}$ = 800 kW and $E_{BESS}$ = 1,200 kWh, and optimal installation in year-1. The total *expected cost* before installing the BESS, $C_0$, is \$66,469,843 which is reduced by 13.87%, 13.65%, 19.11%, and 14.6%, after installing the respective optimal sizes of NaS, VRB, PbA, and Li-ion BESS, at the optimal years. The total cost in the stochastic cases are greater than those in the deterministic and MCS cases because of the presence of scenarios of high demand and low RES generation inherently in the optimization model which increases the microgrid operational cost. Accordingly, earlier installation of BESS with smaller ratings is noted in the stochastic case to compensate for the increase in the operational cost.

To discuss the functioning of the proposed decomposition algorithm, the cases of NaS and PbA are highlighted. It is noted that the optimum BESS ratings at the end of the first iteration are, for NaS, $P_{BESS}$ = 950 kW and $E_{BESS}$ = 5,700 kWh in year-10; while for PbA, are $P_{BESS}$ = 900 kW and $E_{BESS}$ = 1,700 kWh, in year-4. The NPV of the installation cost of the NaS BESS is above $B_0$ until year-9, and hence the BESS can only be installed in year-10. On the other hand, for PbA BESS, it is greater than $B_0$ until year-3, and hence this BESS can be installed in year-4. But since a better solution can exist at lower BESS sizes and earlier installation years, the proposed algorithm updates the budget $BS_{ITR}$ in the next iteration, to less than $INS$ (\$1,324,524) at terminal year for NaS and below \$812,349, for the PbA BESS; and revises the optimal BESS size. In the second iteration, $P_{BESS}$ and $E_{BESS}$ are reduced by 50 kW and 300 kWh, respectively, for NaS BESS, with installation year advanced to year-9; while for PbA BESS the size is reduced by 50 kWh but the installation year remains unchanged at year-4.

It is noted from Table 3.4, and as shown in Figure 3.9 and Figure 3.10 that, as the installation year progresses closer to the optimal year, the total cost reduces. For the same installation year, more cost reduction is achieved with a larger BESS rating, such as in the case of NaS BESS, iteration 3 and 7, and of PbA BESS, in iterations 8-12. The breaks in the plot of the total cost for PbA BESS (Figure 3.10) and hence the significant cost

Table 3.4: Convergence of BESS Plan Decisions: Stochastic Case

| | ITR | 1 | 2 | 3 | 4 | 5 | 6 | 7 | 8 | 9 | 10 | 11 | 12 | 13 | 14 | 15 |
|---|---|---|---|---|---|---|---|---|---|---|---|---|---|---|---|---|
| NaS BESS | $BS_{ITR}$ | $1,400,000 | $1,324,524 | $1,255,300 | $1,186,076 | $1,116,852 | $1,047,627 | $978,403 | $909,179 | $839,955 | **$770,731** | $701,506 | $632,282 | $563,058 | $493,833 | $424,609 |
| | $P_{BESS}$ | 950 | 900 | 850 | 800 | 750 | 700 | 650 | 600 | 550 | **500** | 450 | 400 | 350 | 300 | 250 |
| | $E_{BESS}$ | 5700 | 5400 | 5100 | 4800 | 4500 | 4200 | 3900 | 3600 | 3300 | **3000** | 2700 | 2400 | 2100 | 1800 | 1500 |
| | Year | 10 | 9 | 9 | 8 | 7 | 6 | 6 | 5 | 4 | **3** | 2 | 2 | 1 | 1 | 1 |
| | Total Cost | $65,187,480 | $62,924,474 | $63,001,595 | $61,051,689 | $59,430,184 | $58,181,217 | $58,521,002 | $57,750,936 | $57,303,034 | **$57,247,220** | $57,517,612 | $58,118,384 | $58,734,187 | $59,492,278 | $60,462,751 |
| PbA BESS | $BS_{ITR}$ | $1,400,000 | $812,349 | $805,980 | $799,611 | $793,242 | $786,873 | $780,504 | $747,919 | $741,550 | $728,812 | $722,443 | $716,074 | **$709,705** | $683,488 | $677,119 |
| | $P_{BESS}$ | 900 | 900 | 900 | 900 | 900 | 900 | 850 | 850 | 850 | 850 | 850 | 850 | **800** | 800 | 800 |
| | $E_{BESS}$ | 1700 | 1650 | 1600 | 1550 | 1500 | 1450 | 1450 | 1400 | 1300 | 1250 | 1200 | 1150 | **1200** | 1150 | 1100 |
| | Year | 4 | 4 | 4 | 4 | 4 | 4 | 2 | 2 | 2 | 2 | 2 | 2 | **1** | 1 | 1 |
| | Total Cost | $54,668,981 | $54,623,475 | $54,641,124 | $54,608,795 | $54,649,904 | $54,645,627 | $53,856,208 | $53,842,229 | $53,976,133 | $54,008,142 | $54,119,665 | $54,207,017 | **$53,770,205** | $53,876,794 | $53,920,273 |

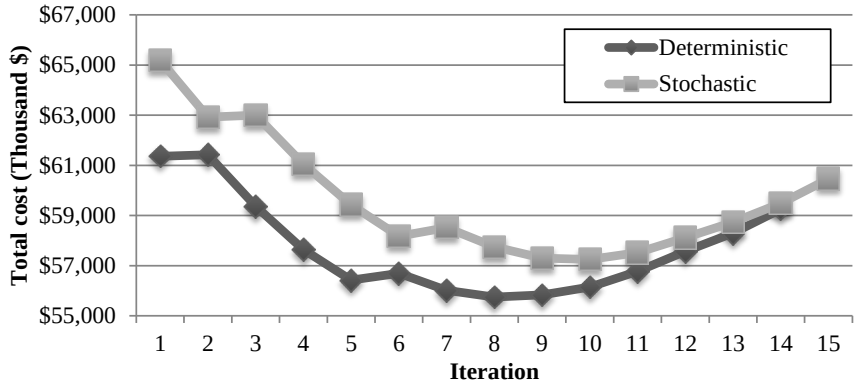


Figure 3.9: Total cost for different NaS BESS installation decisions.

reduction in iterations 7 and 13, are because of the changes in the year of installation to an earlier year.

The algorithm converges after 15 iterations for NaS, and after 31 iterations for PbA, as shown in Figure 3.9 and Figure 3.10, when $C_{ITR}$ is 5.6% and 5.9% of $C^{min}$, respectively. Although an increase in cost is observed in previous iterations, it does not exceed 5% of $C^{min}$, and hence the iterative process is not terminated. For example, in iteration 3 of NaS BESS, $C^{min}$ is $62,924,474, which is determined from iteration 2, and the increase from that value in iteration 3 is only 0.1%. In PbA BESS case, in iteration 12, $C^{min}$ determined from iteration 6 is $53,856,208, and the increase in iteration 12 is only 0.7%.

Figure 3.9 and Figure 3.10 also show the variation in total cost in the deterministic case. The results of MCS are exactly the same as the deterministic case and the variation of cost is also similar, and hence only the deterministic and stochastic cases are presented in Figure 3.9 and Figure 3.10.

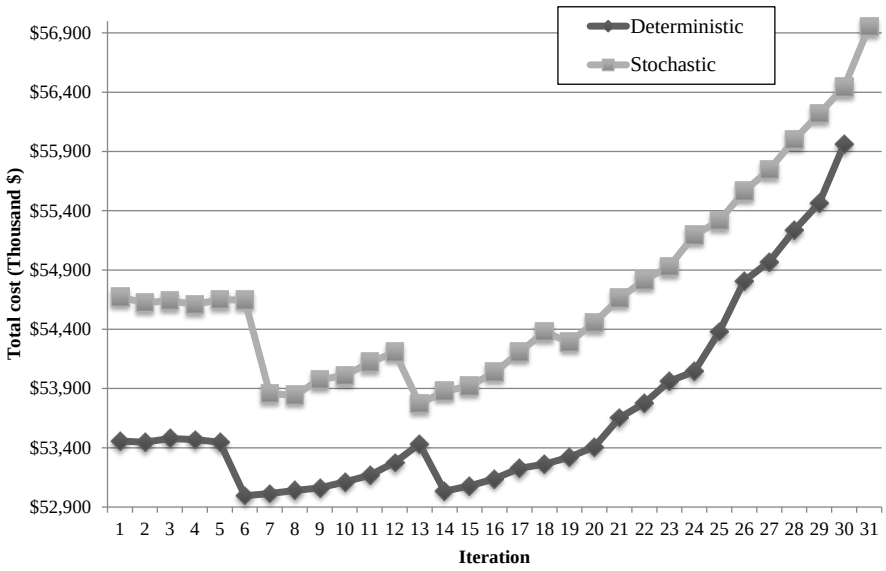


Figure 3.10: Total cost for different PbA BESS installation decisions.

### 3.5.5 Analysis of Different Operational Scenarios

It is noted from Figure 3.9, Figure 3.10, and Table 3.3 that the total cost in the deterministic case studies are always lower than the expected costs in MCS and stochastic case studies. However, the stochastic optimal solution is obtained considering numerous scenarios of possible inputs, and hence the decisions are more robust and close to what can be realistically expected in actual. The deterministic solution depends wholly on the chosen input data for that case study. So, for all practical purposes, the stochastic optimal results are more realistic, unless and until the deterministic case inputs are very precise forecasts and there is very little deviation from the forecast inputs in real life. Note that the total cost of the deterministic case is computed considering the forecasted values, while the stochastic case computes the expected total cost considering several scenarios.

The expected cost is also larger in MCS compared to the deterministic case because of the presence of scenarios with high load and low RES. However, these scenarios have no impact on the optimal solutions since the highest probability solutions are selected in each

iteration; whereas in the stochastic optimization approach all scenarios are considered in determining the optimal solution.

In this section, the decisions of the stochastic and deterministic case studies are evaluated using three scenarios, as follows:

- *Scenario 1- Perfect Forecast*: load, PV, and wind generation are exactly the same as their hourly mean values.
- *Scenario 2- Pessimistic Profiles*: load is 6% higher than the mean, while PV and wind generation are lower than their mean values by 4% and 6%, respectively.
- *Scenario 3- Optimistic Profiles*: load is 6% lower than the mean, while PV and wind generation are higher than their mean values by 4% and 6%, respectively.

Table 3.5 shows the total cost for the considered operational scenarios, when installing BESS using stochastic and deterministic optimal plans. The differences between the two cases are also presented. Note that the total cost presented in Table 3.5 for the stochastic case studies is not the expected cost but the actual deterministic cost considering the profiles of the corresponding scenario and using the stochastic planning decisions presented in Table 3.3.

It is observed that in Scenario-1 and Scenario-3, the deterministic plans always achieve lower cost than the stochastic plans, excluding in Scenario-3 with PbA BESS. However, the differences are small compared to the tremendous savings achieved by the stochastic plans in the pessimistic scenario, Scenario-2. This shows the significance of considering the stochastic models despite their computational challenges.

### 3.5.6 Impact of Degradation

As mentioned in the literature, several papers have addressed the problem of optimal sizing of BESS in microgrids. However, most of the papers do not integrate BESS energy capacity degradation in the operational and planning models. The importance of

Table 3.5: Analysis of Different Operational Scenarios

| BESS Type | Model | Scenario-1 | Scenario-2 | Scenario-3 |
|---|---|---|---|---|
| NaS | Stochastic | $55,838,204 | $70,804,012 | $47,901,641 |
| | Deterministic | $55,748,061 | $71,489,768 | $47,811,027 |
| | Difference | $90,143 | -$685,756 | $90,614 |
| VRB | Stochastic | $55,908,367 | $71,642,717 | $47,988,618 |
| | Deterministic | $55,908,367 | $71,642,717 | $47,988,618 |
| | Difference | - | - | - |
| PbA | Stochastic | $53,113,343 | $62,165,248 | $47,578,992 |
| | Deterministic | $52,995,114 | $62,485,189 | $47,618,478 |
| | Difference | $118,229 | -$319,941 | -$39,486 |
| Li-ion | Stochastic | $55,641,603 | $68,898,113 | $48,399,201 |
| | Deterministic | $55,557,583 | $70,228,068 | $48,305,775 |
| | Difference | $84,020 | -$1,329,955 | $93,426 |

modeling the BESS energy capacity degradation proposed in this work is highlighted in this section. Considering degradation requires installing larger BESS ratings to achieve sufficient BESS capacity at the terminal year when the microgrid demand is highest, considering demand growth. The optimal ratings are also affected by the year of installation since earlier installation means larger degradation of the capacity and lower size at the terminal year. In contrast, when ignoring degradation, the installed size is independent of the installation year since the size remains unchanged after installation. Considering the scenario of forecasted profiles, *i.e.* the deterministic case study, and assuming the degradation factor is zero for all BESS technologies, the new optimal results, without considering degradation, are presented in Table 3.6. It is noted that NaS and Li-ion BESS decisions are not affected by considering the degradation. However, the installation year is advanced to year 2 for VRB BESS and smaller ratings are obtained, while the installation year remains unchanged for PbA BESS but with smaller ratings. In Table 3.6, the objective function is the total cost obtained from the optimization model considering no degradation. However, this cost is not the true cost since it does not take into account the degradation in BESS energy capacity. The true cost is computed by

Table 3.6: Optimal Plan Decisions without Considering Degradation

| BESS Type | NaS | VRB | PbA | Li-ion |
|---|---|---|---|---|
| $P_{BESS}$ | 550 | 500 | 850 | 650 |
| $E_{BESS}$ | 3300 | 600 | 1400 | 700 |
| Year | 4 | 2 | 2 | 4 |
| Objective Function | \$55,659,738 | \$55,726,162 | \$52,836,670 | \$54,894,481 |
| True Cost | \$55,748,061 | \$56,648,057 | \$53,041,158 | \$55,557,583 |

solving the OPES model with fixing all the decisions ($P_{BESS}$, $E_{BESS}$, year of installation) and considering degradation in $E_{BESS}$ starting from its installation. The true cost of the decisions without considering the degradation can be compared with the deterministic results, obtained considering degradation, presented in Table 3.3. It is noted that additional costs are observed when decisions are optimized without considering the capacity degradation. The additional cost is \$739,690 and \$46,044 for VRB and PbA BESS, respectively.

### 3.5.7 Computational Aspects

The original stochastic planning model of BESS, which is an MINLP model (presented in Section 3.2.2) was considered, along with the presence of probabilistic scenarios, in a multi-year inter-temporal planning horizon. The model was executed in several GAMS based MINLP solvers and failed to yield a solution, because of the model dimensionality. This exercise was carried out prior to developing the decomposition based approach, and was the main motivation for this work.

The OPES model in the decomposition appraoch is formulated as an MILP problem and solved in GAMS using the CPLEX solver. The solver uses branch and cut algorithm in which the main problem is divided into linear programming sub-problems [99]. The integer optimal solution is obtained in the two stages by setting the optimality gap to 3%.

The framework is executed on a server with 4 Intel-Xeon 1.87 GHz processors and 64 GB of RAM. The computation times per iteration are presented in Table 3.7. Note that the

Table 3.7: Average Computation Time

| | BESS Type | Deterministic (sec) | MCS (sec/simulation) | Stochastic (hrs) |
|---|---|---|---|---|
| **Stage-I** | NaS | 4 | 6 | 0.22 |
| | VRB | 5 | 6 | 0.38 |
| | PbA | 6 | 9 | 0.33 |
| | Li-ion | 4 | 6 | 0.30 |
| **Stage-II** | NaS | 54 | 53 | 2 |
| | VRB | 80 | 96 | 12 |
| | PbA | 119 | 154 | 5 |
| | Li-ion | 88 | 103 | 9 |

computing time in MCS is relatively similar to the deterministic case, however, the total time depends on the number of simulations performed, *e.g.* 100 scenarios are performed in this case study.

Across all the BESS technologies, the average computational time for the two stages in the deterministic case is 1.62 minutes per iteration. On the other hand, in the stochastic case, the average computational time for Stage-I is about 19 minutes, and about 7 hours for Stage-II, per iteration. Although the computational time in the stochastic case is significantly larger than the deterministic and MCS cases, since the problem is a long-term planning study, fast computation is not the main criterion, and obtaining more reliable results is more important.

## 3.6 Summary

In this chapter, a decomposition-based approach was proposed to determine the optimal year of installation and sizing of BESS in isolated microgrids. Uncertainties in demand and RES generation was considered, which yielded a comprehensive stochastic optimization model, that was computationally large. The proposed decomposition approach determined the optimal plan decisions in two stages. Energy capacity degradation was considered in a novel manner and implemented in Stage-II as a matrix of all possible capacities.

The budget limit affected the solution and did not allow installing a large BESS early. Therefore, the budget constraint was relaxed to ensure the optimal sizing decision, which was then imposed on the model in steps, until arriving at the optimal size and year of installation. Three case studies were conducted to highlight the optimal BESS decisions using deterministic optimization and by considering uncertainty using MCS and scenario-based stochastic optimization.

The proposed BESS planning framework was envisaged to be used by the microgrid community planners, the utility serving the microgrid, or governmental, non-governmental, and private agencies involved in planning, design, and development of microgrid EMS when the BESS was installed and operated by the MGO. The objective of this study was to minimize the operational and investment costs of BESS, and hence the results of this work were specific for the considered case studies and test systems. Other criteria to evaluate ESS investments might examine the cost data of different ESS technologies in power system applications, and hence determine the benefit break-even of these facilities [100].

# Chapter 4

# Third-Party Investment Planning in Battery Energy Storage Systems[1]

In this chapter, investment decisions on BESS installations by a third-party investor in a grid-connected microgrid is studied. The optimal BESS power rating, energy capacity, and the year of installation are determined while maximizing the investor's profit and simultaneously minimizing the grid-connected microgrid operational cost. A bi-objective optimization problem, referred to as "multi-objective" in this thesis, is solved using a goal programming approach with a weight assigned to each objective. The BESS is modeled to participate in energy arbitrage and provision of operating reserves in the microgrid. The BESS performance parameters are considered, and its capacity degradation over the planning horizon is modeled.

[1]This chapter has been published in:

- H. Alharbi, and K. Bhattacharya, "An Optimal Investment Model for Battery Energy Storage Systems in Isolated Microgrids," in *Advances in Energy System Optimization*, Springer Publishing, pp. 105-121, 2017.
- H. Alharbi, and K. Bhattacharya, "A Goal Programming Approach to Sizing and Timing of Third Party Investments in Storage System for Microgrids," in *Proc. IEEE Electrical Power and Energy Conference (EPEC)*, Toronto, ON, 2018, pp. 1-6.

## 4.1 Nomenclature

### *Indices*

| | |
|---|---|
| $h$ | Index for hours, $h = 1, 2, .., H$ |
| $i$ | Index for dispatchable DG units, $i = 1, 2, .., I$ |
| $y$ | Index for years, $y = 1, 2, .., Y_T$ |

### *Parameters*

| | |
|---|---|
| $B_0$ | NPV of budget allocation [$] |
| $C_0$ | Total microgrid operational cost with no BESS installed [$] |
| $C^f$ | Fixed installation cost of BESS [$] |
| $C^{SHED}$ | Cost of load shedding [$/kWh] |
| $Ce^v$ | Variable installation cost of BESS associated with energy capacity [$/kWh] |
| $Cp^v$ | Variable installation cost of BESS associated with power rating [$/kW] |
| $\overline{DOD}$ | Maximum depth of discharge [%] |
| $\overline{EPR}$,$\underline{EPR}$ | Maximum/minimum energy to power ratio |
| $G_i, L_i$ | Initial up-time and down-time required of DG unit $i$ [h] |
| $Min_i^{DW}$ | Minimum down-time of DG unit $i$ [h] |
| $Min_i^{UP}$ | Minimum up-time of DG unit $i$ [h] |
| $OMC^f$ | Yearly fixed O&M cost of BESS [$/kW-year] |
| $OMC^v$ | Variable O&M cost of BESS [$/kWh] |
| $\overline{P}_i$ | Maximum output power of DG unit $i$ [kW] |
| $\underline{P}_i$ | Minimum output power of DG unit $i$ [kW] |
| $\overline{PSS}$ | Maximum substation power limit [kW] |
| $Pd$ | Forecasted demand of isolated microgrid [kW] |
| $PV$ | Forecasted PV generation [kW] |
| $Pw$ | Forecasted wind generation [kW] |

| | |
|---|---|
| $Ramp_i^{DW}$ | Ramp down limit of DG unit $i$ [kW] |
| $Ramp_i^{UP}$ | Ramp up limit of DG unit $i$ [kW] |
| $RC$ | Replacement cost of BESS [$/kW] |
| $R_Y$ | Replacement year of BESS |
| $SD_i$, $SU_i$ | Shut-down and start-up cost of DG unit $i$ [$] |
| $M$ | Large number |
| $\alpha$ | Investor's minimum acceptable rate of return [%] |
| $\beta$ | MGO's discount rate [%] |
| $\gamma$ | Fuel cost escalation rate [%] |
| $\delta_D$,$\delta_{PV}$,$\delta_W$ | Error in forecasted demand, PV and wind [%] |
| $\eta_c$, $\eta_d$ | BESS charging/discharging efficiency [%] |
| $\vartheta$ | Minimum reserve as percentage of demand (%) |
| $\rho^E$ | Forecasted energy price [$/kWh] |
| $\rho^{res}$ | Forecasted reserve provisions price [$/kW] |
| $\sigma$ | BESS energy capacity degradation factor [%] |
| $w$ | Weight assigned for the multi-objective function |

## *Variables*

| | |
|---|---|
| $E_{BESS}$ | Energy capacity of storage system [kWh] |
| $INS$ | NPV of installation cost of storage system [$] |
| $OC^{MG}$ | NPV of microgrid operational cost [$] |
| $OM^S$ | NPV of O&M cost of storage system [$] |
| $P$ | DG output [kW] |
| $P_{BESS}$ | Power rating of storage system [kW] |
| $PB$ | Storage system power; negative when charging, and positive when discharging [kW] |
| $P^{Grid}$ | Power exchange with the main grid [kW] |
| $Pd^{SHED}$ | Load shedding [kWh] |
| $R$ | Total required reserve capacity [kW] |

| | |
|---|---|
| $R^{ES}$ | Reserve capacity from storage system [kW] |
| $R^{DG}$ | Reserve capacity from DG [kW] |
| $R^{Grid}$ | Reserve capacity from the main grid [kW] |
| $SOC$ | Storage state of charge [kWh] |
| $TC^{S}$ | NPV of total cost of storage from the MGO perspective [$] |
| $TC^{Grid}$ | NPV of total cost of energy and reserve provisions from the main grid [$] |
| $U, V, W$ | Binary start-up, shut-down, and commitment decision of DG units |
| $Wp$ | Power rating of storage system at year of installation and zero otherwise [kW] |
| $We$ | Energy capacity of storage system at year of installation and zero otherwise [kWh] |
| $Z$ | Binary installation decision of storage |
| $Zc, Zd$ | Binary charging/discharging decision of storage |
| $\Pi^{CH}$ | NPV of MGO revenue from storage charging [$] |
| $\Pi^{DCH}$ | NPV of MGO cost from storage discharging [$] |
| $\Pi^{RS}$ | NPV of MGO cost from storage reserve provisions [$] |
| $\pi^{CH}$ | NPV of investor cost from storage charging [$] |
| $\pi^{DCH}$ | NPV of investor revenue from storage discharging [$] |
| $\pi^{RS}$ | NPV of investor revenue from storage reserve provisions [$] |

## 4.2 Third-Party BESS Investment Problem

The storage investment problem is formulated considering a multi-objective function where the microgrid operator minimizes its total operational cost, while the third-party investor maximizes its profit. The problem is solved using a goal programming approach to optimize the conflicting objective functions, while satisfying the constraints of each party, in addition to the system constraints.

### 4.2.1 BESS Investor Perspective

The objective function from the perspective of the storage investor is to maximize the NPV of total profit $J_1$, given as follows:

$$J_1 = \left(\pi^{DCH} + \pi^{RS}\right) - \left(\pi^{CH} + INS + OM^S\right) \tag{4.1}$$

The NPV of the cost or revenue for the investor, from the energy exchanged between the BESS and the microgrid, during charging and discharging, and from the provision of reserves, are formulated as follows:

$$\pi^{CH} = 365 \times \sum_{y=1}^{Y_T} \sum_{h=1}^{H} \Big[\frac{1}{(1+\alpha)^y}\ \rho^E_{y,h}\ \Big(\frac{-1}{1-\eta_c\eta_d}\Big)\big(PB_{y,h}\big)\Big] \tag{4.2}$$

$$\pi^{RS} = 365 \times \sum_{y=1}^{Y_T} \sum_{h=1}^{H} \Big[\frac{1}{(1+\alpha)^y}\ \rho^{res}_{y,h}\ R^{ES}_{y,h}\Big] \tag{4.3}$$

$$\pi^{DCH} = 365 \times \sum_{y=1}^{Y_T} \sum_{h=1}^{H} \Big[\frac{1}{(1+\alpha)^y}\ \rho^E_{y,h}\ \Big(\frac{-\eta_c\eta_d}{1-\eta_c\eta_d}\Big)\big(PB_{y,h}\big)\Big] \tag{4.4}$$

where the energy drawn from the microgrid for BESS charging determines the charging cost of the investor in (4.2), and the energy injected to the microgrid by discharging the BESS determines the inverstor's revenue in (4.4).

The $INS$ cost component of BESS comprises costs proportional to the installed power rating ($/kW) and energy capacity ($/kWh), and a fixed installation cost ($) irrespective of the size, as given below:

$$INS = \sum_{y=1}^{Y_T} \Big[\frac{1}{(1+\alpha)^y}\big(Cp^v Wp_y + Ce^v We_y + C^f Z_y\big)\Big] \tag{4.5}$$

The $OM^S$ component comprises the fixed O&M cost, variable O&M cost, and replacement cost. The fixed and replacement costs are proportional to the storage power rating, whereas the variable cost depends on the discharged energy from the BESS, given

as follows:

$$
\begin{aligned}
OM^S = & \sum_{y=1}^{Y_T} \Big[ \frac{1}{(1+\alpha)^y} OMC^f \, P_{BESS_y} \Big] \\
& + 365 \times \sum_{y=1}^{Y_T} \sum_{h=1}^{H} \Big[ \frac{1}{(1+\alpha)^y} \; OMC^v \; \big( \frac{-\eta_c}{1-\eta_c \eta_d} \big) \big( PB_{y,h} \big) \Big] \\
& + \Big[ \frac{1}{(1+\alpha)^{R_Y}} + \frac{1}{(1+\alpha)^{2R_Y}} + ... \Big] \; RC \; P_{BESS_{y=1}} \\
& + \sum_{y=R_Y+1}^{Y_T} \Big[ \Big( \frac{1}{(1+\alpha)^y} + \frac{1}{(1+\alpha)^{y+R_Y}} + ... \Big) \; RC \; \Big( P_{BESS_{y-R_Y+1}} - P_{BESS_{y-R_Y}} \Big) \Big]
\end{aligned}
\tag{4.6}
$$

The first term of (4.6) represents the fixed O&M cost of the BESS. In the second term, the total energy discharged is used to compute the variable O&M cost. Since the model considers one typical day per year, the variable cost is also extrapolated to one year using a factor of 365. The replacement cost of storage is applied when the storage system's years of operation reach its predefined life $R_Y$. The third term of (4.6) denotes the replacement cost for a storage system installed in the first year, while the last term represents the replacement cost if it is installed after the first year. The replacement cost may apply several times if the storage life is reached more than once over the planning horizon.

### 4.2.2 Microgrid Operator Perspective

The operator of the grid-connected microgrid seeks to minimize the NPV of the total operational cost $J_2$ as follows:

$$
J_2 = OC^{MG} + TC^{Grid} + TC^S \tag{4.7}
$$

The term $OC^{MG}$ is the operational cost of the dispatchable DG units in the grid-connected microgrids and cost of load shedding, given as follows:

$$\begin{aligned} OC^{MG} =& 365 \times \sum_{y=1}^{Y_T} \sum_{h=1}^{H} \sum_{i=1}^{I} \Bigg[ \frac{1}{(1+\beta)^y} \Big[ C^{SHED} Pd_{y,h}^{SHED} \\ & + \big(1+\gamma\big)^{y-1} F_i\big(P_{y,h,i}\big) W_{y,h,i} + SU_i U_{y,h,i} + SD_i V_{y,h,i} \Big] \Bigg] \end{aligned} \tag{4.8}$$

The microgrid energy and reserve exchanged with the main grid and the BESS are formulated as follows:

$$TC^{Grid} = 365 \times \sum_{y=1}^{Y_T} \sum_{h=1}^{H} \left[ \frac{1}{(1+\beta)^y} \rho_{y,h}^{E} P^{Grid} + \rho_{y,h}^{R} R^{Grid} \right] \tag{4.9}$$

$$TC^{S} = \big(\Pi^{DCH} + \Pi^{RS}\big) - \big(\Pi^{CH}\big) \tag{4.10}$$

The MGO's NPV revenue/cost $\Pi^{DCH}$, $\Pi^{RB}$, and $\Pi^{CH}$ can be formulated as follows:

$$\Pi^{DCH} = 365 \times \sum_{y=1}^{Y_T} \sum_{h=1}^{H} \big[ \frac{1}{(1+\beta)^y} \ \rho_{y,h}^{E} \ \big( \frac{-\eta_c \eta_d}{1-\eta_c \eta_d} \big) \big( PB_{y,h} \big) \big] \tag{4.11}$$

$$\Pi^{RS} = 365 \times \sum_{y=1}^{Y_T} \sum_{h=1}^{H} \big[ \frac{1}{(1+\beta)^y} \ \rho_{y,h}^{res} \ R_{y,h}^{ES} \big] \tag{4.12}$$

$$\Pi^{CH} = 365 \times \sum_{y=1}^{Y_T} \sum_{h=1}^{H} \big[ \frac{1}{(1+\beta)^y} \ \rho_{y,h}^{E} \ \big( \frac{-1}{1-\eta_c \eta_d} \big) \big( PB_{y,h} \big) \big] \tag{4.13}$$

## 4.3 Proposed Goal Programming Approach

The objective function in the proposed goal programming based approach is to maximize $J$ which comprises the objectives of the MGO and the BESS investor with a weight assigned

for each objective $\omega$, as follows:

$$J = (1 - \omega)D_1 - \omega D_2 \tag{4.14}$$

where $D1$ and $D2$ are given as follows:

$$D_1 = J_1 - A_1 \tag{4.15}$$

$$D_2 = J_2 - A_2 \tag{4.16}$$

The aspiration level for each objective $A1$ and $A2$ are set to achieve a required value of the objective function. In this work, $A1$ is the break-even point of the investor's profit, *i.e.* the NPV of profit in (4.1) is zero considering a discount rate equal to the investor's MARR, while $A2$ is set by the microgrid operator, which represents the total microgrid operational cost in the base case without BESS installation ($C_0$).

The objective function (4.14) is subject to the following constraints:

### 4.3.1 Microgrid Cost Limit

The NPV of the total microgrid operational cost should not exceed $C_0$, the base case cost without BESS installation, given as follows:

$$OC^{MG} + TC^{Grid} + TC^{S} \leq C_0 \tag{4.17}$$

It is noted that the costs in (4.17) is calculated based on the discount rate $\beta$.

### 4.3.2 Investor's Revenue Constraint

Although the investor's objective function is to maximize the profit, it does not ensure the profitability of the investment. Therefore, this constraint is considered to ensure that the IRR is at least equal to the investor's MARR, while minimizing the total microgrid costs.

$$\left(\pi^{DCH} + \pi^{RS}\right) - \left(\pi^{CH} + INS + OM^{S}\right) \geq 0 \tag{4.18}$$

The costs/revenues in (4.18) are calculated based on MARR ($\alpha$).

### 4.3.3 Operational and Planning Constraints

#### 4.3.3.1 Demand-Supply Balance

This constraint ensures sufficient generation to meet the microgrid demand at an hour, as follows:

$$\sum_{i=1}^{I} P_{y,h,i} + P_{y,h}^{Grid} + PB_{y,h} + PV_{y,h} + Pw_{y,h} = Pd_{y,h} - Pd_{y,h}^{SHED} \quad \forall y, \forall h \tag{4.19}$$

#### 4.3.3.2 Microgrid Reserve Requirements

The MGO ensures a minimum reserve level of $\vartheta$ of the demand plus factors accounting for uncertainty in demand and RES forecasting errors [40]. The reserve constraint is modeled as follows:

$$R_{y,h}^{DG} + R_{y,h}^{Grid} + R_{y,h}^{ES} \geq \big(\vartheta + \delta_D\big) Pd_{y,h} + \delta_{PV} PV_{y,h} + \delta_W Pw_{y,h} \quad \forall y, \forall h \tag{4.20}$$

$$R_{y,h}^{DG} \leq \sum_{i=1}^{I} \big(\overline{P_i} W_{y,h,i} - P_{y,h,i}\big) \quad \forall y, \forall h \tag{4.21}$$

$$R_{y,h}^{Grid} \leq \overline{PSS} - P_{y,h}^{Grid} \quad \forall y, \forall h \tag{4.22}$$

$$R_{y,h}^{ES} \leq -PB_{y,h} + \min\Big\{ \big[SOC_{y,h} - E_{BESS_y}(1 - \overline{DOD})\big]\eta_d, P_{BESS_y} \Big\} \quad \forall y, \forall h \tag{4.23}$$

#### 4.3.3.3 DG Units Constraints

Each generating unit has upper and lower bounds on its power production, as follows:

$$\underline{P_i} W_{y,h,i} \leq P_{y,h,i} \leq \overline{P_i} W_{y,h,i} \quad \forall y, \forall h, \forall i \tag{4.24}$$

The inter-hour increase/decrease in generation should satisfy the ramp rate limits of generating units, as follows:

$$P_{y,h,i} - P_{y,h-1,i} - U_{y,h,i}\ \overline{P_i} \leq Ramp_i^{UP} \qquad \forall y, \forall i, \forall h; h \neq 1 \tag{4.25}$$

$$P_{y,h-1,i} - P_{y,h,i} - V_{y,h,i}\ \overline{P_i} \leq Ramp_i^{DW} \qquad \forall y, \forall i, \forall h; h \neq 1 \tag{4.26}$$

When a generating unit is turned on, it must not be de-committed before satisfying its minimum up time. These constraints are formulated as follows [91]:

$$\sum_{h=1}^{G_i}(1 - W_{y,h,i}) = 0 \quad \forall y, \forall i \tag{4.27}$$

$$\sum_{q=h}^{h+Min_i^{UP}-1} W_{y,q,i} \geq Min_i^{UP}[W_{y,h,i} - W_{y,h-1,i}] \qquad \forall y, \forall i, h = G_i + 1, ....H - Min_i^{UP} + 1 \tag{4.28}$$

$$\sum_{q=h}^{H} \left[W_{y,q,i} - (W_{y,h,i} - W_{y,h-1,i})\right] \geq 0 \qquad \forall y, \forall i, h = H - Min_i^{UP} + 2, ....H \tag{4.29}$$

When a generating unit is turned off, the minimum down time should be satisfied before committing it again. The constraints are formulated as follows [91]:

$$\sum_{h=1}^{L_i} W_{y,h,i} = 0 \quad \forall y, \forall i \tag{4.30}$$

$$\sum_{q=h}^{h+Min_i^{DW}-1} (1 - W_{y,q,i}) \geq Min_i^{DW}[W_{y,h-1,i} - W_{y,h,i}] \qquad \forall y, \forall i, h = L_i + 1, ....H - Min_i^{DW} + 1 \tag{4.31}$$

$$\sum_{q=h}^{H} \left[1 - W_{y,q,i} - (W_{y,h-1,i} - W_{y,h,i})\right] \geq 0 \qquad \forall y, \forall i, h = H - Min_i^{DW} + 2, ....H \tag{4.32}$$

To ensure proper coordination between the generator status and the start-up/shut down variables, the following constraint is formulated, as below:

$$U_{y,h,i} - V_{y,h,i} = W_{y,h,i} - W_{y,h-1,i} \qquad \forall y, \forall h, \forall i \tag{4.33}$$

It is noted that the ramping and minimum-up and -down time constraints can be relaxed in some microgrid EMS models, to reduce the computational time in operational problems, because of the fast ramping capability of dispatchable DG units, and fewer restrictions on their minimum-up and -down times. However, in practice, these constraints indeed impact the microgrid operations [96], and since planning problems are less restricted by the computational time, these are considered in this study for the sake of accuracy.

#### 4.3.3.4 Storage Power Rating Constraints

Two variables are defined for power rating, $P_{BESS_y}$ and $Wp_y$. The first denotes the power rating of BESS, and once the BESS is installed, it remains constant over the plan horizon. On the other hand, while $Wp_y$ also denotes the installed BESS size, it is used to compute the installation cost, and is active only at the year of installation; otherwise, it is zero. The BESS power rating constraints are given as follows:

$$P_{BESS_y} = Wp_y \qquad ; y = 1 \tag{4.34}$$

$$P_{BESS_y} = Wp_y + P_{BESS_{y-1}} \qquad \forall y; y \neq 1 \tag{4.35}$$

$$Wp_y \geq Z_y \qquad \forall y \tag{4.36}$$

$$Wp_y \leq M\ Z_y \qquad \forall y \tag{4.37}$$

#### 4.3.3.5 Storage Energy Capacity Constraints

Similar to the power rating, two variables are defined for energy capacity $E_{BESS_y}$ and $We_y$, and the capacity constraints are given as follows:

$$We_y \geq Z_y \quad \forall y \tag{4.38}$$

$$We_y \leq M\ Z_y \quad \forall y \tag{4.39}$$

$$\underline{EPR}\ P_{BESS_y} \leq E_{BESS_y} \leq \overline{EPR}\ P_{BESS_y} \quad \forall y \tag{4.40}$$

Energy storage capacity considering its degradation is formulated as follows:

$$E_{BESS_y} = \sum_{y'=1}^{y} \Big[We_{y'}\big[1-\sigma(y-y')\big]\Big] \qquad ; y = 1, 2, ..R_Y \tag{4.41}$$

$$\begin{aligned} E_{BESS_y} = &\sum_{y'=1}^{y-R_Y} \Big[We_{y'}\big[1-\sigma(y-R_Y-y')\big]\Big] + \sum_{y'=y-R_Y+1}^{R_Y} \Big[We_{y'}\big[1-\sigma(y-y')\big]\Big] \\ &+ \sum_{y'=1}^{y-R_Y} \Big[We_{y'+R_Y}\big[1-\sigma(y-R_Y-y')\big]\Big] \\ &\qquad\qquad ; y = R_Y+1, ..Y_T \end{aligned} \tag{4.42}$$

The storage capacity $E_{BESS_y}$ depends on the installed energy capacity and the year of installation, represented by $We_y$, and the capacity degradation factor $\sigma$. The energy size $E_{BESS_y}$ before the replacement year $R_Y$ is formulated in (4.41), while $E_{BESS_y}$ in the preceding years is formulated in (4.42).

#### 4.3.3.6 BESS Operational Constraints

The charging and discharging power of the BESS and its SOC are formulated as follows [97]:

$$-PB_{y,h}\ \eta_c - M\ Zd_{y,h} \leq SOC_{y,h+1} - SOC_{y,h} \qquad \forall y, \forall h; h \neq H \tag{4.43}$$

$$SOC_{y,h+1} - SOC_{y,h} \leq -PB_{y,h}\ \eta_c + M\ Zd_{y,h} \qquad \forall y, \forall h; h \neq H \tag{4.44}$$

$$\frac{-PB_{y,h}}{\eta_d} - M\big(Zc_{y,h} - Zd_{y,h} + 1\big) \leq SOC_{y,h+1} - SOC_{y,h} \qquad \forall y, \forall h; h \neq H \tag{4.45}$$

$$SOC_{y,h+1} - SOC_{y,h} \leq \frac{-PB_{y,h}}{\eta_d} + M\big(Zc_{y,h} - Zd_{y,h} + 1\big) \qquad \forall y, \forall h; h \neq H \tag{4.46}$$

The initial SOC of the BESS is assumed to be 50% of the installed energy capacity, as follows:

$$SOC_{y,h} = 0.5\ E_{BESS_y} \qquad \forall y, h = 1 \tag{4.47}$$

The final status of SOC is implemented in the constraints (4.43)-(4.46) by replacing $SOC_{y,h+1}$ to the desired level, *i.e.*,

$$SOC_{y,h+1} = 0.5\ E_{BESS_y} \qquad \forall y, h = H \tag{4.48}$$

In order to force the binary variables $Zc$ and $Zd$ to be activated during the charging and discharging process in (4.43)-(4.46), and to prevent simultaneous charging and discharging, the following constraints are considered:

$$-M\ Zc_{y,h} \leq PB_{y,h} \qquad \forall y, \forall h \tag{4.49}$$

$$M\ Zd_{y,h} \geq PB_{y,h} \qquad \forall y, \forall h \tag{4.50}$$

$$(1 - \overline{DOD})E_{BESS_y} \leq SOC_{y,h} \leq E_{BESS_y} \qquad \forall y, \forall h \tag{4.51}$$

$$-P_{BESS_y} \leq PB_{y,h} \leq P_{BESS_y} \qquad \forall y, \forall h \tag{4.52}$$

$$Zc_{y,h} + Zd_{y,h} \leq 1 \qquad \forall y, \forall h \tag{4.53}$$

$$\sum_{y=1}^{Y_T} Z_y \leq 1 \tag{4.54}$$

#### 4.3.3.7 Budget Constraint

The NPV of the installation cost should not exceed the NPV of the allocated budget for the year, as follows:

$$INS \leq B_0 \tag{4.55}$$

The investment planning model (4.1)-(4.55) is formulated as an MILP problem and solved in GAMS using CPLEX solver.

## 4.4 Results and Discussions

### 4.4.1 Test System

The proposed investment planning model is tested on the modified CIGRE medium voltage microgrid [88]. The PV and wind capacity is 1,100 kW and 1,900 kW, respectively, while the total capacity of dispatchable DG units is 5,510 kW. The microgrid is considered to be connected to the main grid and the line capacity is 500 kW. The microgrid peak demand in the first year of the planning horizon is 6,240 kW with an annual increase of 1%, over a plan period of 10 years. The investor's MARR is assumed 14%, while the discount rate set by the microgrid operator is 8%. The annual fuel price escalation rate is assumed to be 3%, while the energy price profile is obtained from [40].

The microgrid operator considers an operating reserve of 10% of the demand, in addition to the forecasting errors of demand ($\delta_D$), generation of PV ($\delta_{PV}$), and wind ($\delta_W$), which are assumed to be 3%, 9%, 13%, respectively [40].

The Li-ion BESS is considered in this case study, while its performance and cost parameters are shown in Table 3.2. The maximum size for BESS is assumed as, $P_{BESS}$ = 6,500 kW, and $E_{BESS}$ = 6,500 kWh, the options are considered to be available in multiples of 50 kW and 50 kWh, respectively.

The impact of microgrid operation on the storage investment decisions is studied considering the following scenarios:

### 4.4.2 Case-I

The microgrid generation capacity considering its dispatchable DG capacity and RES generation is not adequate to meet the demand, particularly when approaching the terminal year. Therefore, load shedding is included in this case to maintain the supply-demand balance, as shown in Figure 4.1. The microgrid operational cost without storage installation ($C_0$) is \$29,688,315.

The BESS investment decisions are examined considering different weights for the objective functions ($\omega$), as shown in Table 4.1. For $\omega$ = zero, which represents the investor's perspective, the installation of BESS is at year-1 with large power rating and energy capacity 1($P_{BESS}$ = 900 kW and $E_{BESS}$ = 1150 kWh) to maximize the investor revenue, for a high rate of return of 46%. However, the NPV of total microgrid costs remains the same at \$29,688,315 since the the high cost of load shedding and energy imported from the main grid during high energy price hours is avoided. When $\omega = 0.5$, the investor's MARR of 14% is maintained, and a reduction in the microgrid operational cost from the base case by \$3,347,874 is achieved. This reduction reaches \$3,978,824 when $\omega = 1$, which represents the MGO's perspective. The optimal BESS installation from the MGO perspective is less in ratings with deferred installation year compared to the investor's perspective. The optimal BESS ratings are 750 kW and 900 kWh, while the optimal installation year is year-2 of the planning horizon.

Figure 4.2 shows the optimal BESS and microgrid operation at the terminal year considering $\omega = 0.5$. The BESS charging and discharging operations help the microgrid to meet the entire demand without the need for load shedding during the peak hours, while relatively less energy import is observed to minimize the cost of buying energy when the energy price is high. Furthermore, the microgrid load is levelized, which reduces the need for starting up expensive dispatchable DG units.

### 4.4.3 Case-II

The RES generation is assumed 50% higher in this case with respect to that in Case-I. Therefore, the MGO is not required to shed microgrid load to maintain the supply-demand

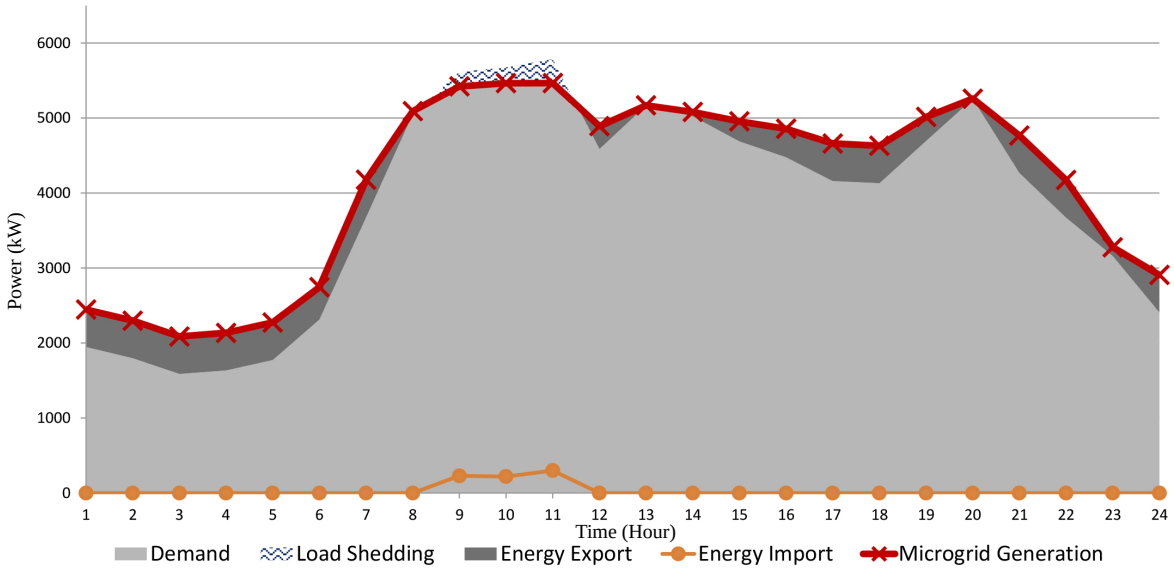


Figure 4.1: Optimal operation of microgrid without storage installation (Case-I).

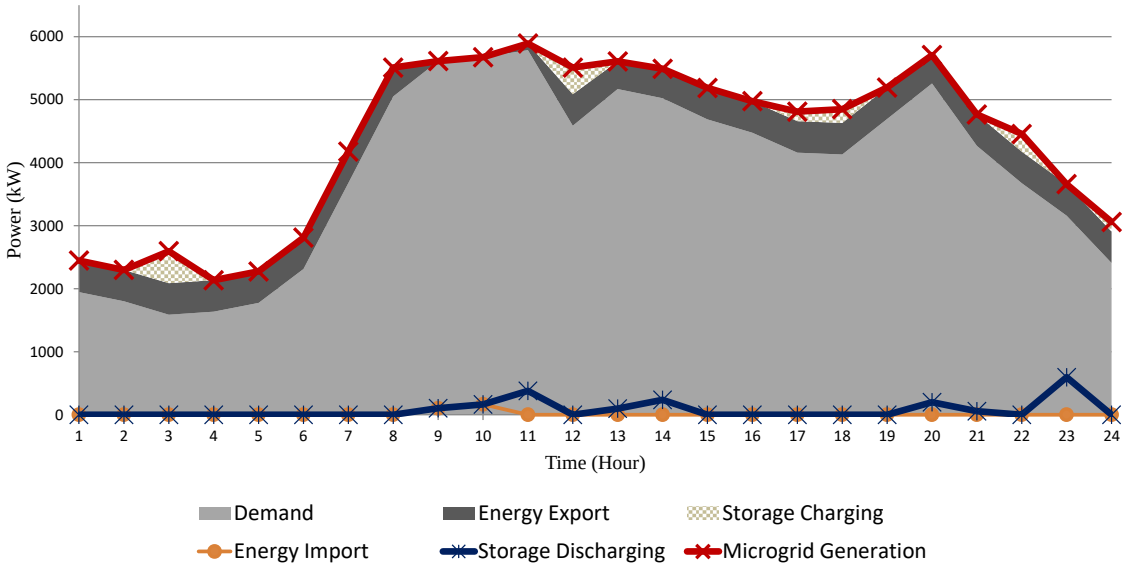


Figure 4.2: Optimal operation of storage and microgrid at $\omega = 0.5$ (Case-I).

Table 4.1: Optimal Investment Decisions and Associated Costs (Case-I)

| $\omega$ | Cost Reduction (MGO) | IRR (Investor) | $P_{BESS}$ | $E_{BESS}$ | Year |
|---|---|---|---|---|---|
| 0 | 0 | 46% | 900 | 1150 | 1 |
| 0.25 | \$582,784 | 46% | 800 | 1000 | 1 |
| 0.5 | \$3,347,874 | 14% | 750 | 900 | 2 |
| 0.75 | \$3,961,544 | 14% | 750 | 900 | 2 |
| 1 | \$3,978,824 | 14% | 750 | 900 | 2 |

balance, as shown in Figure 4.3, which presents the optimal microgrid operation in year-10 without BESS installations. Therefore, the operational cost of the microgrid ($C_0$) is reduced to \$19,109,328, compared to that in Case-I.

The BESS optimal decision from the investor's perspective is to install 300 kW/400 kWh of energy storage, while the optimal year of installation is year-2. This reduction in the ratings is also represented by a reduction in the rate of return to 38% since the microgrid operational cost $C_0$ in Case-II is lower than that in Case-I, and therefore, there is less margin of reduction in the microgird operational cost, as shown in Table 4.2. The storage installation decisions at $\omega = 100\%$ is 250 kW and 300 kWh, while the optimal year of installation is year-4. The reduction in the microgrid cost reaches \$713,277.

The optimal BESS and microgrid operation at year-10 with $\omega = 0.5$ in Case-II is shown in Figure 4.4. Because of the lower ratings of BESS, there are fewer charging and discharging cycles, which are mainly to minimize the cost of starting up expensive DG units by levelizing the load of the microgrid.

### 4.4.4 Case-III

The RES generation profile is increased further to about 100% with respect to the RES generation profile in Case-I. The surplus in microgrid generation is large allowing the

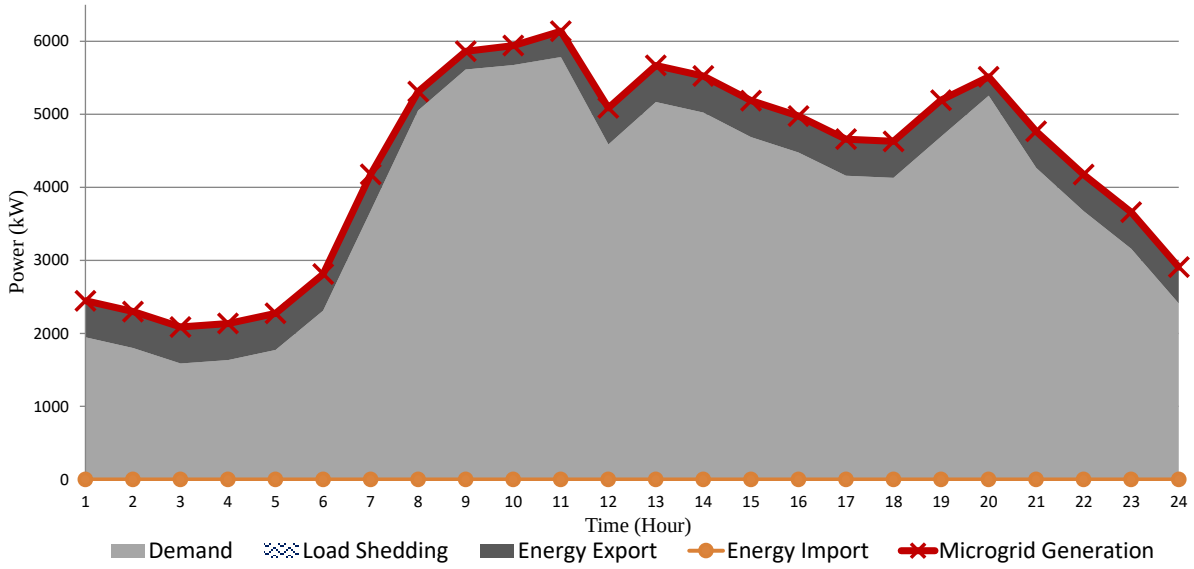


Figure 4.3: Optimal operation of microgrid without storage installation (Case-II).

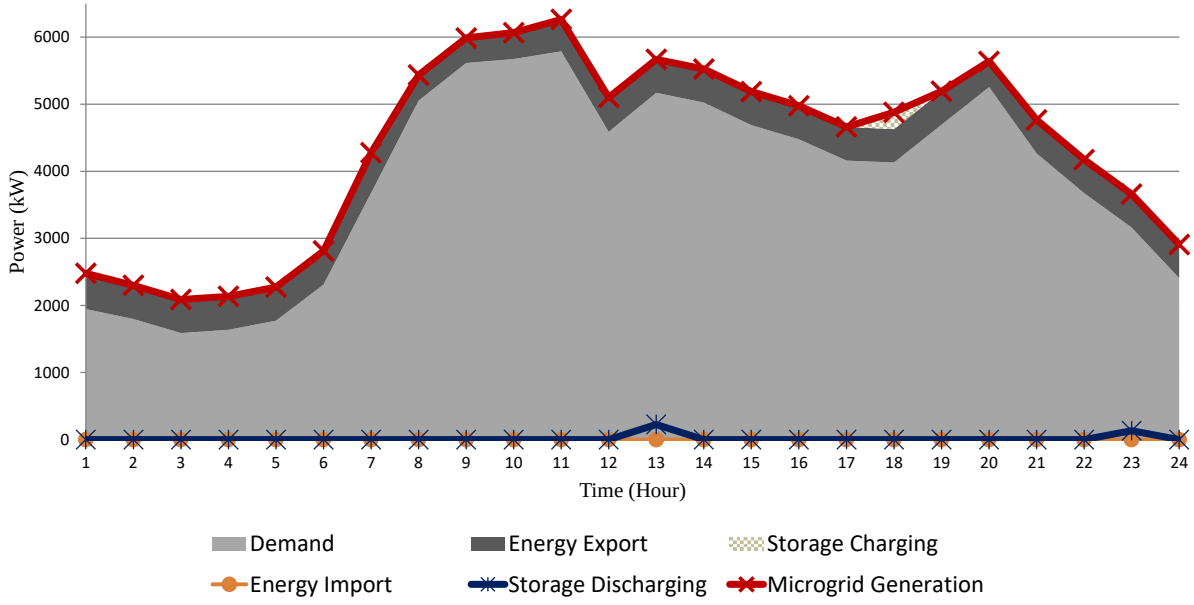


Figure 4.4: Optimal operation of storage and microgrid at $\omega = 0.5$ (Case-II).

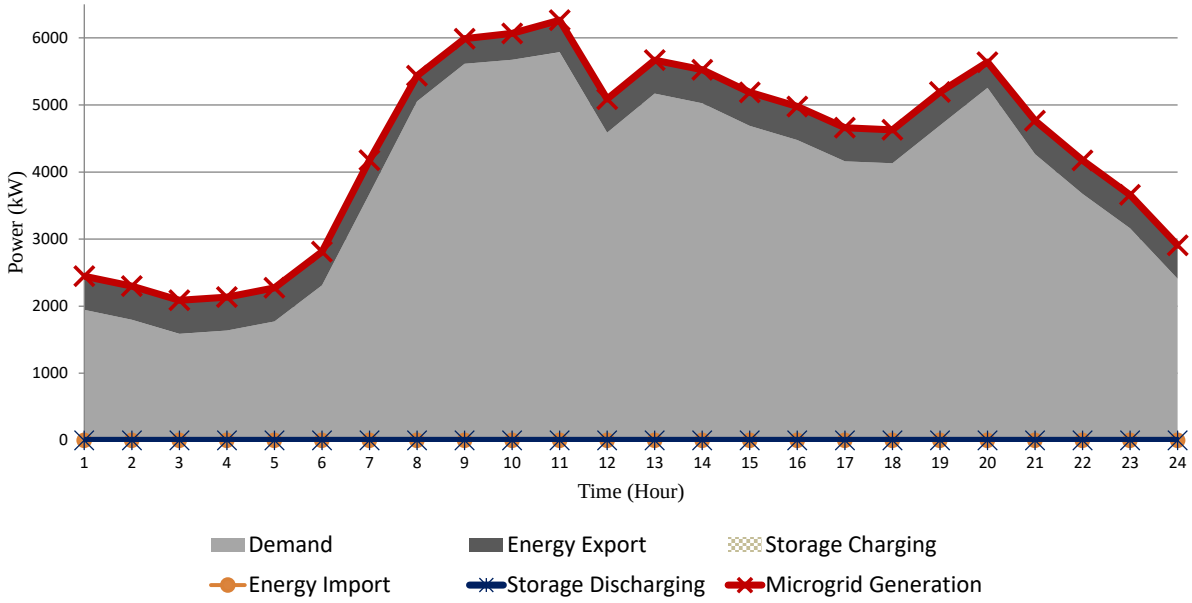


Figure 4.5: Optimal operation of microgrid (Case-III).

Table 4.2: Optimal Investment Decisions and Associated Costs (Case-II)

| $\omega$ | Cost Reduction (MGO) | IRR (Investor) | $P_{BESS}$ | $E_{BESS}$ | Year |
|---|---|---|---|---|---|
| 0 | 0 | 38% | 300 | 400 | 2 |
| 0.25 | 0 | 38% | 300 | 400 | 2 |
| 0.5 | \$696,925 | 14% | 250 | 300 | 3 |
| 0.75 | \$702,761 | 14% | 250 | 300 | 4 |
| 1 | \$713,277 | 14% | 250 | 300 | 4 |

MGO to sell energy to the main grid during peak hours and offset some of the microgrid operational costs. The total microgrid operational cost without the installation of BESS is \$11,724,286.

Figure 4.5 shows the optimal microgrid operation at year-10. Since there is less margin

for further reduction in microgrid operational cost, the investor's IRR of 14% cannot be met within the planning horizon. The optimal investment decision is to not install BESS, either from the perspective of the investor or from that of the MGO.

## 4.5 Summary

In this chapter, a new method based on goal programming approach was proposed to determine the BESS investment decisions by a third-party investor while it was operated and scheduled by the MGO. The proposed model was validated on the CIGRE microgrid test system considering different microgrid operational scenarios. The results demonstrated the effectiveness of the proposed work in determining if the storage installation accrued a reduction in the total microgrid operational costs and satisfied the investor MARR considering the microgrid generation mix and load profiles.

# Chapter 5

# Participation of Pumped Hydro Storage in Energy and Performance-Based Regulation Markets[1]

This chapter examines the non-strategic and strategic participation of a PHES facility in day-ahead energy and PBR (regulation capacity and mileage) markets. The PHES is modeled with the capability of operating in HSC mode with detailed representation of its operational constraints, and integrated with an energy-cum-PBR market clearing model. For its strategic participation, a bi-level market framework is proposed to determine the optimal offers and bids of the PHES that maximize its profit. The operation of PHES is modeled at the upper level, while the market clearing is modeled in the lower level problem. The bi-level problem is formulated as an MPEC model, which is linearized and solved as an MILP problem. Several case studies are carried out to demonstrate the impact of PHES' non-strategic and strategic operations on market outcomes. Furthermore, stochastic case

[1]This chapter has been accepted for publication in:
H. Alharbi, and K. Bhattacharya, "Participation of Pumped Hydro Storage in Energy and Performance-Based Regulation Markets," *IEEE Transactions on Power Systems*, (in print).

studies are conducted to determine the PHES strategies considering the uncertainty of the net demand and rivals' price and quantity offers.

## 5.1 Nomenclature

### *Indices*

| | |
|---|---|
| $h$ | Index for PHES units, $h = 1, 2, .., Nh$ |
| $i$ | Index for generation units, $i = 1, 2, .., I$ |
| $j$ | Index for customers, $j = 1, 2, .., J$ |
| $s$ | Index for scenarios, $s = 1, 2, .., S$ |
| $t$ | Index for time, $t = 1, 2, .., T$ |
| $w$ | Index for RES units, $w = 1, 2, .., W$ |

### *Parameters*

| | |
|---|---|
| $C^D$ | Demand bid in energy market [$/MWh] |
| $C^g$ | Generator offer in energy market [$/MWh] |
| $C^{g,uM/dM}$ | Generator regulation up/down mileage offer [$/MW] |
| $C^{g,uR/dR}$ | Generator regulation up/down capacity offer [$/MW] |
| $C^{RE}$ | RES generation offer [$/MWh] |
| $M^{sys,u/d}$ | Required regulation up/down mileage [MW] |
| $m^{h,u/d}$ | Mileage capability multiplier of a PHES unit. |
| $m^{g,u/d}$ | Mileage capability multiplier of a generator. |
| $\overline{P}^{HG}, \underline{P}^{HG}$ | Generation limits of PHES unit [MW] |
| $\overline{P}^{HP}$ | Fixed PHES pumping power [MW] |
| $\overline{P}^{D}, \underline{P}^{D}$ | Limits of demand $j$ [MW] |
| $\overline{P}^{g}, \underline{P}^{g}$ | Limits of generation unit $i$ [MW] |
| $\overline{P}^{RE}$ | Maximum available RES generation [MW] |
| $\overline{Q}^{HG}, \underline{Q}^{HG}$ | Water discharge limits during generation [$m^3/h$] |
| $\overline{Q}^{HP}$ | Fixed pumped water in pumping mode [$m^3/h$] |

| | |
|---|---|
| $R^{sys,u/d}$ | Required up/down regulation capacity [MW] |
| $\overline{R}^{H,u/d}$ | PHES regulation up/down capacity limit [MW] |
| $\overline{R}^{g,u/d}$ | Generator regulation up/down capacity limit [MW] |
| $SU^{HG/HP}$ | Start-up cost in generating/pumping mode [$] |
| $\overline{V}^{H}$, $\underline{V}^{H}$ | Water volume limits of PHES [$m^3$] |
| $\eta_G$, $\eta_P$ | Efficiency in generating and pumping mode |
| $\alpha$ | PHES energy conversion coefficient [MW/$m^3$] |
| $\gamma$ | Regulation capacity as a ratio of the total unit rating |
| $\rho$ | Scenario probability. |

## *Variables*

| | |
|---|---|
| $M^{H,u/d}$ | PHES regulation up/down mileage cleared [MW] |
| $M^{g,u/d}$ | Generator regulation up/down mileage [MW] |
| $\hat{M}^{H,u/d}$ | PHES regulation up/down mileage offer [MW] |
| $P^{HG/HP}$ | PHES generating/pumping power [MW] |
| $P^{g}$ | Cleared generation of a generator [MW] |
| $P^{D}$ | Cleared demand of a customer [MW] |
| $P^{RE}$ | Cleared generation of a RES unit [MW] |
| $\hat{P}^{HP}$ | PHES demand quantity bid [MWh] |
| $\hat{P}^{HG}$ | PHES generation quantity offer [MWh] |
| $Q'$ | Water discharge above the minimum limit [$m^3$] |
| $Q^{HG}$ | Water discharged in generation mode [$m^3$] |
| $Q^{HP}$ | Water pumped in pumping mode [$m^3$] |
| $R^{H,u/d}$ | PHES regulation up/down capacity cleared [MW] |
| $R^{g,u/d}$ | Generator regulation up/down capacity [MW] |
| $\hat{R}^{H,u/d}$ | PHES regulation up/down capacity offer [MW] |
| $v^{H}$ | Water volume of the reservoir [$m^3$] |
| $Y^{HG/HP}$ | PHES generating/pumping start-up [0,1] |
| $Z^{HG/HP}$ | PHES unit mode status [0,1] |

| | |
|---|---|
| $Z^{PP}$ | Conventional PHES binary coordination [0,1] |
| $\beta^{H,uM/dM}$ | PHES regulation up/down mileage offer price [$/MW] |
| $\beta^{HP}$ | Bid price of PHES as a customer [$/MWh] |
| $\beta^{HG}$ | Offer price of PHES as a generator [$/MWh] |
| $\beta^{H,uR/dR}$ | PHES regulation up/down capacity offer price [$/MW] |
| $\lambda^{E}$ | Energy market marginal price [$/MWh] |
| $\lambda^{u,M}, \lambda^{d,M}$ | Regulation up/down mileage price [$/MW] |
| $\lambda^{u,R}, \lambda^{d,R}$ | Regulation up/down capacity price [$/MW] |

## 5.2 Bi-Level Optimization Problem

### 5.2.1 Upper Level: PHES Profit Maximization Operations

The objective function in the upper level problem is to maximize the expected value of the PHES profit considering a risk-neutral approach, given as follows:

$$J_U = \sum_{s=1}^{S} \rho_s \sum_{t=1}^{T} \sum_{h=1}^{Nh} \Big[ (\lambda_{s,t}^{E} P_{s,h,t}^{HG} + \lambda_{s,t}^{u,R} R_{s,h,t}^{H,u} + \lambda_{s,t}^{d,R} R_{s,h,t}^{H,d} + \lambda_{s,t}^{u,M} M_{s,h,t}^{H,u} + \lambda_{s,t}^{d,M} M_{s,h,t}^{H,d}) - (\lambda_{s,t}^{E} P_{s,h,t}^{HP} + SU^{HG} Y_{h,t}^{HG} + SU^{HP} Y_{h,t}^{HP}) \Big] \tag{5.1}$$

In (5.1), the first set of terms denote the revenue of the PHES, accrued from its participation in the day-ahead energy, and regulation up/down capacity and up/down mileage markets. The PHES operations cost denoted by the second set of terms in (5.1) includes the cost of energy drawn during pumping, and the start-up costs of the PHES units. Note that the market prices are variables, determined from the lower level market settlement model.

In this work, only day-ahead market is modeled without considering real-time operations, to keep the MPEC problem tractable. It is to be noted that while the regulation capacity is procured in the day-ahead market, it is deployed in real-time

operations. The regulation capacity cleared in the day-ahead market receives a payment, regardless of its deployment in the real-time, hence this term is included in (5.1).

In the case of mileage, the payment is made after real-time operations, based on the PHES facility's performance in following the signal and actual movements. But since the procurement of regulation capacity and mileage is carried out simultaneously in the day-ahead market, they being inter-related variables, the mileage component is also included in (5.1). For example, a large regulation capacity from a unit may not necessarily yield a large mileage, and the market operator would need to select another unit to meet the system mileage requirement.

Although the actual PHES mileage revenue may differ from that determined in (5.1), maximizing the mileage participation in the day-ahead market leads to a higher profit potential for the PHES, considering its performance. The objective function (5.1) is subject to the following constraints:

#### 5.2.1.1 Offer/Bid Constraints of PHES

The optimal PHES offers and bids in the energy and regulation capacity markets are limited by the PHES unit ratings and the maximum regulation capacity, respectively, as follows:

$$0 \leq \hat{P}^{HP}_{h,t} \leq Z^{HP}_{h,t}\overline{P}^{HP}_{h} \;\;,\;\; 0 \leq \hat{P}^{HG}_{h,t} \leq Z^{HG}_{h,t}\overline{P}^{HG}_{h} \qquad \forall h,t \tag{5.2}$$

$$0 \leq \hat{R}^{H,u/d}_{h,t} \leq Z^{HG}_{h,t}\overline{R}^{H,u/d}_{h} \qquad \forall h,t \tag{5.3}$$

$$\overline{R}^{H,u/d}_{h} = \gamma\overline{P}^{HG}_{h} \qquad \forall h \tag{5.4}$$

The participation of a PHES unit $h$ in regulation provisions is only activated if it is in the generating mode, *i.e.* when $Z^{HG}$=1, as noted from (5.3).

The energy and regulation capacity offers are also constrained by the PHES unit ratings and the available water volume in the reservoir, as follows:

$$\hat{P}^{HG}_{h,t} + \hat{R}^{H,u}_{h,t} \leq Z^{HG}_{h,t}\overline{P}^{HG}_{h} \;\;,\;\; Z^{HG}_{h,t}\underline{P}^{HG}_{h} \leq \hat{P}^{HG}_{h,t} - \hat{R}^{H,d}_{h,t} \;\; \forall h,t \tag{5.5}$$

$$\sum_{h=1}^{Nh}\left[(\hat{P}_{h,t}^{HG}+\hat{R}_{h,t}^{H,u})\frac{1}{\eta_G\alpha}-\hat{P}_{h,t}^{HP}\frac{\eta_P}{\alpha}\right]\leq v_{s,t}^{H}-\underline{V}^{H}\qquad\forall s,t \tag{5.6}$$

$$\sum_{h=1}^{Nh}\left[\hat{P}_{h,t}^{HP}\frac{\eta_P}{\alpha}-(\hat{P}_{h,t}^{HG}-\hat{R}_{h,t}^{H,d})\frac{1}{\eta_G\alpha}\right]\leq \overline{V}^{H}-v_{s,t}^{H}\qquad\forall s,t \tag{5.7}$$

The constraints (5.6)-(5.7) are needed to ensure the feasibility of the PHES offer/bid strategy for the entire range of scenarios considered. Although participation of the PHES may be reduced because of the scenario of lowest volume for (5.6) or the scenario of highest volume for (5.7), such "conservative" constraints are necessary in order to avoid water shortages during discharging/pumping when the binding offer/bid is cleared in the market.

The PHES mileages are dependent on the regulation capacity and the PHES mileage multiplier. The resource-specific mileage multiplier is a parameter computed by the ISO considering both the historic regulation performance and the certified ramping capability of a resource [79]. Therefore, the slow resources which are limited by their ramping capability have a lower mileage multiplier, and vice versa.

$$\hat{R}_{h,t}^{H,u/d}\leq\hat{M}_{h,t}^{H,u/d}\leq m_h^{h,u/d}\hat{R}_{h,t}^{H,u/d}\qquad\forall h,t \tag{5.8}$$

The lower bound in (5.8) ensures that the full regulation capacity offer can be utilized by the PHES mileage. If this constraint is not considered, the cleared regulation capacity may not be fully available for regulation provision.

Although the HSC PHES can operate in HSC mode, where some of the units are pumping and the others are generating, an individual PHES unit $h$ cannot simultaneously operate in pumping and generating mode, as follows:

$$Z_{h,t}^{HG}+Z_{h,t}^{HP}\leq 1\qquad\forall h,t \tag{5.9}$$

#### 5.2.1.2 PHES Power and Water (Generating Mode)

The relationship between the water discharged and the generated power is formulated in the following constraints:

$$P^{HG}_{s,h,t} = Z^{HG}_{h,t}\underline{P}^{HG}_{h} + Q'_{s,h,t}\alpha \ , \ Q^{HG}_{s,h,t} = Z^{HG}_{h,t}\underline{Q}^{HG}_{h} + Q'_{s,h,t} \quad \forall s,h,t \tag{5.10}$$

$$0 \leq Q'_{s,h,t} \leq (\overline{Q}^{HG}_{h} - \underline{Q}^{HG}_{h})Z^{HG}_{h,t} \qquad \forall s,h,t \tag{5.11}$$

$$P^{HG}_{s,h,t} \leq Z^{HG}_{h,t}\overline{P}^{HG}_{h} \qquad \forall s,h,t \tag{5.12}$$

It is noted that the operation of the PHES depends on the water head of the reservoir and the water discharge function $P^{HG}_{h} = f(Q^{HG}_{h})$, which is non-linear. The linear relationship between water discharge and power generation has been widely used in the literature of hydro-thermal coordination [21, 54, 101]. This relationship adequately represents the participation of PHES in energy and regulation markets, and captures the main operational and physical constraints associated with their participation.

#### 5.2.1.3 PHES Power and Water (Pumping Mode)

In the pumping mode, a PHES unit $h$ operates at a fixed speed, and hence the pumped water and its corresponding power consumption are formulated as follows:

$$P^{HP}_{s,h,t} = Z^{HP}_{h,t}\overline{P}^{HP}_{h} \ , \ Q^{HP}_{s,h,t} = Z^{HP}_{h,t}\overline{Q}^{HP}_{h} \qquad \forall s,h,t \tag{5.13}$$

#### 5.2.1.4 PHES Start-up Binary Variables

In order to ensure a proper coordination between the operating status of PHES turbines and pumps and their start-up binary variables, the following constraints are considered:

$$Y^{HG}_{h,t} \geq Z^{HG}_{h,t} - Z^{HG}_{h,t-1} \ , \ Y^{HP}_{h,t} \geq Z^{HP}_{h,t} - Z^{HP}_{h,t-1} \quad \forall h, t > 1 \tag{5.14}$$

#### 5.2.1.5 Reservoir Water Volume Balance Constraints

This constraint ensures a balance in the reservoir water volume considering the water inflows during pumping and water discharged in generation mode, as follows:

$$v_{s,t}^{H} = v_{s,t-1}^{H} + \sum_{h=1}^{Nh}(Q_{s,h,t}^{HP}\eta_P - \frac{Q_{s,h,t}^{HG}}{\eta_G})\Delta t \qquad \forall s,t \tag{5.15}$$

$$\underline{V}^{H} \leq v_{s,t}^{H} \leq \overline{V}^{H} \qquad \forall s,t \tag{5.16}$$

$$v_{s,t}^{H} = 0.5\ \overline{V}^{H} \qquad \forall s; t = 0, T \tag{5.17}$$

where $\Delta t$ denotes the time interval considered in the relationship between the water volume and water discharged. In this work, since the day-ahead problem is solved for each hour, $\Delta t$ is assumed to take the value 1 hour, or, $\Delta t = 1$.

It is to be noted that the deployment of regulation is not considered in (5.15) assuming that the net energy of regulation is zero for each interval. This can be either managed by the PHES or the system operator, as described in [60, 76]. Therefore, the PHES is able to maintain the same level of water volume over a period of time, even after deploying the regulation-up and -down services. When maintaining the water volume is not possible, the uncertainty of the regulation offset should be considered, as in [11, 12].

The following constraints are additionally considered for the conventional PHES to prevent simultaneous generation and pumping operations:

$$Z_t^{PP} \geq Z_{h,t}^{HP} \qquad \forall h,t \tag{5.18}$$

$$Z_{h,t}^{HG} \leq 1 - Z_t^{PP} \qquad \forall h,t \tag{5.19}$$

### 5.2.2 Lower Level: Market Clearing

In this level, the market clearing process is modeled considering the offers and bids of all generators, customers and PHES. The objective function is to maximize the social welfare,

given as follows:

$$
\begin{aligned}
J_L = \sum_{t=1}^{T} \Big\{ & \sum_{j=1}^{J} C_{s,j}^{D} P_{s,j,t}^{D} \\
& + \sum_{h=1}^{Nh} \Big[ \beta_{h,t}^{HP} P_{s,h,t}^{HP} - \beta_{h,t}^{HG} P_{s,h,t}^{HG} - \beta_{h,t}^{H,uR} R_{s,h,t}^{H,u} - \beta_{h,t}^{H,uM} M_{s,h,t}^{H,u} - \beta_{h,t}^{H,dR} R_{s,h,t}^{H,d} - \beta_{h,t}^{H,dM} M_{s,h,t}^{H,d} \Big] \\
& - \sum_{i=1}^{I} \Big[ C_{s,i}^{g} P_{s,i,t}^{g} + C_{s,i}^{g,uR} R_{s,i,t}^{g,u} + C_{s,i}^{g,uM} M_{s,i,t}^{g,u} + C_{s,i}^{g,dR} R_{s,i,t}^{g,d} + C_{s,i}^{g,dM} M_{s,i,t}^{g,d} \Big] \\
& - \sum_{w=1}^{W} \Big[ C_{s,w}^{RE} P_{s,w,t}^{RE} ] \Big\} \quad \forall s
\end{aligned} \tag{5.20}
$$

The following constraints are considered in the problem:

#### 5.2.2.1 System Requirements

The supply and demand balance, as well as the minimum regulation up/down capacity and mileage requirements, are formulated as follows:

$$
\sum_{i=1}^{I} P_{s,i,t}^{g} + \sum_{w=1}^{W} P_{s,w,t}^{RE} + \sum_{h=1}^{Nh} (P_{s,h,t}^{HG} - P_{s,h,t}^{HP}) - \sum_{j=1}^{J} P_{s,j,t}^{D} = 0 \quad : (\lambda_{s,t}^{E}) \quad \forall s,t \tag{5.21}
$$

$$
\sum_{i=1}^{I} R_{s,i,t}^{g,u/d} + \sum_{h=1}^{Nh} R_{s,h,t}^{H,u/d} \geq R_{s,t}^{sys,u/d} \quad : (\lambda_{s,t}^{u/d,R}) \quad \forall s,t \tag{5.22}
$$

$$
\sum_{i=1}^{I} M_{s,i,t}^{g,u/d} + \sum_{h=1}^{Nh} M_{s,h,t}^{H,u/d} \geq M_{s,t}^{sys,u/d} \quad : (\lambda_{s,t}^{u/d,M}) \quad \forall s,t \tag{5.23}
$$

The dual variables in parentheses in (5.21)-(5.23) represent the marginal prices of energy and regulation up/down capacity and mileage up/down services.

It is noted that transmission constraints can impact the planning (sizing and siting) and operation of ESS and the energy market prices [102]. However, because of the significant

computational challenges arising when the transmission constraints are considered, they are not included in the proposed MPEC model.

#### 5.2.2.2 PHES Strategic Operation

The PHES strategic operation at this level are constrained by the offers and bids determined at the upper level, as follows:

$$0 \leq P^{HP}_{s,h,t} \leq \hat{P}^{HP}_{h,t} \qquad : (\mu^{HP^{min}}_{s,h,t}, \mu^{HP^{max}}_{s,h,t}) \qquad \forall s,h,t \tag{5.24}$$

$$0 \leq P^{HG}_{s,h,t} \leq \hat{P}^{HG}_{h,t} \qquad : (\mu^{HG^{min}}_{s,h,t}, \mu^{HG^{max}}_{s,h,t}) \qquad \forall s,h,t \tag{5.25}$$

$$0 \leq R^{H,u/d}_{s,h,t} \leq \hat{R}^{H,u/d}_{h,t} : (\mu^{HUR/HDR^{min}}_{s,h,t}, \mu^{HUR/HDR^{max}}_{s,h,t}) \;\; \forall s,h,t \tag{5.26}$$

$$\hat{R}^{H,u/d}_{h,t} \leq M^{H,u/d}_{s,h,t} \leq \hat{M}^{H,u/d}_{h,t} : (\mu^{HUM/HDM^{min}}_{s,h,t}, \mu^{HUM/HDM^{max}}_{s,h,t}) \;\; \forall s,h,t \tag{5.27}$$

#### 5.2.2.3 Generators and Customers Quantity Offers/Bids

The energy and regulation market clearing dispatches of generation and customer loads are constrained by their respective offer/bid quantities. It is assumed that the hourly demand and RES offer/bid quantities are based on their forecasted values in the deterministic case and the simulated scenario in the stochastic case, while traditional generator offer quantities are their rated capacities, and remain unchanged over the operational period.

$$\underline{P}^{D}_{j} \leq P^{D}_{s,j,t} \leq \overline{P}^{D}_{j} \qquad : (\mu^{D^{min}}_{s,j,t}, \mu^{D^{max}}_{s,j,t}) \qquad \forall s,j,t \tag{5.28}$$

$$0 \leq P^{RE}_{s,w,t} \leq \overline{P}^{RE}_{s,w,t} \qquad : (\mu^{RE^{min}}_{s,w,t}, \mu^{RE^{max}}_{s,w,t}) \qquad \forall s,w,t \tag{5.29}$$

$$\underline{P}^{g}_{i} \leq P^{g}_{s,i,t} \leq \overline{P}^{g}_{i} \qquad : (\mu^{g^{min}}_{s,i,t}, \mu^{g^{max}}_{s,i,t}) \quad \forall s,i,t \tag{5.30}$$

$$0 \leq R^{g,u/d}_{s,i,t} \leq \overline{R}^{g,u/d}_{i} : (\mu^{g,ur/dr^{min}}_{s,i,t}, \mu^{g,ur/dr^{max}}_{s,i,t}) \quad \forall s,i,t \tag{5.31}$$

$$P^{g}_{s,i,t} + R^{g,u}_{s,i,t} \leq \overline{P}^{g}_{i} \qquad : (\mu^{g^{up}}_{s,i,t}) \qquad \forall s,i,t \tag{5.32}$$

$$\underline{P}^{g}_{i} \leq P^{g}_{s,i,t} - R^{g,d}_{s,i,t} \qquad : (\mu^{g^{dn}}_{s,i,t}) \qquad \forall s,i,t \tag{5.33}$$

$$R^{g,u/d}_{s,i,t} \leq M^{g,u/d}_{s,i,t} \leq m^{g,u/d}_{i} R^{g,u/d}_{s,i,t} \qquad : (\mu^{g,um/dm^{min}}_{s,i,t}, \mu^{g,um/dm^{max}}_{s,i,t}) \qquad \forall s,i,t \tag{5.34}$$

The generation and demand quantities cleared in the energy market are upper-bounded by their offers/bids, while their lower bounds are specified by their minimum power limits (5.28)-(5.30). The cleared regulation up/down capacities are upper-bounded by their maximum bids and the generators' rating, net of the cleared quantity in the energy market (5.31)-(5.33). The cleared regulation up/down mileage quantities are limited by their cleared regulation capacity and mileage multipliers (5.34).

## 5.3 Proposed MPEC Problem

The MPEC problem comprises the objective function defined in (5.1) and subject to the upper level constraints, (5.2)-(5.17) for the HSC PHES and (5.2)-(5.19) for the conventional PHES. Furthermore, the Karush-Kuhn-Tucker (KKT) conditions derived from the Lagrangian of the lower level problem are considered in the MPEC problem, which will be presented in Section 5.3.1.

The complementarity conditions associated with the inequality constraints of the lower level problem are non-linear. Therefore, additional constraints and binary variables are used to linearize them, following the same approach used in other MPEC problems [15–18].

Furthermore, the non-linear objective function in (5.1) is linearized by equating the primal and dual objective functions using the strong duality theorem [103] since the lower level problem is convex and linear. The linearization of the MPEC model will be discussed in Section 5.3.2.

It is noted that this MPEC model is solved from the perspective of one agent, *i.e.* the PHES facility, and hence assuming the PHES can anticipate the market clearing and

other market participants do not change their strategies. However, in practice, the other generation utilities also have the ability to anticipate the market and may change their strategies. Because of the computational issues, this proposed framework did not consider the interaction between several strategic players who can anticipate the market. This can be solved using Equilibrium Problem with Equilibrium Constraints (EPEC) framework, which is computationally more challenging than the MPEC problem.

### 5.3.1 KKT Conditions of the Lower Level Problem

For the lower level problem, defined by (5.20)-(5.34), the KKT conditions for optimality comprise stationary, primal feasibility, dual feasibility, and complementary slackness conditions [103]. The stationary conditions are formulated, as follows:

$$-\beta_{h,t}^{HP} + \lambda_{s,t}^{E} - \mu_{s,h,t}^{HP^{min}} + \mu_{s,h,t}^{HP^{max}} = 0 \qquad \forall s, h, t \tag{5.35}$$

$$\beta_{h,t}^{HG} - \lambda_{s,t}^{E} - \mu_{s,h,t}^{HG^{min}} + \mu_{s,h,t}^{HG^{max}} = 0 \qquad \forall s, h, t \tag{5.36}$$

$$\beta_{h,t}^{H,u/dR} - \lambda_{s,t}^{u/d,R} - \mu_{s,h,t}^{HUR/HDR^{min}} + \mu_{s,h,t}^{HUR/HDR^{max}} = 0 \qquad \forall s, h, t \tag{5.37}$$

$$\beta_{h,t}^{H,u/dM} - \lambda_{s,t}^{u/d,M} - \mu_{s,h,t}^{HUM/HDM^{min}} + \mu_{s,h,t}^{HUM/HDM^{max}} = 0 \qquad \forall s, h, t \tag{5.38}$$

$$-C_{s,j}^{D} + \lambda_{s,t}^{E} - \mu_{s,j,t}^{D^{min}} + \mu_{s,j,t}^{D^{max}} = 0 \qquad \forall s, j, t \tag{5.39}$$

$$C_{s,w}^{RE} - \lambda_{s,t}^{E} - \mu_{s,w,t}^{RE^{min}} + \mu_{s,w,t}^{RE^{max}} = 0 \qquad \forall s, w, t \tag{5.40}$$

$$C_{s,i}^{g} - \lambda_{s,t}^{E} - \mu_{s,i,t}^{g^{min}} + \mu_{s,i,t}^{g^{max}} + \mu_{s,i,t}^{g^{up}} - \mu_{s,i,t}^{g^{dn}} = 0 \qquad \forall s, i, t \tag{5.41}$$

$$C^{g,uR}_{s,i} - \lambda^{u,R}_{s,t} - \mu^{g,ur^{min}}_{s,i,t} + \mu^{g,ur^{max}}_{s,i,t} + \mu^{g^{up}}_{s,i,t} + \mu^{g,um^{min}}_{s,i,t} - m^{g,u}_{i}\mu^{g,um^{max}}_{s,i,t} = 0 \quad \forall s,i,t \tag{5.42}$$

$$C^{g,dR}_{s,i} - \lambda^{d,R}_{s,t} - \mu^{g,dr^{min}}_{s,i,t} + \mu^{g,dr^{max}}_{s,i,t} + \mu^{g^{dn}}_{s,i,t} + \mu^{g,dm^{min}}_{s,i,t} - m^{g,d}_{i}\mu^{g,dm^{max}}_{s,i,t} = 0 \quad \forall s,i,t \tag{5.43}$$

$$C^{g,u/dM}_{s,i} - \lambda^{u/d,M}_{s,t} - \mu^{g,um/dm^{min}}_{s,i,t} + \mu^{g,um/dm^{max}}_{s,i,t} = 0 \quad \forall s,i,t \tag{5.44}$$

The primal feasibility conditions comprise the equality constraint (5.21) and the inequality constraints (5.22)-(5.34); the latter can be formulated as $0 \leq \mathcal{K}$. Hence, the dual feasibility conditions can be formulated as $0 \leq \mu^{\mathcal{K}}$, where $\mu^{\mathcal{K}}$ denotes the dual variable associated with the inequality constraint. The KKT complementary slackness conditions are formulated as $\mathcal{K}\mu^{\mathcal{K}} = 0$.

It is noted that the primal feasibility conditions for the inequality constraints and their associated dual feasibility and complementary slackness conditions can be formulated as follows:

$$0 \leq \mathcal{K} \quad \perp \quad 0 \leq \mu^{\mathcal{K}} \tag{5.45}$$

For example, the KKT conditions corresponding to the upper-bound limits in (5.24) are formulated as follows:

$$0 \leq \hat{P}^{HP}_{h,t} - P^{HP}_{s,h,t} \quad \perp \quad 0 \leq \mu^{HP^{max}}_{s,h,t} \qquad \forall s,h,t \tag{5.46}$$

The set of KKT conditions represented by (5.45) are linearized considering each constraint separately, *i.e.* $0 \leq \mathcal{K}$ and $0 \leq \mu^{\mathcal{K}}$, in addition to the following constraints:

$$\mathcal{K} \leq M(1 - Z^{\mathcal{K}}) \tag{5.47}$$

$$\mu^{\mathcal{K}} \leq M\ Z^{\mathcal{K}} \tag{5.48}$$

where $Z^{\mathcal{K}}$ is a vector of binary variables.

### 5.3.2 Linearization of the MPEC Objective Function

The MPEC problem comprises the upper level problem in which the PHES maximizes its profit from market participation considering the market prices determined from the lower level market clearing problem. Since the lower level problem is linear and convex, the primal and dual optimal objective function values are equal, which can be used, along with the KKT conditions of the lower level problem, to derive a relation for the PHES market clearing decisions in terms of the other participants' clearing decisions. Therefore, the bilinear product of the market prices and the PHES cleared quantities in the MPEC objective function (5.1) can be substituted by linear terms obtained by the derived relation.

In the primal objective function of the lower level problem (5.20), the PHES offers/bids ($\beta^{HP}$,$\beta^{HG}$,$\beta^{H,u/dR}$, and $\beta^{H,u/dM}$) are substituted using the KKT conditions (5.35)-(5.38), as follows:

$$\begin{aligned} J_L^{Primal} = \sum_{t=1}^{T}\Big\{ \sum_{j=1}^{J} C_{s,j}^{D} P_{s,j,t}^{D} + \sum_{h=1}^{Nh} \Big[ (\lambda_{s,t}^{E} - \mu_{s,h,t}^{HP^{min}} + \mu_{s,h,t}^{HP^{max}}) P_{s,h,t}^{HP} - (\lambda_{s,t}^{E} + \mu_{s,h,t}^{HG^{min}} \\ - \mu_{s,h,t}^{HG^{max}}) P_{s,h,t}^{HG} - (\lambda_{s,t}^{u,R} + \mu_{s,h,t}^{HUR^{min}} - \mu_{s,h,t}^{HUR^{max}}) R_{s,h,t}^{H,u} - (\lambda_{s,t}^{u,M} + \mu_{s,h,t}^{HUM^{min}} \\ - \mu_{s,h,t}^{HUM^{max}}) M_{s,h,t}^{H,u} - (\lambda_{s,t}^{d,R} + \mu_{s,h,t}^{HDR^{min}} - \mu_{s,h,t}^{HDR^{max}}) R_{s,h,t}^{H,d} - (\lambda_{s,t}^{d,M} + \mu_{s,h,t}^{HDM^{min}} \\ - \mu_{s,h,t}^{HDM^{max}}) M_{s,h,t}^{H,d} \Big] - \sum_{i=1}^{I} \Big[ C_{s,i}^{g} P_{s,i,t}^{g} + C_{s,i}^{g,uR} R_{s,i,t}^{g,u} + C_{s,i}^{g,uM} M_{s,i,t}^{g,u} + C_{s,i}^{g,dR} R_{s,i,t}^{g,d} \\ + C_{s,i}^{g,dM} M_{s,i,t}^{g,d} \Big] - \sum_{w=1}^{W} \Big[ C_{s,w}^{RE} P_{s,w,t}^{RE} \Big] \Big\} \quad \forall s \end{aligned} \tag{5.49}$$

It is noted from (5.47) and (5.48) that $\mathcal{K}\,\mu^{\mathcal{K}} = 0$. Therefore, the terms ($\mu^{HG/HP^{min}} P^{HG/HP}$) and ($\mu^{HUR/HDR^{min}} R^{H,u/d}$) are zeros, while the following terms can be substituted in the primal objective:

$$\mu^{HG/HP^{max}} P^{HG/HP} = \mu^{HG/HP^{max}} \hat{P}^{HG/HP} \tag{5.50}$$

$$\mu^{HUR/HDR^{max}} R^{H,u/d} = \mu^{HUR/HDR^{max}} \hat{R}^{H,u/d} \tag{5.51}$$

$$\mu^{HUM/HDM^{min}} M^{H,u/d} = \mu^{HUM/HDM^{min}} \hat{R}^{H,u/d} \tag{5.52}$$

$$\mu^{HUM/HDM^{max}} M^{H,u/d} = \mu^{HUM/HDM^{max}} \hat{M}^{H,u/d} \tag{5.53}$$

Accordingly, the primal objective function is given as follows:

$$\begin{aligned} J_L^{Primal} = \sum_{t=1}^{T} \Big\{ & \sum_{j=1}^{J} C_{s,j}^{D} P_{s,j,t}^{D} + \sum_{h=1}^{Nh} \Big[ \lambda_{s,t}^{E} P_{s,h,t}^{HP} + \mu_{s,h,t}^{HP^{max}} \hat{P}_{h,t}^{HP} - \lambda_{s,t}^{E} P_{s,h,t}^{HG} + \mu_{s,h,t}^{HG^{max}} \hat{P}_{h,t}^{HG} \\ & - \lambda_{s,t}^{u,R} R_{s,h,t}^{H,u} + \mu_{s,h,t}^{HUR^{max}} \hat{R}_{h,t}^{H,u} - \lambda_{s,t}^{u,M} M_{s,h,t}^{H,u} - \mu_{s,h,t}^{HUM^{min}} \hat{R}_{h,t}^{H,u} + \mu_{s,h,t}^{HUM^{max}} \hat{M}_{h,t}^{H,u} \\ & - \lambda_{s,t}^{d,R} R_{s,h,t}^{H,d} + \mu_{s,h,t}^{HDR^{max}} \hat{R}_{h,t}^{H,d} - \lambda_{s,t}^{d,M} M_{s,h,t}^{H,d} - \mu_{s,h,t}^{HDM^{min}} \hat{R}_{h,t}^{H,d} + \mu_{s,h,t}^{HDM^{max}} \hat{M}_{h,t}^{H,d} \Big] \\ & - \sum_{i=1}^{I} \Big[ C_{s,i}^{g} P_{s,i,t}^{g} + C_{s,i}^{g,uR} R_{s,i,t}^{g,u} + C_{s,i}^{g,uM} M_{s,i,t}^{g,u} + C_{s,i}^{g,dR} R_{s,i,t}^{g,d} + C_{s,i}^{g,dM} M_{s,i,t}^{g,d} \Big] \\ & - \sum_{w=1}^{W} \Big[ C_{s,w}^{RE} P_{s,w,t}^{RE} \Big] \Big\} \quad \forall s \end{aligned} \tag{5.54}$$

The dual objective function of the lower level problem is formulated as follows:

$$\begin{aligned} J_L^{Dual} = \sum_{t=1}^{T} \Big\{ & - \lambda_{s,t}^{u,R} R_{s,t}^{sys,u} - \lambda_{s,t}^{d,R} R_{s,t}^{sys,d} - \lambda_{s,t}^{u,M} M_{s,t}^{sys,u} - \lambda_{s,t}^{d,M} M_{s,t}^{sys,d} \\ & + \sum_{h=1}^{Nh} \Big[ \mu_{s,h,t}^{HP^{max}} \hat{P}_{h,t}^{HP} + \mu_{s,h,t}^{HG^{max}} \hat{P}_{h,t}^{HG} + \mu_{s,h,t}^{HUR^{max}} \hat{R}_{h,t}^{H,u} + \mu_{s,h,t}^{HDR^{max}} \hat{R}_{h,t}^{H,d} \\ & - \mu_{s,h,t}^{HUM^{min}} \hat{R}_{h,t}^{H,u} + \mu_{s,h,t}^{HUM^{max}} \hat{M}_{h,t}^{H,u} - \mu_{s,h,t}^{HDM^{min}} \hat{R}_{h,t}^{H,d} + \mu_{s,h,t}^{HDM^{max}} \hat{M}_{h,t}^{H,d} \Big] \\ & + \sum_{i=1}^{I} \Big[ - (\mu_{s,i,t}^{g^{min}} + \mu_{s,i,t}^{g^{dn}}) \underline{P}_{i}^{g} + (\mu_{s,i,t}^{g^{max}} + \mu_{s,i,t}^{g^{up}}) \overline{P}_{i}^{g} + \mu_{s,i,t}^{g,ur^{max}} \overline{R}_{i}^{g,u} + \mu_{s,i,t}^{g,dr^{max}} \overline{R}_{i}^{g,d} \Big] \\ & + \sum_{j=1}^{J} \Big[ - \mu_{s,j,t}^{D^{min}} \underline{P}_{j}^{D} + \mu_{s,j,t}^{D^{max}} \overline{P}_{j}^{D} \Big] + \sum_{w=1}^{W} \Big[ \mu_{s,w,t}^{RE^{max}} \overline{P}_{s,w,t}^{RE} \Big] \Big\} \quad \forall s \end{aligned} \tag{5.55}$$

Since the lower level problem is linear and convex, the primal and dual optimal

objectives are equal, as per the strong duality theorem. Equating the primal and dual objectives of the lower level problem (5.54) and (5.55), respectively, yields the following relation:

$$\sum_{t=1}^{T}\sum_{h=1}^{Nh}\Big[(\lambda_{s,t}^{E}P_{s,h,t}^{HG}+\lambda_{s,t}^{u,R}R_{s,h,t}^{H,u}+\lambda_{s,t}^{d,R}R_{s,h,t}^{H,d}+\lambda_{s,t}^{u,M}M_{s,h,t}^{H,u}+\lambda_{s,t}^{d,M}M_{s,h,t}^{H,d})-(\lambda_{s,t}^{E}P_{s,h,t}^{HP})\Big]=$$
$$\sum_{t=1}^{T}\Bigg\{\lambda_{s,t}^{u,R}R_{s,t}^{sys,u}+\lambda_{s,t}^{d,R}R_{s,t}^{sys,d}+\lambda_{s,t}^{u,M}M_{s,t}^{sys,u}+\lambda_{s,t}^{d,M}M_{s,t}^{sys,d}$$
$$-\sum_{i=1}^{I}\Big[C_{s,i}^{g}P_{s,i,t}^{g}+C_{s,i}^{g,uR}R_{s,i,t}^{g,u}+C_{s,i}^{g,uM}M_{s,i,t}^{g,u}+C_{s,i}^{g,dR}R_{s,i,t}^{g,d}+C_{s,i}^{g,dM}M_{s,i,t}^{g,d}$$
$$-(\mu_{s,i,t}^{g^{min}}+\mu_{s,i,t}^{g^{dn}})\underline{P}_{i}^{g}+(\mu_{s,i,t}^{g^{max}}+\mu_{s,i,t}^{g^{up}})\overline{P}_{i}^{g}+\mu_{s,i,t}^{g,ur^{max}}\overline{R}_{i}^{g,u}+\mu_{s,i,t}^{g,dr^{max}}\overline{R}_{i}^{g,d}\Big]$$
$$+\sum_{j=1}^{J}\Big[C_{s,j}^{D}P_{s,j,t}^{D}+\mu_{s,j,t}^{D^{min}}\underline{P}_{j}^{D}-\mu_{s,j,t}^{D^{max}}\overline{P}_{j}^{D}\Big]-\sum_{w=1}^{W}\Big[C_{s,w}^{RE}P_{s,w,t}^{RE}+\mu_{s,w,t}^{RE^{max}}\overline{P}_{s,w,t}^{RE}\Big]\Bigg\}\quad\forall s \tag{5.56}$$

Therefore, the relation derived in (5.56) is used to substitute the non-linear terms in the MPEC objective function (5.1).

## 5.4 Results and Discussions

### 5.4.1 Test System

The formulated MPEC optimization model is tested using the IEEE RTS [104]. The system comprises 26 generators and 17 customer demands. The six hydro units are replaced by a four-unit PHES facility. The RES are considered as negative loads which affects the net demand. It is assumed that the offers from the thermal generators and RES units are based on their marginal costs. The marginal cost of RES units are assumed to be zero, and hence they are price-taker participants. Table 5.1 shows the energy and regulation offers, and the mileage capability multipliers of the 26 thermal generators, categorized by their types.

It is noted that the resource-specific mileage multipliers ($m_i^{g,u}$,$m_i^{g,d}$) are determined by the ISO based on the historical performance of the resource [79]. The maximum regulation capacity of a unit is assumed 40% of its rating. The 17 customer bid prices in the energy market are all assumed to be 50 \$/MWh. The PHES comprises four identical units, and their parameters are given in Table 5.2. The hourly net demand, as a percentage of the peak demand, and system regulation requirements are given in Table 5.3. The hourly regulation mileage equals the regulation capacity times the system multipliers, shown in Table 5.3.

In the following sections, deterministic and stochastic case studies are considered, and the main aspects of each case are summarized in Table 5.4.

The impact of PHES presence, strategic and non-strategic market participation, and PHES operational aspects considering conventional and HSC PHES are demonstrated through five deterministic case studies (D1-D5). The market clearing model is solved in Case-D1 without the presence of PHES. The HSC PHES market participation is considered in Case-D2 and Case-D3, highlighting the differences between non-strategic and strategic participation. In Case-D4 and Case-D5, the non-strategic and strategic participation of conventional PHES are considered to highlight the impact of PHES type on the market outcomes.

The impact of uncertainty on net demand and rival generators' offers are demonstrated through four stochastic case studies (S1-S4). The stochastic case studies consider only the strategic operation of HSC PHES in order to highlight the impact of uncertainty on the market participation decisions. In Case-S1, the uncertainty in net demand is considered, while in Case-S2 and Case-S3, the uncertainty in rival generators' price and quantity offers, respectively, is considered. Case-S4 considers both the net demand and rival generators' offers uncertainties.

### 5.4.2 Deterministic Case Studies

In these cases, the system peak demand, net of the RES generation, is 3,000 MW, while the peak regulation up/down capacity requirement is 100 MW. The forecasted deterministic demand and RES generation profiles are presented in Figure 5.1.

Table 5.1: Generators Parameters

| Gen. | $\overline{P_i^g}$ (MW) | $C_i^g$ (\$/MWh) | $C_i^{g,u/dR}$ (\$/MW) | $C_i^{g,u/dM}$ (\$/MW) | $m_i^{g,u/d}$ |
|---|---|---|---|---|---|
| G1-G2 | 400 | 7 | 50 | 50 | 1 |
| G3-G6 | 155 | 20 | 8 | 1 | 1.5 |
| G7 | 350 | 22 | 10 | 2 | 3 |
| G8-G10 | 197 | 25 | 14 | 3 | 2.5 |
| G11-G14 | 76 | 29 | 17 | 4 | 3.5 |
| G15-G17 | 100 | 32 | 19 | 5 | 3 |
| G18-G21 | 20 | 36 | 24 | 8 | 2 |
| G22-G26 | 12 | 45 | 29 | 12 | 1 |

Table 5.2: PHES Parameters

| $\overline{P}_h^{HG/HP}$ | $\underline{P}_h^{HG}$ | $\overline{Q}_h^{HG/HP}$ | $\underline{Q}_h^{HG}$ | $\alpha$ | $\overline{V^H}$ | $\eta_G$,$\eta_P$ | $m_h^{h,u/d}$ |
|---|---|---|---|---|---|---|---|
| 10 MW | 3 MW | 14 $m^3$ | 4.2 $m^3$ | 0.71 MW/$m^3$ | 1120 $m^3$ | 90% | 4 |

Table 5.3: Hourly System Requirements

| Hour | 1 | 2 | 3 | 4 | 5 | 6 | 7 | 8 | 9 | 10 | 11 | 12 |
|---|---|---|---|---|---|---|---|---|---|---|---|---|
| % of peak | 67 | 63 | 60 | 59 | 59 | 60 | 74 | 86 | 95 | 96 | 96 | 95 |
| Mileage multip. | 1 | 1.2 | 1.3 | 1 | 1.4 | 1.8 | 2 | 2.3 | 2.5 | 2.6 | 2.7 | 2.5 |
| Hour | 13 | 14 | 15 | 16 | 17 | 18 | 19 | 20 | 21 | 22 | 23 | 24 |
| % of peak | 95 | 95 | 93 | 94 | 99 | 100 | 100 | 96 | 91 | 83 | 73 | 63 |
| Mileage multip. | 2.8 | 2.9 | 2.4 | 2.9 | 2.9 | 2.5 | 2.4 | 2.9 | 2.5 | 2.3 | 1.9 | 1.6 |

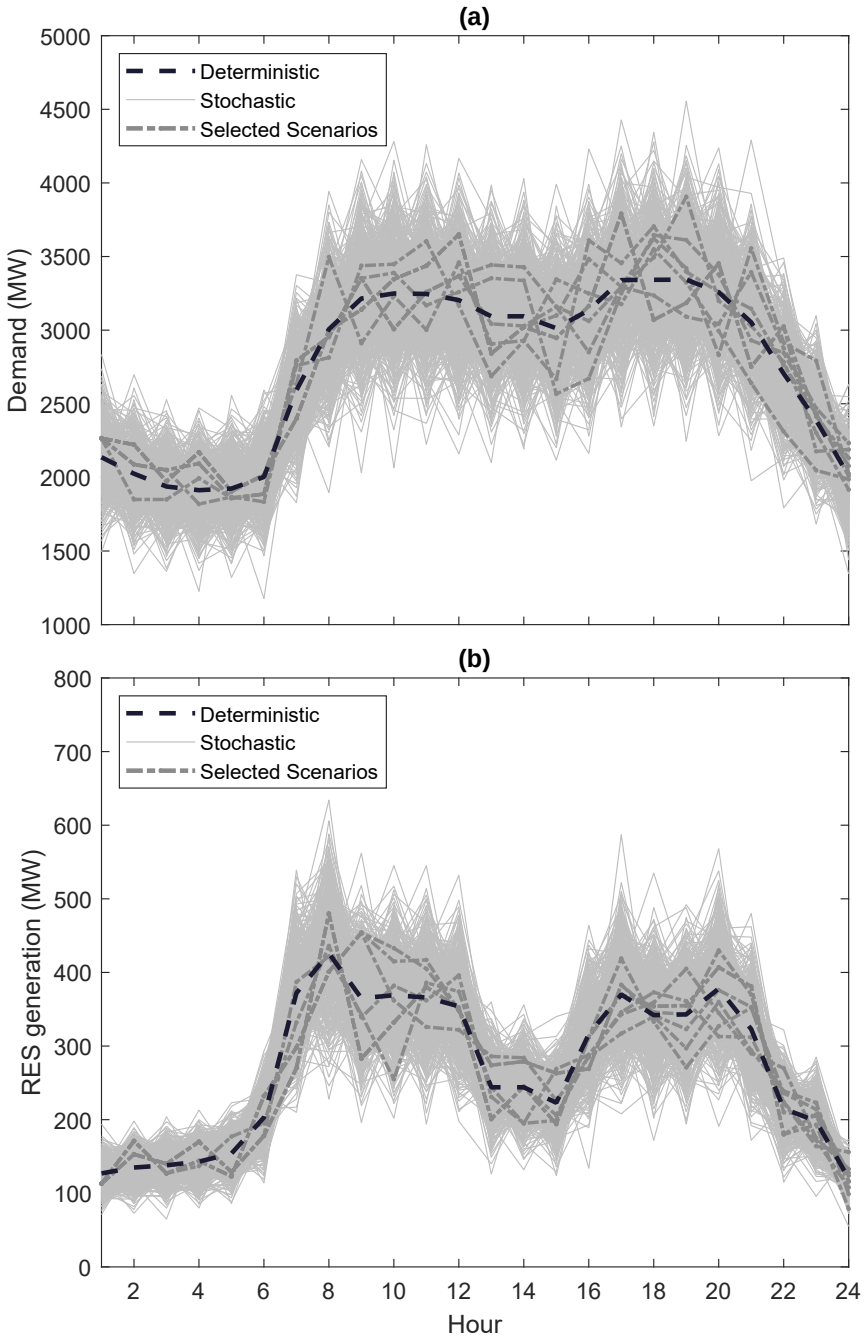


Figure 5.1: The forecasted deterministic profiles, and the 500 simulated profiles for stochastic analysis: (a) Demand profiles (b) RES generation profiles.

Table 5.4: Case Studies Overview

| | Case | PHES Type | Market Participation | Uncertainty |
|---|---|---|---|---|
| Deterministic | D1 | No PHES | - | - |
| | D2 | HSC | Non-strategic | - |
| | D3 | HSC | Strategic | - |
| | D4 | Conventional | Non-strategic | - |
| | D5 | Conventional | Strategic | - |
| Stochastic | S1 | HSC | Strategic | RES, demand |
| | S2 | HSC | Strategic | Rivals' price offers |
| | S3 | HSC | Strategic | Rivals' quantity offers |
| | S4 | HSC | Strategic | RES, demand, and rivals' price/quantity offers, simultaneously |

#### 5.4.2.1 Case-D1

In this case, without PHES participation, the market is settled considering the lower level optimization model to maximize the social welfare and simultaneously include energy, regulation capacity and mileage. Therefore, the system requirements are met by the thermal generators only, as shown in Table 5.5, and yields a social welfare of $1,760,664. Figure 5.2 depicts the participation of each generator in energy and regulation-up capacity markets, while the regulation-down capacity share of these generators are identical to their regulation-up capacity.

It is noted that the energy market clearing prices (Figure 5.3) match the offers of the marginal generators (shown in column-3 of Table 5.1). On the contrary, since the regulation up/down capacity and mileage are coherently linked, these market clearing prices (Figure 5.3) may not match the offers of the thermal generators (shown in column-4 and 5 of Table 5.1). For example, in hour-1, the regulation-up capacity price is 13 $/MW since an additional unit of regulation-up capacity is met by reducing the energy market dispatch of G6 (offer price, $20), and increasing its participation in regulation (offer price, $8), while also increasing the generation of the marginal generator G9 by 1 MW (offer price, $25).

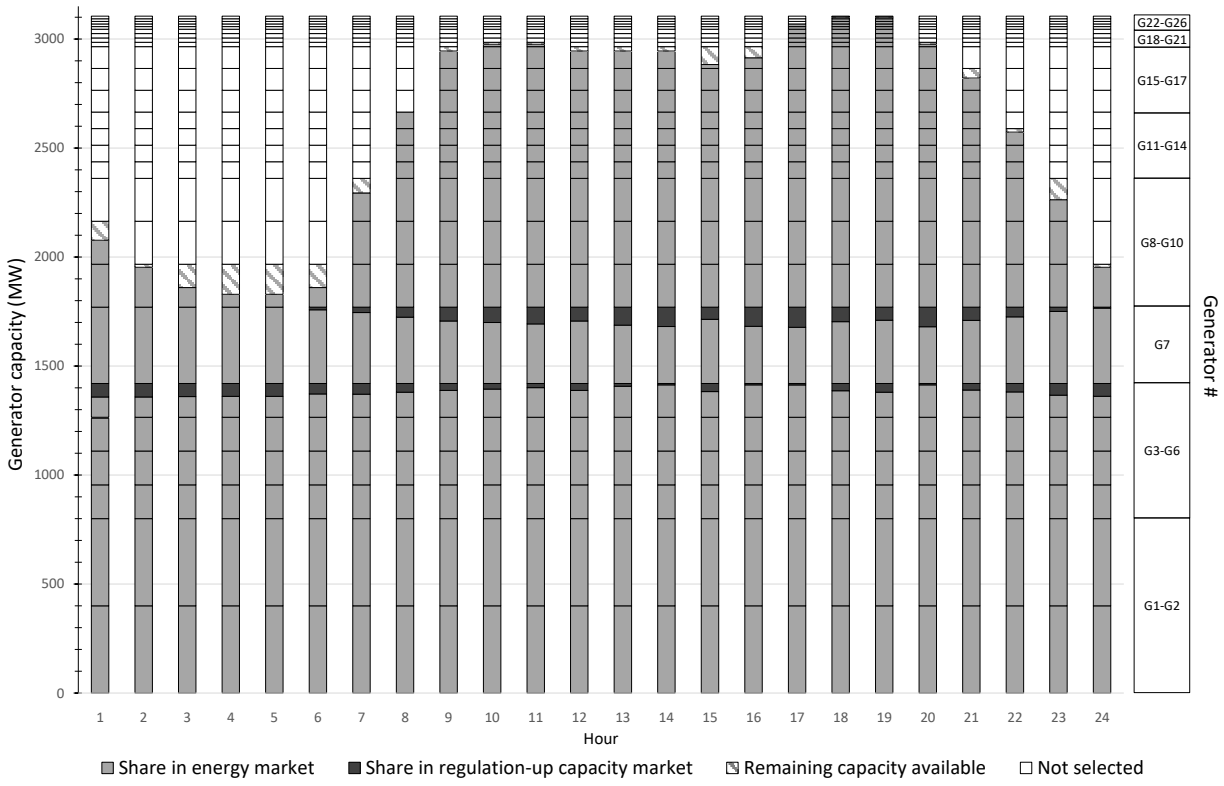


Figure 5.2: The participation of generators in energy and regulation-up capacity markets in Case-D1.

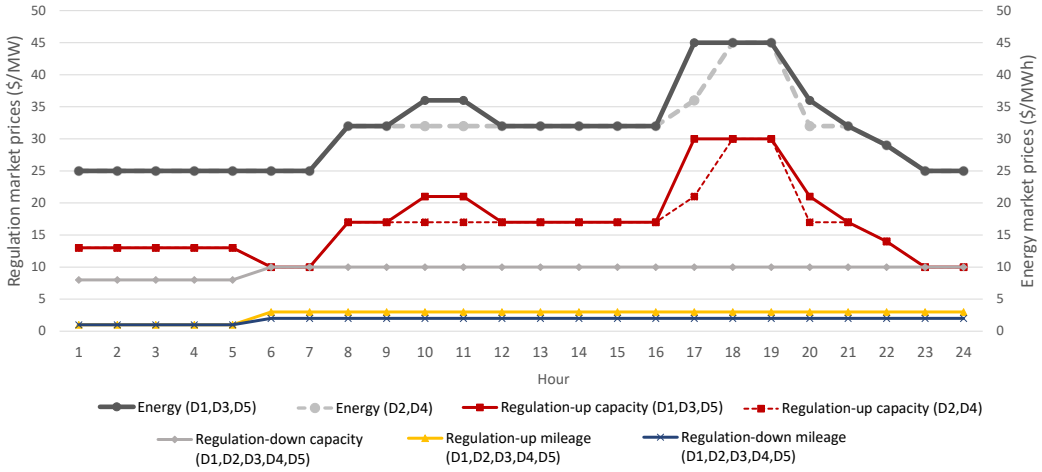


Figure 5.3: Energy and regulation market prices in the deterministic case studies.

Therefore, the impact on the objective function is: (-20+8+25) which is 13 $/MW.

The regulation market clearing price may need to be determined by adjusting more than two generators. For example, at hour-6, the least impact on the objective function when adding 1 MW of regulation-up capacity is by: a) reducing the output of G6 by 2 MW while increasing its regulation capacity and mileage by 2 MW and 3 MW, respectively, and (b) increasing the output of G7 by 1 MW while decreasing its regulation capacity and mileage by 1 MW and 3 MW, respectively, and (c) increasing the output of G8 by 1 MW. These changes will decrease the objective function by $10, which is the regulation market clearing price.

Note that in hours 1-5, the regulation capacity and mileage requirement is met by the least-expensive generator G6, only. For the other hours, including hour-6 discussed above, adjustments in multiple generators are required because of the limited mileage capability of G6 (which is 1.5, as given in Table 5.1). In hour-6, the mileage required is 1.8 times the regulation capacity of 60 MW, which is shared by G6 and G7, where G6 accounts for 72 MW of regulation mileage while G7 for the remaining 36 MW, as shown in Figure 5.4.

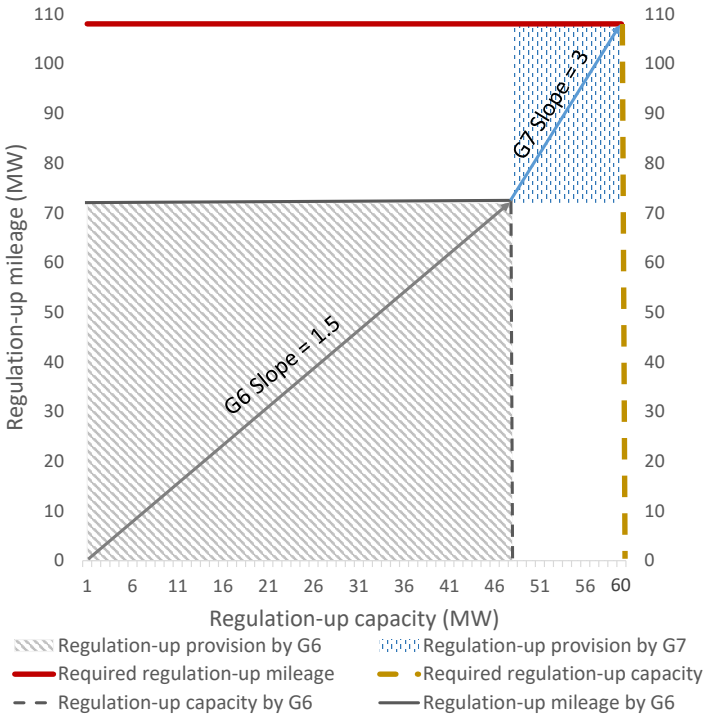


Figure 5.4: Regulation-up capacity and mileage share at hour 6 (Case-D1).

#### 5.4.2.2 Case-D2

In this case, when the PHES is considered a price-taker (non-strategic) participant, the lower level problem is only solved, but by including the constraints of the HSC PHES from the upper level problem, (5.2)-(5.17). The PHES energy and regulation sell offers are assumed to be zero, because it is a price-taker, whereas its energy buy bid price is assumed 50 $/MWh, which is at par with the load side participants.

It is noted from the obtained solution that the PHES helps in increasing the social welfare by about 2.5% from Case-D1, as shown in Table 5.5. The total thermal generation has increased, while the total cleared thermal capacities in the different regulation markets are reduced. The PHES participates more in the regulation-down market (207 MW as against 163 MW in regulation-up) since most of its capacity is cleared in the energy market, thus leaving less capacity for regulation-up provisions.

The impact of PHES on the market prices is shown in Figure 5.3. During the off-peak hours, the PHES operates in pumping mode, which increases the output of the marginal generators, but with no impact on the market prices, while during peak hours, the energy generated by the PHES helps in reducing the market price. For example, in Case-D1 during hour 10, the marginal generator G18 generated 11 MW, which is not required in Case-D2 when the PHES generates 28 MW. This change in schedule renders G17 the marginal generator. Since the PHES does not act strategically, the market clearing price is reduced to 32 $/MWh during this hour.

Furthermore, the PHES also helps in reducing the regulation market price. From the market operator's perspective, to maximize the social welfare, the least expensive generator is selected to provide both the regulation capacity and mileage. However, when the mileage capability of the least expensive generator does not meet the mileage requirement, the next expensive generator is selected to provide the excess mileage and the corresponding regulation capacity. In the case of PHES, the mileage capability is large but the regulation capacity is limited. Therefore, the participation of PHES in regulation markets allows the system to increase the share of the least expensive generator, while the excess mileages are provided by the combination of PHES and the next least expensive generator.

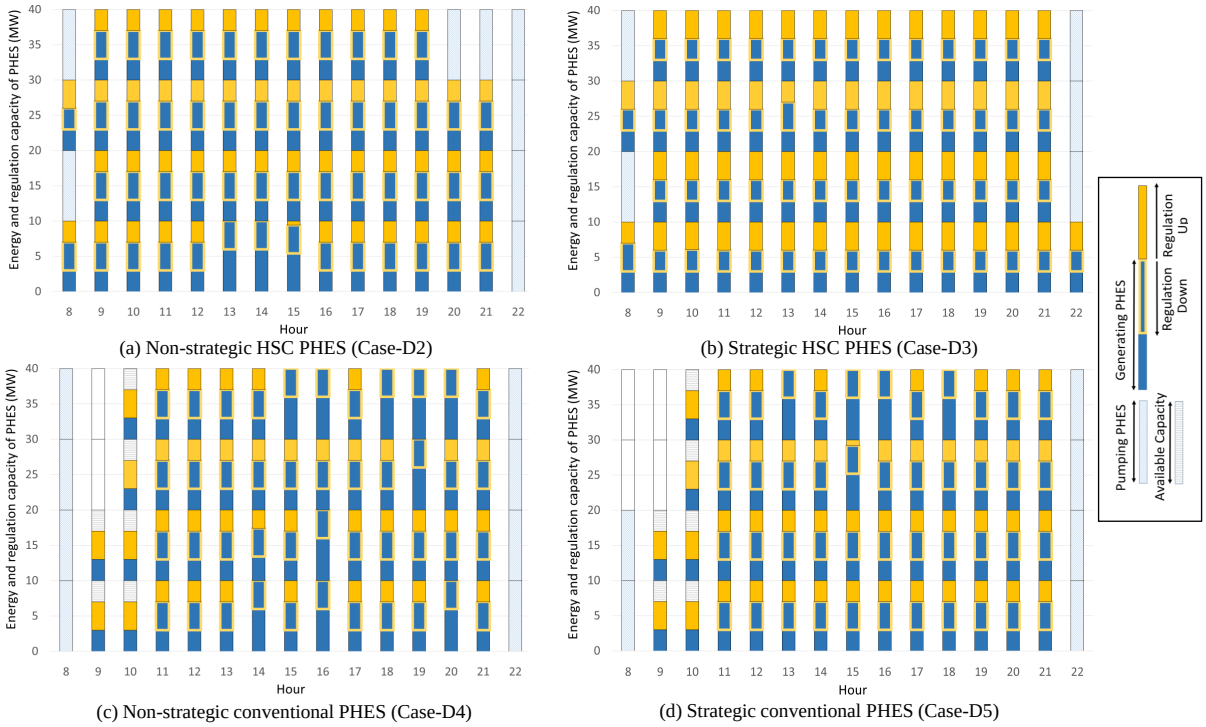


(a) Non-strategic HSC PHES (Case-D2)

(b) Strategic HSC PHES (Case-D3)

(c) Non-strategic conventional PHES (Case-D4)

(d) Strategic conventional PHES (Case-D5)

Figure 5.5: Comparison of the HSC and conventional PHES for non-strategic and strategic operations.

Table 5.5: Deterministic Market Clearing Results

| Case No. | Case-D1 | Case-D2 | Case-D3 | Case-D4 | Case-D5 |
|---|---|---|---|---|---|
| PHES Type | - | HSC | HSC | Conventional | Conventional |
| Market Participation | - | Non-strategic | Strategic | Non-strategic | Strategic |
| Total Thermal Generation [MWh] | 59,759 | 59,842 | 59,837 | 59,842 | 59,839 |
| Total PHES $P^{HG/HP}$ [MWh] | - | 357/440 | 332/410 | 357/440 | 340/420 |
| Total Cleared $R^{g,u/d}$ [MW] | 1,992/1,992 | 1,829/1,785 | 1,774/1,825 | 1,866/1,816 | 1,850/1,816 |
| Total Cleared $R^{H,u/d}$ [MW] | - | 163/207 | 218/167 | 126/176 | 142/176 |
| Total Cleared $M^{g,u/d}$ [MW] | 4,551/4,551 | 3,957/3,723 | 3,679/3,883 | 4,047/3,847 | 3,983/3,847 |
| Total Cleared $M^{H,u/d}$ [MW] | - | 594/828 | 872/668 | 504/704 | 568/704 |
| Social Welfare | $1,760,664 | $1,804,910 | $1,773,070 | $1,798,214 | $1,774,843 |
| PHES Profit | - | $8,660 | $10,434 | $7,955 | $9,338 |

#### 5.4.2.3 Case-D3

In this case, the PHES participates strategically in the market, and the proposed MPEC problem discussed in Section III is solved for the HSC PHES. The MPEC problem incorporates the KKT conditions of the lower level market clearing model into the PHES profit maximizing upper level problem. From the obtained solution, it is noted that the sell offers from the PHES ought to be the same as the market clearing prices of Case-D1, for it to maximize profit. Although, the social welfare increases in this case with participation of PHES, as compared to Case-D1, it is lower than that in Case-D2 because of its strategic behavior of seeking to maximize its profit (Table 5.5). Because of the higher regulation-up prices as compared to regulation-down (Figure 5.3), more PHES capacity is strategically cleared by the MPEC model for regulation-up, as shown in Table 5.5. Consequently, the energy market participation of PHES decreases in Case-D3. Overall, the strategic participation of PHES yields an increased profit of 20%, as compared to its non-strategic participation in Case-D2.

Since the PHES has a higher mileage capability than thermal generators, the system can still increase the share of the least expensive generator, as in Case-D2, and therefore increase the social welfare. However, the PHES minimizes the share of the second least expensive generator, particularly in mileage-up market, while offering at the system marginal price.

A comparison of the operations profile of the HSC PHES for its non-strategic (Case-D2) versus strategic (Case-D3) market participation, referring to Figure 5.5(a) and Figure 5.5(b), can be summarized as follows:

- Off-peak hours 1-7 and 23, 24: The PHES participates in the market as a load, operating in the pumping mode, in both cases. However, its 40 MW of pumping load is not significant enough, for the considered example, to influence the market price. Hence, the market outcomes from the non-strategic and strategic operation of the PHES during these hours are identical.

- Hours-8,9,12-16,18,19,21,22: The PHES can idle some units if only partial pumping

capacity is required, *i.e.* less than 40 MW. However, operating in the HSC mode, maximizes its profit since it allows some of its units to participate in up/down regulation provisions. The PHES operates in HSC mode before transitioning from pumping to generating, or vice versa, *i.e.* when the market prices are not high enough for generating or low enough that all its units are pumping. Since the PHES in Case-D2 generates more energy during all these hours compared to that in Case-D3, particularly notable during hours 13-15, the PHES is required to pump more water in Case-D2, to meet the terminal target of reservoir water level, by operating in HSC mode in hours 20-21 and in pumping mode in hour-22, as opposed to Case-D3 when it only operates in HSC mode in hour-22. During these hours, the PHES strategic operation differs from the non-strategic operation to maximize its profit, however, there is no impact on the market clearing prices.

- Hours-10,11,17,20: During these hours, the PHES has the capacity to impact the market clearing prices. In both cases, the PHES generation alters the thermal generation schedule, however, only in Case-D3, the PHES offers higher price, matching the marginal generator of Case-D1 to maximize the profit.

#### 5.4.2.4 Case-D4

This case is similar to Case-D2 but considers a conventional PHES. The lower level problem is solved but including the upper level constraints of conventional PHES, (5.2)-(5.19). From the obtained solution, it is noted that the social welfare increased by 2.1% from Case-D1, as shown in Table 5.5. The market prices obtained in Case-D4 are identical to those in Case-D2, (Figure 5.3), and the cleared energy quantities in the two cases are also identical; however, the HSC PHES participates more in regulation provisions, as seen from Table 5.5 because of its higher flexibility as compared to the conventional. For example, the values of $R^{H,u/d}$ reduces from 163/207 MW to 126/176 MW, from HSC PHES to conventional PHES.

Since the first and terminal reservoir water volume should be at the same level, *i.e.* the ratio of total generation to total pumping, $P^{HG}/P^{HP}$, is always constant, as may be noted

from Table 5.5, and is equal to the round-trip efficiency of the PHES, which is 0.81 in the considered case study. Accordingly, note that the total generation is always constrained by the fixed pumping power of the PHES and the constraints on reservoir water volume. Therefore, since the conventional PHES cannot operate in HSC mode, this constrained generation requires idling some of its units at hour-9, as shown in Figure 5.5(c) and also operating at partial load during hours 9-10.

#### 5.4.2.5 Case-D5

The strategic participation of a conventional PHES is studied in this case. The MPEC model is solved by considering the conventional PHES upper level problem (5.2)-(5.19), and the linearized KKT of the lower level problem, as discussed in Section III. It is noted that the social welfare increases as compared to Case-D1 (without PHES), but is understandably lower than when the PHES is non-strategic (Case-D4), as shown in Table 5.5. Furthermore, the PHES profit increases because of the strategic bidding in Case-D5 as compared to Case-D4 by about 17%. Note that the market clearing prices are identical for the strategic operation of conventional PHES (Case-D5) and HSC PHES (Case-D3) (Figure 5.3).

From Table 5.5, it is seen that the conventional PHES provides 142/176 MW of regulation-up/down capacity, while the HSC PHES provides 218/167 MW of the same, respectively. Therefore, it can be inferred that the conventional PHES does not exploit the higher regulation-up prices unlike the HSC PHES. This can be attributed to the lower degree of flexibility in conventional PHES in allocating the capacities according to the market prices.

Note also from Figure 5.5(d) that the strategic conventional PHES in Case-D5 idles two additional units when pumping at hour-8, as compared to its non-strategic operation in Case-D4, in order to reduce its generation at later hours while meeting the terminal hour reservoir water level target. Reducing generation allows the PHES to allocate more capacity to regulation-up which increases the profit of the strategic PHES.

Following are the observations on the operations of the conventional PHES vis-a-vis the HSC PHES:

- The type of PHES configuration (conventional or HSC) has no bearing on the electricity market prices. That means, non-strategic operation by HSC or conventional PHES results in identical market prices; and similarly, strategic operation by HSC and conventional yields another set of identical market prices.
- However, when a PHES facility (either HSC or conventional) transitions from non-strategic to strategic operation, the market prices increase at some hours; the impacts are identical with conventional or HSC PHES facilities.
- The HSC PHES has more flexibility in allocating its capacity to different markets according to their prices, while the conventional PHES operation is restricted by its need to idle some units during some hours, which impacts its capacity allocation in different markets.

### 5.4.3 Stochastic Case Studies

It was stated earlier that the PBR market provides more incentives for fast response resources, however, these benefits are subject to uncertainties, when considering stochastic power dispatch [105]. This section presents case studies to demonstrate the impact of uncertainty in net demand and in rival generators' offers on market settlement in the presence of PHES. For conciseness, only strategic market participation of an HSC PHES facility has been considered in these cases. The results of the stochastic cases, Case S1-S4, are discussed along with the corresponding deterministic case with strategic HSC PHES facility, Case-D3.

The uncertainty in demand and RES generation are modeled considering a time-independent normal pdf for each hour, with its mean being the forecasted value of the respective profile, which was considered for the deterministic case studies (Figure 5.1), and a standard deviation of 10% and 15% of the mean for the demand and RES generation, respectively. The uncertainty in each rival generator's price offers is modeled considering a uniform pdf with a range of 100% to 150% of the generator's marginal cost, while the uncertainty in quantity offers is modeled considering a uniform pdf with a maximum 10% withhold capacity of the unit rating. In this work, 500 scenarios of

uncertainty are generated, and the plot of the demand and RES generation profiles are shown in Figure 5.1. Because of the computational challenges of the MPEC problem, a scenario reduction is performed to select a representative subset of 8 scenarios using the backward reduction of scenario sets algorithm reported in [94]. In this technique, the full number of scenarios are initially selected, then scenarios are removed based on the distance between similar scenarios, *i.e.* if the distance between two scenarios is small, one of the two is deleted in the next iteration. The final selected set of scenarios of demand and RES generation are presented in Figure 5.1.

The MPEC problem is solved considering the KKT conditions of the lower level optimization problem pertaining to each scenario, and the optimal PHES strategy is obtained at the upper level problem considering all the scenarios.

#### 5.4.3.1 Case-S1

In this case, the uncertainty in demand and RES generation are considered using normal pdfs, whose parameters are stated above. On the other hand, the rival generator's offers are same as those used in the deterministic cases. The expected social welfare is \$1,838,413, and the expected profit of the PHES facility is \$12,556, as shown in Table 5.6. The expected profit of the PHES facility is higher in Case-S1 as compared to Case-D3, which can be attributed to the noticeably high expected values of energy market prices, at hours 9-12, the regulation-up capacity prices for the same hours, and also the overall increase in regulation-up mileage prices after hour-6 (Figure 5.6).

The PHES quantity offers/bids determined from the stochastic model solution, follow the same pattern as the deterministic case (Case-D3), shown in Figure 5.5(b), as can be noted from the expected values of the cleared PHES quantities in Table 5.6. However, the PHES price offers/bids are indeed impacted by the stochastic scenarios.

The obtained PHES generation price offers are lower than the expected and deterministic energy market prices, Figure 5.7, while the PHES pumping price bids are higher than the expected and deterministic energy market prices, Figure 5.8. This strategy ensures that the obtained PHES offers/bids are always cleared based on the

Table 5.6: Stochastic Market Clearing Results

| Case No. | Case-S1 | Case-S2 | Case-S3 | Case-S4 |
|---|---|---|---|---|
| Thermal Generation [MWh] | 60,255 | 59,763 | 59,595 | 59,477 |
| PHES $P^{HG/HP}$ [MWh] | 332/410 | 332/410 | 332/410 | 324/400 |
| Cleared $R^{g,u/d}$ [MW] | 1,775/1,827 | 1,782/1,822 | 1,779/1,825 | 1,769/1,836 |
| Cleared $R^{H,u/d}$ [MW] | 217/165 | 210/170 | 213/167 | 223/156 |
| Cleared $M^{g,u/d}$ [MW] | 3,683/3,891 | 3,711/3,871 | 3,699/3,883 | 3,659/3,927 |
| Cleared $M^{H,u/d}$ [MW] | 868/660 | 840/680 | 852/668 | 892/624 |
| Social Welfare | $1,838,413 | $1,566,990 | $1,628,619 | $1,511,556 |
| PHES Profit | $12,556 | $11,212 | $13,524 | $12,074 |

most conservative scenario of highest buying bid and lowest selling offer, which is required because of the need to meet the target reservoir water volume at the end of the day, in all the considered scenarios.

On the other hand, in the regulation-up capacity market, the PHES offer prices are lower than those in Case-D3, excluding some hours when prices are significantly high, *e.g.* hours 10 and 12 (Figure 5.9). At hours-10 and 12, the PHES takes a risk to offer higher prices to maximize its expected profit, accrued from the scenarios with high market prices, while the PHES regulation-up offers may not be selected in the scenarios with lower market prices.

It is observed that the impact of uncertainty in demand and RES generation on regulation-down capacity market prices is not significant. Furthermore, since the absolute difference in the mileage up/down market prices are very small, the PHES tends to submit conservative offers, which follow the same pattern of the deterministic mileage offers.

#### 5.4.3.2 Case-S2

The uncertainty in rivals' price offers is considered in this case, while the net demand

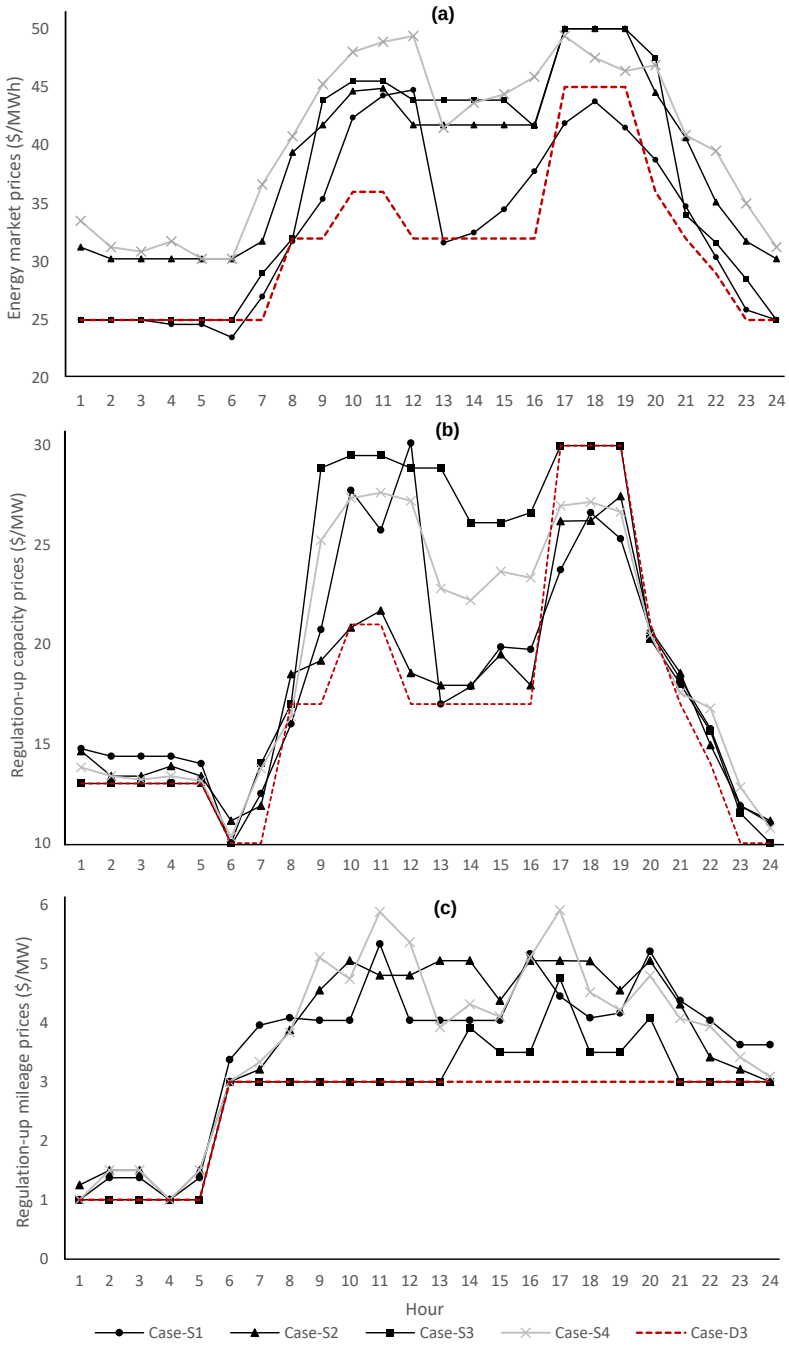


Figure 5.6: Impact of uncertainty on the market prices of (a) energy (b) regulation-up capacity (c) regulation-up mileage.

profile is same as in the deterministic studies. It is noted from the results in Table 5.6, the expected thermal generation is decreased as compared to the deterministic Case-D3 since the customers are not willing to buy from generators with offer prices above the demand price bid of 50 $/MWh. Therefore, the demand is reduced during some hours, which also yields a significant reduction in the expected social welfare.

On the other hand, the expected profit of the PHES increases by about 7.5% from that in Case-D3 because of the increase in market prices due to rival generators' bidding above their marginal cost in energy market and regulation-up capacity market Figure 5.6(a) and Figure 5.6(b). The impact of uncertainty in Case-S2 on the regulation-down capacity and up/down mileage markets is marginal.

#### 5.4.3.3 Case-S3

The uncertainty in rivals' quantity offers is considered in this case, while the net demand profile and the rivals' price offers remain the same as in the deterministic studies. The expected thermal generation, presented in Table 5.6, is decreased since the generators are withholding some of their capacities. Therefore, the expected social welfare has decreased too, as compared to Case-D3, but it is more than that in Case-S2 since the offer prices in Case-S3 are set at the generators' marginal prices.

The expected profit of the PHES increases by about 29.6% from that in Case-D3 because of the increase in market prices during only the peak hours, *i.e.* when the PHES is selling, due to the shortage of generation in energy market and regulation-up capacity market Figure 5.6(a) and Figure 5.6(b). There is a marginal impact of uncertainty in Case-S3 on the regulation-down capacity and up/down mileage markets.

It is noted that during the hours 1-6, 8, and 24, the impact of withholding the quantities is minimum on the market prices because there is enough available capacities from the marginal generator and also the generators with the same offer prices as the marginal generators, as shown in Figure 5.2. Because of the higher margin between the PHES pumping price and generating price, as compared to Case-S1 and Case-S2, the PHES profit is significantly increased in Case-S3.

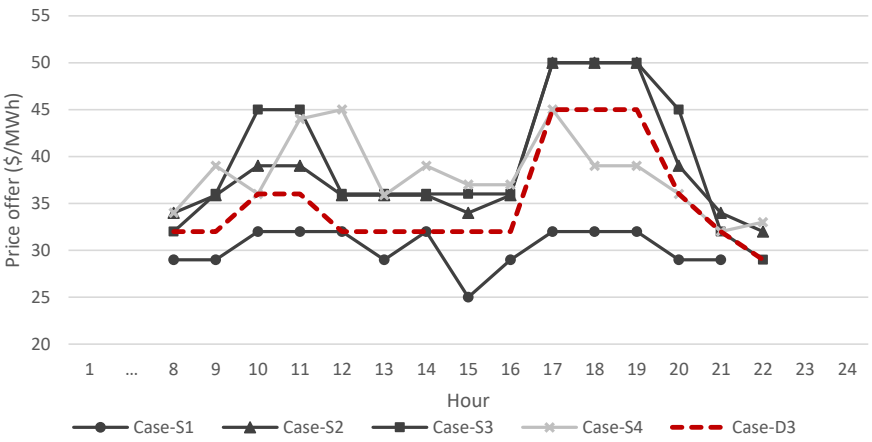


Figure 5.7: Stochastic PHES generating price offers.

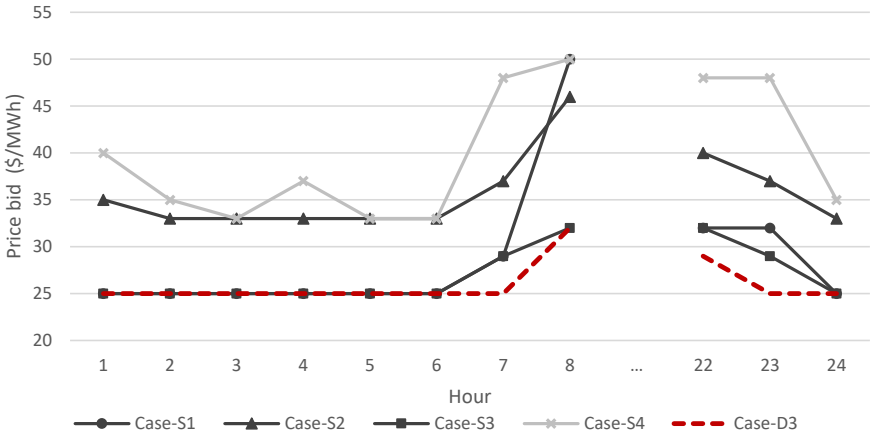


Figure 5.8: Stochastic PHES pumping price bids.

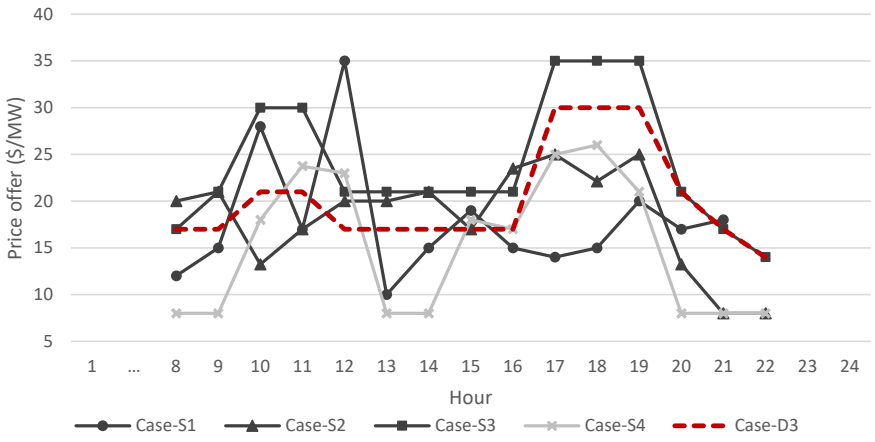


Figure 5.9: Stochastic PHES regulation-up capacity price offers.

#### 5.4.3.4 Case-S4

In this case, the uncertainty in net demand and rival generators' price/quantity offers are considered simultaneously. The expected values of the various decision variables are shown in Table 5.6. The expected thermal generation is reduced compared to Cases S1-S3 because of the high offer prices beyond the demand bids and the reduction in available capacities. The expected social welfare is reduced further, even lower than that in Case-S2 and Case-S3, since the generation offer prices are high in Case-S4, compared to Case-S3, and the cleared quantities are low, compared to Case-S2. It is noted that there is a slightly reduced participation of the PHES in energy and regulation-down markets, and a marginal increase in regulation-up markets compared to Cases S1-S3. The expected PHES profit is higher than Case-D3 by 15.7%, but less than that in Case-S3 because of the overall high prices even during pumping hours.

The energy market price profile of Case-S4 is similar to that of Case-S1, but is somewhat higher because of the increased prices from rival generators, Figure 5.6(a). Similarly, the regulation-up market prices are also impacted by both sources of uncertainty, Figure 5.6(b) and Figure 5.6(c).

Furthermore, the conservative strategy of the PHES in the energy market yields lower

generation offer prices as compared to Case-S2 and Case-S3, notable during the peak hours 17-20 (Figure 5.7), but generally higher than those in Case-S1. On the other hand, the PHES pumping bid prices in Case-S4 (Figure 5.8) are higher than Case S1-S3. It is noted that the optimal PHES regulation-up capacity offer price in Case-S4, shown in Figure 5.9, is low, in order to ensure clearing more quantity. Consequently, there is less participation of PHES in the energy market, and more in the regulation-up market, as compared to Case S1-S3, since the energy market prices in Case-S4 are higher at all hours, affecting both the energy revenue and cost.

### 5.4.4 Out-of-Sample Analysis

The PHES bidding decisions determined in the case studies S1-S4 are validated through an out-of-sample analysis considering all the 500 scenarios of uncertainty in RES generation, demand, and rivals' price/quantity offers. The optimal bids for the PHES obtained earlier from the proposed MPEC model were considered to be fixed, for this analysis.

Table 5.7 shows the average of social welfare and PHES profit obtained from the 500 scenarios, and their deviation from the expected values obtained from the MPEC model shown in Table 5.6. The average social welfare values are within less than 3.4% from the MPEC expected values, while the average PHES profit is decreased by at most 7% from the expected values obtained from the MPEC model.

The PHES profit for Case-S4 depicts a normal pdf as shown in Figure 5.10, with an average of \$11,491 and standard deviation of \$1,186. The histogram of PHES profit for Case-S4 is also presented in Figure 5.10, with a very close expected value of \$11,487.

### 5.4.5 Computational Aspects

The computational burden of MPEC problems is complex because of the large number of constraints in the bi-level models and the presence of non-linear constraints, which are linearized in this work using the big M method. The selection of the constant big M is important to avoid numerical ill-conditioning. In this work, the value of big M is selected

Table 5.7: Out-of-Sample Results

| | Case No. | Case-S1 | Case-S2 | Case-S3 | Case-S4 |
|---|---|---|---|---|---|
| Social | Average | $1,814,020 | $1,526,164 | $1,574,803 | $1,484,213 |
| Welfare | Deviation from MPEC | -1.3% | -2.7% | -3.4% | -1.8% |
| PHES | Average | $12,189 | $10,480 | $12,728 | $11,491 |
| Profit | Deviation from MPEC | -3% | -7% | -6% | -5% |

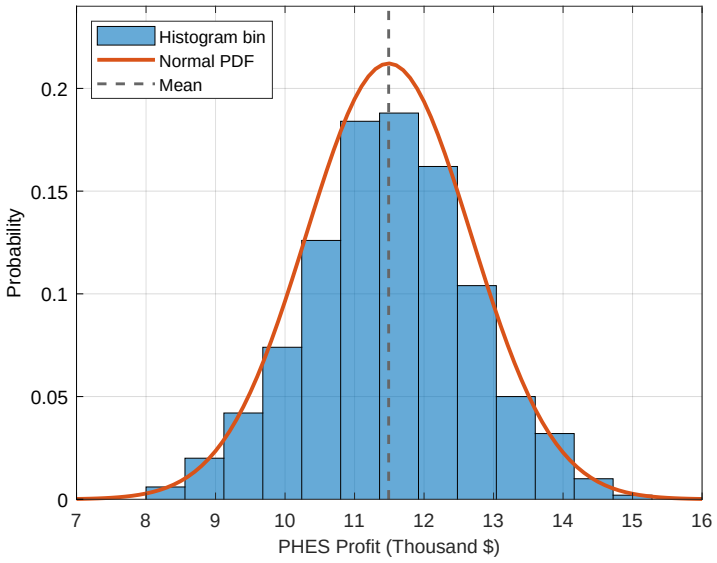


Figure 5.10: Histogram of the PHES profit considering its strategy determined from Case-S4.

using a trial-and-error approach. Initially, a large number is selected for the constant M, in which no feasible solution is obtained for the MPEC problem. Then, the value of M is reduced in small steps, until an optimal solution is found, while the obtained results are validated and the constraints are checked to hold. The optimal solution is also compared considering arbitrary different values of M to ensure that the MPEC problem is not ill-conditioned or that the solution obtained is not a suboptimal solution. As reported in [106], there is a risk of arriving at a suboptimal solution if the value of M is not selected properly. However, to the best of our knowledge, there is no reported effective method for the selection of M value that guarantees a global optimal solution for power system problems.

The proposed models are solved using the CPLEX solver in GAMS and executed on a server with 4 Intel-Xeon 1.87 GHz processors and 256 GB of RAM.

The optimization model in Case-D1 is a linear programming problem, and an optimal solution is obtained within 11 seconds. Since the PHES constraints are included in Case-D2 and Case-D4, these optimization models are formulated as MILP problems, and the solution times are 122 and 181 seconds, respectively. The MPEC problem in Cases D3 and D5, formulated as MILP models, are solved in 19 and 14 minutes, respectively.

The stochastic scenarios resulted in significant increase in the computational complexity of the MPEC problem. As discussed earlier, a scenario reduction technique was applied for case studies S1-S4, wherein 8 representative scenarios are considered. The solution times for Cases-S1, S2, S3, and S4 are 58, 33, 72, and 69 minutes, respectively. Since the proposed model is solved for the day-ahead problem, these computational times are within reasonable limits.

## 5.5 Summary

In this chapter, the ESS was considered to participate in a competitive electricity market, as is being discussed in several markets in USA and Canada. This is contrary to the ESS business models presented in Chapter 3 and Chapter 4 wherein the system operator centrally managed the ESS operation along with other generation resources and demand.

The objective of market clearing was to maximize the social welfare, while the PHES operator sought to maximize its profit from the market participation. Therefore, a bi-level MPEC framework was proposed to determine the optimal offers and bids of conventional and HSC PHES participating in joint energy-PBR markets. The effectiveness of the model was validated on the IEEE RTS considering deterministic and stochastic case studies.

# Chapter 6

# Conclusions

## 6.1 Summary

This thesis focused on the development of electricity market participation and investment planning frameworks for ESS considering different business models and ownership structures. The motivations for this research were presented in Chapter 1. A literature review of these topics was carried out to identify the main research objectives.

In Chapter 2, some essential background topics required for this research were discussed. The state-of-art energy storage technologies, systems, and their important properties and parameters were presented. An overview of ancillary services provision and ancillary services markets in North America (USA and Canada) was presented, followed by a brief discussion of some investment planning aspects for microgrids. Finally, uncertainty management techniques in power systems were presented.

In Chapter 3, a decomposition-based approach was proposed to determine the optimal year of installation and sizing of BESS in isolated microgrids. Uncertainties in demand and RES generation was considered, which yielded a comprehensive stochastic optimization model, that was computationally large. The proposed decomposition approach determined the optimal plan decisions in two stages. Energy capacity degradation was considered in a novel manner and implemented in Stage-II as a matrix of all possible capacities.

The budget limit affected the solution and did not allow installing a large BESS early. Therefore, the budget constraint was relaxed to ensure the optimal sizing decision, which was then imposed on the model in steps, until arriving at the optimal size and year of installation. Three case studies were conducted to highlight the optimal BESS decisions using deterministic optimization and by considering uncertainty using MCS and scenario-based stochastic optimization.

The proposed BESS planning framework was envisaged to be used by the microgrid community planners, the utility serving the microgrid, or governmental, non-governmental, and private agencies involved in planning, design, and development of microgrid energy management systems when the BESS was installed and operated by the MGO.

In Chapter 4, a new method based on goal programming approach was proposed to determine the BESS investment decisions by a third-party investor while it was operated and scheduled by the MGO. The proposed model was validated on the CIGRE microgrid test system considering different microgrid operational scenarios. The results demonstrated the effectiveness of the proposed work in determining if the storage installation accrued a reduction in the total microgrid operational costs and satisfied the investor MARR considering the microgrid generation mix and load profiles.

In Chapter 5, the ESS was considered to participate in a competitive electricity market, as is being discussed in several markets in USA and Canada. This is contrary to the ESS business models presented in Chapter 3 and Chapter 4 wherein the system operator centrally managed the ESS operation along with other generation resources and demand. The objective of market clearing was to maximize the social welfare, while the PHES operator sought to maximize its profit from the market participation. Therefore, a bi-level MPEC framework was proposed to determine the optimal offers and bids of conventional and HSC PHES participating in joint energy-PBR markets. The effectiveness of the model was validated on the IEEE RTS considering deterministic and stochastic case studies.

The following conclusions can be drawn from the thesis:

- The studies revealed that the optimal sizing, timing and scheduling of ESS determined by the proposed investment planning frameworks have contributed to a reduction in the microgrid's operational costs. In order to accurately examine such

impact of ESS, which have unique characteristics and inter-temporal constraints, *i.e.* the charging/discharging and SOC relations, it was important to consider the inter-temporal operational constraints of dispatchable units and the uncertainties in RES generation and demand.

- It was noted that the considered MCS method had the same plan decisions as the deterministic case, while the decisions obtained from the stochastic optimization model showed more robust results in different operational scenarios.

- The impact of BESS capacity degradation on the optimal plan decisions and the associated costs was examined. It was noted that the BESS capacity, without modeling its degradation, was smaller, and installation year was earlier. However, ignoring degradation in the planning model fails to capture the costs properly and the plan decisions resulted in higher microgrid operational cost than that obtained when degradation was considered within the planning model.

- When the BESS was installed by a third-party investor and operated by the MGO, the economic viability of such a business structure was dependent on the load profiles and generation mix which determined the economical value of the BESS installation.

- Both strategic and non-strategic participation of PHES in the energy-cum-PBR markets increased the social welfare, while the strategic HSC PHES accrued more profit compared to conventional PHES because of its flexibility in the regulation-up capacity and mileage provisions.

- Considering the stochastic scenarios of demand, RES generation, and rivals' offers, the offer/bid strategies of the PHES were more conservative in the energy market than that in the regulation markets, to ensure the selection of PHES offers and hence maintain its reservoir water volume, in all the considered stochastic scenarios.

## 6.2 Contributions

The main contributions of the research presented in this thesis can be summarized as follows:

- Using a new representation of the energy diagram of the BESS, a novel investment planning framework from the system operator's perspective is developed to determine the optimal power and energy size of BESS and its optimal year of installation considering the long-term demand profile of an isolated microgrid, in the presence of other energy resources. Different BESS technologies and their inherent characteristics including energy capacity degradation, and cost parameters, are considered to arrive at the optimal selection of BESS technology.

- A stochastic optimization model for BESS planning is developed for isolated microgrids to capture the uncertainty of solar radiation, wind speed, and power demand, using different probabilistic scenarios. A two-stage decomposition-based approach is developed to solve the stochastic optimization model: in the first stage, the optimal power and final degraded energy size of BESS is determined; in the second stage, the optimal year of installation is obtained considering a novel matrix representing BESS energy capacity degradation.

- An investment planning framework is developed to determine the optimal BESS power rating and energy capacity in microgrids wherein the BESS is installed by a third-party investor to maximize its profits, while the MGO minimizes its operational costs. The BESS participates in energy arbitrage and provision of operating reserves in the microgrid. The BESS performance parameters are considered, and its capacity degradation over the planning horizon is modeled.

- The investment planning problem is solved using a goal programming approach to consider the objectives of the investor and MGO simultaneously. The aspiration level for the MGO is set to achieve a reduction in the operational costs as compared to the costs without BESS, while the aspiration level for the investor is to achieve the MARR. These are also considered as boundary constraints in the optimization

model to ensure that both targets are achieved when determining the optimal BESS investment plan.

- A new market participation model for PHES technologies is developed to determine their bidding strategies in joint energy and PBR markets, considering both the regulation capacity and mileage. The PBR market formulation developed in this work is in line with FERC Order 755 to facilitate PHES participation in regulation markets.

- The PHES flexibility aspects in regulation provisions during pumping operation while behaving as a strategic participant are considered for the first time. The thesis models and analyzes such operation features of a price-maker HSC PHES participating in the joint energy-PBR markets.

- A novel bi-level MPEC framework is developed to solve the problem of strategic participation of PHES in the joint energy-PBR markets. In the upper level, the optimal PHES offers and bids are determined to maximize its profit considering the technical constraints of conventional and HSC PHES facilities. The bidding strategy determined at the upper level is constrained by the lower level problem, which models the joint energy-PBR markets.

- To complete the full picture, non-strategic operation of PHES is also examined and compared with strategic operations for both, conventional and HSC PHES. Also, the impact of uncertainties of net demand and rivals' price and quantity offers on the strategic operation of the HSC PHES are studied in detail using an MCS based approach.

Some parts of Chapter 2 have been published in the Proceedings of 2019 CIGRE Canada Conference [107]. The main contents of Chapter 3 have been published in IEEE Transactions on Sustainable Energy [108]. The main contents of Chapter 4 have been reported in a book chapter published by Springer [109] and in the Proceedings of 2018 IEEE Canada Electrical Power and Energy Conference (EPEC) [110]. The main contents of Chapter 5 have been accepted for publication in IEEE Transactions on Power Systems [111].

## 6.3 Future Work

Based on the work presented in this thesis, the following issues can be examined in further research problems:

- The proposed ESS investment planning frameworks can further examine the impact of ESS on other operational aspects such as improving the reliability of the system and minimizing the costs of load losses.
- The conflicting objectives in the third-party investment planning problem can be solved in a bi-level MPEC framework. However, some essential operational constraints that require considering integer and binary variables, need to be simplified or avoided in order to formulate the lower level problem as a linear programming model. It is noted that the bi-level model solves the optimization problem from the perspective of either the MGO or ESS investor, while the proposed goal programming approach considers a variable weight that can determine the optimal decisions considering the two perspectives simultaneously.
- The proposed investment planning model for third-party investors can be extended to integrate pricing mechanisms for BESS in the operation stage, after its installation, to ensure fair operation of the BESS by MGO considering the impact of degradation on a cycle-by-cycle basis.
- Although the bi-level MPEC problem for PHES market participation was focused on determining its optimal offers and bids, more analysis can be conducted by market operators to examine the potential impact of such ESS on energy and regulation markets.
- The impact of strategic behavior of rival agents on the PHES' strategy and its market power can be examined by extending the framework to an EPEC model.
- The real-time energy-PBR market participation and dispatch models, which require representing the PHES dynamic behavior and inclusion of the AGC signal, can be considered in a future work.

# References


[1] "Ontario's long-term energy plan: Achieving balance," Ministry of Energy, 2013. [Online]. Available: https://www.ontario.ca/document/2013-long-term-energy-plan

[2] "Ontario's energy capacity," Ontario Independent Electricity System Operator (IESO), 2020. [Online]. Available: http://www.ieso.ca/Learn/Ontario-Supply-Mix/Ontario-Energy-Capacity

[3] "IESO report: Energy storage," Ontario Independent Electricity System Operator (IESO), Mar. 2016. [Online]. Available: http://www.ieso.ca/-/media/files/ieso/document-library/energy-storage/ieso-energy-storage-report_march-2016.pdf

[4] "Frequency regulation compensation in the organized wholesale power markets," FERC, Washington, DC, FERC Order No. 755, 2011.

[5] "Electric storage participation in markets operated by regional transmission organizations and independent system operators," FERC, Washington, DC, FERC Order No. 841, 2018.

[6] D. Bhatnagar, A. Currier, J. Hernandez, O. Ma, and B. Kirby, "Market and policy barriers to energy storage deployment," Sandia National Laboratories, Albuquerque, NM, USA, SAND2013-7606, Sep. 2013.

[7] R. D. Masiello, B. Roberts, and T. Sloan, "Business models for deploying and operating energy storage and risk mitigation aspects," *Proc. of the IEEE*, vol. 102, no. 7, pp. 1052–1064, Jul. 2014.

[8] K. Malek and J. Nathwani, "Typology of business models for adopting grid-scale emerging storage technologies," in *Proc. Portland International Conference on Management of Engineering and Technology*, 2017, pp. 1–6.

[9] A. Akhil *et al.*, "DOE/EPRI electricity storage handbook in collaboration with NRECA," Sandia National Laboratories, Albuquerque, NM, USA, SAND2015-1002, 2015.

[10] C. G. Baslis and A. G. Bakirtzis, "Mid-term stochastic scheduling of a price-maker hydro producer with pumped storage," *IEEE Trans. Power Syst.*, vol. 26, no. 4, pp. 1856–1865, Nov. 2011.

[11] M. Chazarra, J. I. Perez-Diaz, and J. Garcia-Gonzalez, "Value of perfect information of spot prices in the joint energy and reserve hourly scheduling of pumped storage plants," *Electric Power Systems Research*, vol. 148, pp. 303–310, 2017.

[12] M. Chazarra, J. I. Perez-Diaz, J. Garcia-Gonzalez, and A. Helseth, "Economic effects of forecasting inaccuracies in the automatic frequency restoration service for the day-ahead energy and reserve scheduling of pumped storage plants," *Electric Power Systems Research*, vol. 174, 2019, Art. no. 105850.

[13] A. Awad, J. Fuller, T. EL-Fouly, and M. Salama, "Impact of energy storage systems on electricity market equilibrium," *IEEE Trans. Sustain. Energy*, vol. 5, no. 3, pp. 875–885, Jul. 2014.

[14] P. Zou, Q. Chen, Q. Xia, G. He, and C. Kang, "Evaluating the contribution of energy storages to support large-scale renewable generation in joint energy and ancillary service markets," *IEEE Trans. Sustain. Energy*, vol. 7, no. 2, pp. 808–818, Apr. 2016.

[15] Y. Wang, Y. Dvorkin, R. Fernndez-Blanco, B. Xu, T. Qiu, and D. S. Kirschen, "Look-ahead bidding strategy for energy storage," *IEEE Trans. Sustain. Energy*, vol. 8, no. 3, pp. 1106–1117, Jul. 2017.

[16] E. Nasrolahpour, J. Kazempour, H. Zareipour, and W. Rosehart, "A bilevel model for participation of a storage system in energy and reserve markets," *IEEE Trans. Sustain. Energy*, vol. 9, no. 2, pp. 582–598, Apr. 2018.

[17] E. Nasrolahpour, J. Kazempour, H. Zareipour, and W. D. Rosehart, "Impacts of ramping inflexibility of conventional generators on strategic operation of energy storage facilities," *IEEE Trans. Smart Grid*, vol. 9, no. 2, pp. 1334–1344, Mar. 2018.

[18] K. Hartwig and I. Kockar, "Impact of strategic behavior and ownership of energy storage on provision of flexibility," *IEEE Trans. Sustain. Energy*, vol. 7, no. 2, pp. 744–754, Apr. 2016.

[19] "ISO and RTO energy storage market modeling working group white paper: Current state of the art in modeling energy storage in electricity markets and alternative designs for improved economic efficiency and reliability," Electric Power Research Institute (EPRI), Palo Alto, CA, USA, 3002012327, Mar. 2018.

[20] J. I. Perez-Diaz, M. Chazarra, J. Garcia-Gonzalez, G. Cavazzini, and A. Stoppato, "Trends and challenges in the operation of pumped-storage hydropower plants," *Renewable and Sustain. Energy Reviews*, vol. 44, pp. 767–784, 2015.

[21] M. Chazarra, J. I. Perez-Diaz, and J. Garcia-Gonzalez, "Optimal energy and reserve scheduling of pumped-storage power plants considering hydraulic short-circuit operation," *IEEE Trans. Power Syst.*, vol. 32, no. 1, pp. 344–353, Jan. 2017.

[22] T. K. A. Brekken, A. Yokochi, A. von Jouanne, Z. Z. Yen, H. M. Hapke, and D. A. Halamay, "Optimal energy storage sizing and control for wind power applications," *IEEE Trans. Sustain. Energy*, vol. 2, no. 1, pp. 69–77, Jan. 2011.

[23] H. Bludszuweit and J. A. Dominguez-Navarro, "A probabilistic method for energy storage sizing based on wind power forecast uncertainty," *IEEE Trans. Power Syst.*, vol. 26, no. 3, pp. 1651–1658, Aug. 2011.

[24] Q. Li, S. S. Choi, Y. Yuan, and D. L. Yao, "On the determination of battery energy storage capacity and short-term power dispatch of a wind farm," *IEEE Trans. Sustain. Energy*, vol. 2, no. 2, pp. 148–158, Apr. 2011.

[25] Y. Ru, J. Kleissl, and S. Martinez, "Storage size determination for grid-connected photovoltaic systems," *IEEE Trans. Sustain. Energy*, vol. 4, no. 1, pp. 68–81, Jan. 2013.

[26] B. Hartmann and A. Dan, "Methodologies for storage size determination for the integration of wind power," *IEEE Trans. Sustain. Energy*, vol. 5, no. 1, pp. 182–189, Jan. 2014.

[27] P. Xiong and C. Singh, "Optimal planning of storage in power systems integrated with wind power generation," *IEEE Trans. Sustain. Energy*, vol. 7, no. 1, pp. 232–240, Jan. 2016.

[28] E. Nasrolahpour, S. J. Kazempour, H. Zareipour, and W. D. Rosehart, "Strategic sizing of energy storage facilities in electricity markets," *IEEE Trans. Sustain. Energy*, vol. 7, no. 4, pp. 1462–1472, Oct. 2016.

[29] Y. Dvorkin *et al.*, "Co-planning of investments in transmission and merchant energy storage," *IEEE Trans. Power Syst.*, vol. 33, no. 1, pp. 245–256, Jan. 2018.

[30] T. Qiu, B. Xu, Y. Wang, Y. Dvorkin, and D. S. Kirschen, "Stochastic multistage coplanning of transmission expansion and energy storage," *IEEE Trans. Power Syst.*, vol. 32, no. 1, pp. 643–651, Jan. 2017.

[31] Y. Dvorkin, R. Fernandez-Blanco, D. S. Kirschen, H. Pandzic, J. Watson, and C. A. Silva-Monroy, "Ensuring profitability of energy storage," *IEEE Trans. Power Syst.*, vol. 32, no. 1, pp. 611–623, Jan. 2017.

[32] F. A. Chacra, P. Bastard, G. Fleury, and R. Clavreul, "Impact of energy storage costs on economical performance in a distribution substation," *IEEE Trans. Power Syst.*, vol. 20, no. 2, pp. 684–691, May 2005.

[33] Y. Yang, H. Li, A. Aichhorn, J. Zheng, and M. Greenleaf, "Sizing strategy of distributed battery storage system with high penetration of photovoltaic for voltage regulation and peak load shaving," *IEEE Trans. Smart Grid*, vol. 5, no. 2, pp. 982–991, Mar. 2014.

[34] X. Shen, M. Shahidehpour, Y. Han, S. Zhu, and J. Zheng, "Expansion planning of active distribution networks with centralized and distributed energy storage systems," *IEEE Trans. Sustain. Energy*, vol. 8, no. 1, pp. 126–134, Jan. 2017.

[35] S. W. Alnaser and L. F. Ochoa, "Optimal sizing and control of energy storage in wind power-rich distribution networks," *IEEE Trans. Power Syst.*, vol. 31, no. 3, pp. 2004–2013, May 2016.

[36] X. Zhu, J. Yan, and N. Lu, "A graphical performance-based energy storage capacity sizing method for high solar penetration residential feeders," *IEEE Trans. Smart Grid*, vol. 8, no. 1, pp. 3–12, Jan. 2017.

[37] H. Akhavan-Hejazi and H. Mohsenian-Rad, "Energy storage planning in active distribution grids: A chance-constrained optimization with non-parametric probability functions," *IEEE Trans. Smart Grid*, vol. 9, no. 3, pp. 1972–1985, May 2018.

[38] A. S. A. Awad, T. H. M. EL-Fouly, and M. M. A. Salama, "Optimal ESS allocation and load shedding for improving distribution system reliability," *IEEE Trans. Smart Grid*, vol. 5, no. 5, pp. 2339–2349, Sep. 2014.

[39] M. Sedghi, A. Ahmadian, and M. Aliakbar-Golkar, "Optimal storage planning in active distribution network considering uncertainty of wind power distributed generation," *IEEE Trans. Power Syst.*, vol. 31, no. 1, pp. 304–316, Jan. 2016.

[40] S. X. Chen, H. B. Gooi, and M. Q. Wang, "Sizing of energy storage for microgrids," *IEEE Trans. Smart Grid*, vol. 3, no. 1, pp. 142–151, Mar. 2012.

[41] T. A. Nguyen, M. L. Crow, and A. C. Elmore, "Optimal sizing of a vanadium redox battery system for microgrid systems," *IEEE Trans. Sustain. Energy*, vol. 6, no. 3, pp. 729–737, Jul. 2015.

[42] R. Rigo-Mariani, B. Sareni, and X. Roboam, "Integrated optimal design of a smart microgrid with storage," *IEEE Trans. Smart Grid*, vol. 8, no. 4, pp. 1762–1770, Jul. 2017.

[43] J. Xiao, L. Bai, F. Li, H. Liang, and C. Wang, "Sizing of energy storage and diesel generators in an isolated microgrid using Discrete Fourier Transform (DFT)," *IEEE Trans. Sustain. Energy*, vol. 5, no. 3, pp. 907–916, Jul. 2014.

[44] I. Miranda, N. Silva, and H. Leite, "A holistic approach to the integration of battery energy storage systems in island electric grids with high wind penetration," *IEEE Trans. Sustain. Energy*, vol. 7, no. 2, pp. 775–785, Apr. 2016.

[45] C. Yuan, M. S. Illindala, and A. S. Khalsa, "Co-optimization scheme for distributed energy resource planning in community microgrids," *IEEE Trans. Sustain. Energy*, vol. 8, no. 4, pp. 1351–1360, Oct. 2017.

[46] J. Dong, F. Gao, X. Guan, Q. Zhai, and J. Wu, "Storage-reserve sizing with qualified reliability for connected high renewable penetration micro-grid," *IEEE Trans. Sustain. Energy*, vol. 7, no. 2, pp. 732–743, Apr. 2016.

[47] R. Atia and N. Yamada, "Sizing and analysis of renewable energy and battery systems in residential microgrids," *IEEE Trans. Smart Grid*, vol. 7, no. 3, pp. 1204–1213, Mar. 2016.

[48] P. Yang and A. Nehorai, "Joint optimization of hybrid energy storage and generation capacity with renewable energy," *IEEE Trans. Smart Grid*, vol. 5, no. 4, pp. 1566–1574, Jul. 2014.

[49] S. Bahramirad, W. Reder, and A. Khodaei, "Reliability-constrained optimal sizing of energy storage system in a microgrid," *IEEE Trans. Smart Grid*, vol. 3, no. 4, pp. 2056–2062, Dec. 2012.

[50] H. Khorramdel, J. Aghaei, B. Khorramdel, and P. Siano, "Optimal battery sizing in microgrids using probabilistic unit commitment," *IEEE Trans. Industrial Informatics*, vol. 12, no. 2, pp. 834–843, Apr. 2016.

[51] C. Abbey and G. Joos, "A stochastic optimization approach to rating of energy storage systems in wind-diesel isolated grids," *IEEE Trans. Power Syst.*, vol. 24, no. 1, pp. 418–426, Feb. 2009.

[52] E. Hajipour, M. Bozorg, and M. Fotuhi-Firuzabad, "Stochastic capacity expansion planning of remote microgrids with wind farms and energy storage," *IEEE Trans. Sustain. Energy*, vol. 6, no. 2, pp. 491–498, Apr. 2015.

[53] H. Wang and J. Huang, "Joint investment and operation of microgrid," *IEEE Trans. Smart Grid*, vol. 8, no. 2, pp. 833–845, Mar. 2017.

[54] J. Garcia-Gonzalez, R. M. R. de la Muela, L. M. Santos, and A. M. Gonzalez, "Stochastic joint optimization of wind generation and pumped-storage units in an electricity market," *IEEE Trans. Power Syst.*, vol. 23, no. 2, pp. 460–468, May 2008.

[55] M. Chazarra, J. I. Perez-Diaz, and J. Garcia-Gonzalez, "Optimal joint energy and secondary regulation reserve hourly scheduling of variable speed pumped storage hydropower plants," *IEEE Trans. Power Syst.*, vol. 33, no. 1, pp. 103–115, Jan. 2018.

[56] A. Vargas-Serrano, A. Hamann, S. Hedtke, C. M. Franck, and G. Hug, "Economic benefit analysis of retrofitting a fixed-speed pumped storage hydropower plant with an adjustable-speed machine," in *Proc. IEEE Manchester PowerTech*, Jun. 2017, pp. 1–6.

[57] S. A. Gabriel, A. J. Conejo, B. F. Hobbs, D. Fuller, and C. Ruiz, *Complementarity Modeling in Energy Markets*. New York, NY, USA: Springer, 2013.

[58] B. F. Hobbs, C. B. Metzler, and J. Pang, "Strategic gaming analysis for electric power systems: An MPEC approach," *IEEE Trans. Power Syst.*, vol. 15, no. 2, pp. 638–645, May 2000.

[59] N. Padmanabhan, M. Ahmed, and K. Bhattacharya, "Battery energy storage systems in energy and reserve markets," *IEEE Trans. Power Syst.*, vol. 35, no. 1, pp. 215–226, Jan. 2020.

[60] B. Xu, Y. Shi, D. S. Kirschen, and B. Zhang, "Optimal battery participation in frequency regulation markets," *IEEE Trans. Power Syst.*, vol. 33, no. 6, pp. 6715–6725, Nov. 2018.

[61] T. A. Nguyen, D. A. Copp, R. H. Byrne, and B. R. Chalamala, "Market evaluation of energy storage systems incorporating technology-specific nonlinear models," *IEEE Trans. Power Syst.*, vol. 34, no. 5, pp. 3706–3715, Sep. 2019.

[62] A. Sadeghi-Mobarakeh and H. Mohsenian-Rad, "Optimal bidding in performance-based regulation markets: An MPEC analysis with system dynamics," *IEEE Trans. Power Syst.*, vol. 32, no. 2, pp. 1282–1292, Mar. 2017.

[63] L. Liang, Y. Hou, and D. J. Hill, "GPU-based enumeration model predictive control of pumped storage to enhance operational flexibility," *IEEE Trans. Smart Grid*, vol. 10, no. 5, pp. 5223–5233, Sep. 2019.

[64] M. V. Pereira, S. Granville, M. H. C. Fampa, R. Dix, and L. A. Barroso, "Strategic bidding under uncertainty: A binary expansion approach," *IEEE Trans. Power Systs.*, vol. 20, no. 1, pp. 180–188, Feb. 2005.

[65] B. Fanzeres, S. Ahmed, and A. Street, "Robust strategic bidding in auction-based markets," *European Journal of Operational Research*, vol. 272, no. 3, pp. 1158–1172, 2019.

[66] P. B. V. Viswanathan, M. Kintner-Meyer and C. Jin, "National assessment of energy storage for grid balancing and arbitrage: Phase 2, Volume 2: Cost and performance characterization," Pacific Northwest National Laboratory, Richland, WA, USA, PNNL-21388, Sep. 2013.

[67] J. Eyer and G. Corey, "Energy storage for the electricity grid: Benefits and market potential assessment guide," Sandia National Laboratories, Albuquerque, NM, USA, SAND2010-0815, Feb. 2010.

[68] A. F. Zobaa, *Energy Storage - Technologies and Applications*. IntechOpen, 2013.

[69] T. Kousksou, P. Bruel, A. Jamil, T. El Rhafiki, and Y. Zeraouli, "Energy storage: Applications and challenges," *Solar Energy Materials and Solar Cells*, vol. 120, pp. 59–80, Jan. 2014.

[70] J. Leadbetter and L. G. Swan, "Selection of battery technology to support grid-integrated renewable electricity," *Journal of Power Sources*, vol. 216, pp. 376–386, Oct. 2012.

[71] M. Beaudin, H. Zareipour, A. Schellenberglabe, and W. Rosehart, "Energy storage for mitigating the variability of renewable electricity sources: An updated review," *Energy for Sustainable Development*, vol. 14, no. 4, pp. 302–314, Dec. 2010.

[72] S. Rehman, L. M. Al-Hadhrami, and M. Alam, "Pumped hydro energy storage system: A technological review," *Renewable and Sustainable Energy Reviews*, vol. 44, pp. 586–598, 2015.

[73] "Pumped hydroelectric storage," Energy Storage Association, 2016. [Online]. Available: http://energystorage.org/energy-storage/technologies/pumped-hydroelectric-storage

[74] "NERC operating manual," North American Electric Reliability Corporation (NERC), Aug. 2016. [Online]. Available: https://www.nerc.com/comm/OC/Pages/Operating-Manual.aspx

[75] J. Ellison, L. Tesfatsion, V. Loose, and R. Byrne, "Project report: A survey of operating reserve markets in U.S. ISO/RTO-managed electric energy regions," Sandia National Laboratories, Albuquerque, NM, USA, SAND2012-1000, Sep. 2012.

[76] B. Xu, Y. Dvorkin, D. S. Kirschen, C. A. Silva-Monroy, and J. Watson, "A comparison of policies on the participation of storage in U.S. frequency regulation markets," in *Proc. IEEE Power and Energy Society General Meeting*, Jul. 2016, pp. 1–5.

[77] "U.S. battery storage market trends," The Energy Information Administration, 2018. [Online]. Available: https://www.eia.gov/analysis/studies/electricity/batterystorage/pdf/battery_storage.pdf

[78] "PJM manual 11: Energy and ancillary services market operations," PJM, 2019. [Online]. Available: https://www.pjm.com/~/media/documents/manuals/m11.ashx

[79] "Section 8: Ancillary services," California Independent System Operator (CAISO), 2018. [Online]. Available: http://www.caiso.com/Documents/Section8-AncillaryServices-asof-Nov6-2018.pdf

[80] "Manual 2: Ancillary services manual," New York Independent System Operator (NYISO), 2018. [Online]. Available: https://www.nyiso.com/documents/20142/2923301/ancserv.pdf

[81] "Ancillary services market," Ontario Independent Electricity System Operator (IESO), 2020. [Online]. Available: http://www.ieso.ca/en/Sector-Participants/Market-Operations/Markets-and-Related-Programs/Ancillary-Services-Market

[82] "Dispatchable renewables and energy storage," The Alberta Electric System Operator (AESO), May 2018. [Online]. Available: https://www.aeso.ca/assets/Uploads/AESO-Dispatchable-Renewables-Storage-Report-May2018.pdf

[83] B. Baker, I. Sklokin, L. Coad, and T. Crawford, "Canada's electricity infrastructure: Building a case for investment," The Conference Board of Canada, Ottawa, ON, Canada, 11-257, Apr. 2011.

[84] T. Gonen, *Electric Power Distribution System Engineering*. New York, NY, USA: McGraw-Hill, 1986.

[85] D. L. Whitman and R. E. Terry, *Fundamentals of Engineering Economics and Decision Analysis*. San Rafael, CA, USA: Morgan & Claypool Publishers, 2012.

[86] D. E. Olivares *et al.*, "Trends in microgrid control," *IEEE Trans. Smart Grid*, vol. 5, no. 4, pp. 1905–1919, Jul. 2014.

[87] M. Farrokhabadi *et al.*, "Microgrid stability definitions, analysis, and examples," *IEEE Trans. Power Syst.*, vol. 35, no. 1, pp. 13–29, Jan. 2020.

[88] D. E. Olivares, C. A. Canizares, and M. Kazerani, "A centralized energy management system for isolated microgrids," *IEEE Trans. Smart Grid*, vol. 5, no. 4, pp. 1864–1875, Jul. 2014.

[89] A. L. Dimeas and N. D. Hatziargyriou, "Operation of a multiagent system for microgrid control," *IEEE Trans. Power Syst.*, vol. 20, no. 3, pp. 1447–1455, Aug. 2005.

[90] G. B. Sheble and G. N. Fahd, "Unit commitment literature synopsis," *IEEE Trans. Power Syst.*, vol. 9, no. 1, pp. 128–135, Feb. 1994.

[91] M. Carrion and J. M. Arroyo, "A computationally efficient mixed-integer linear formulation for the thermal unit commitment problem," *IEEE Trans. Power Syst.*, vol. 21, no. 3, pp. 1371–1378, Aug. 2006.

[92] Z. Shu and P. Jirutitijaroen, "Latin hypercube sampling techniques for power systems reliability analysis with renewable energy sources," *IEEE Trans. Power Syst.*, vol. 26, no. 4, pp. 2066–2073, Nov. 2011.

[93] S. Zhang, H. Cheng, L. Zhang, M. Bazargan, and L. Yao, "Probabilistic evaluation of available load supply capability for distribution system," *IEEE Trans. Power Syst.*, vol. 28, no. 3, pp. 3215–3225, Aug. 2013.

[94] J. Dupačová, N. Gröwe-Kuska, and W. Römisch, "Scenario reduction in stochastic programming: An approach using probability metrics," *Mathematical Programming*, vol. 95, no. 3, pp. 493–511, Mar. 2003.

[95] P. A. Ruiz, C. R. Philbrick, E. Zak, K. W. Cheung, and P. W. Sauer, "Uncertainty management in the unit commitment problem," *IEEE Trans. Power Syst.*, vol. 24, no. 2, pp. 642–651, May 2009.

[96] B. V. Solanki, C. A. Canizares, and K. Bhattacharya, "Practical energy management systems for isolated microgrids," *IEEE Trans. Smart Grid*, vol. 10, no. 5, pp. 4762–4775, Sep. 2019.

[97] F. Ramos-gaete, C. Canizares, and K. Bhattacharya, "Effect of price responsive demand on the operation of microgrids," in *Proc. Power Syst. Comput. Conf.*, 2014, pp. 1–7.

[98] S. A. Arefifar, M. Ordonez, and Y. A. I. Mohamed, "Energy management in multi-microgrid systems–Development and assessment," *IEEE Trans. Power Syst.*, vol. 32, no. 2, pp. 910–922, Mar. 2017.

[99] GAMS Documentation Center. [Online]. Available: https://www.gams.com/

[100] J. Nathwani *et al.*, "Equinox blueprint: Energy 2030 - A technological roadmap for a low-carbon, electrified future," Waterloo Global Science Initiative, Waterloo, ON, Canada, Feb. 2012.

[101] A. J. Wood, B. F. Wollenberg, and G. B. Sheble, *Power Generation, Operation, and Control*. Hoboken, NJ, USA: Wiley, 2013.

[102] C. Bustos, E. Sauma, S. de la Torre, J. A. Aguado, J. Contreras, and D. Pozo, "Energy storage and transmission expansion planning: substitutes or complements?" *IET Gener., Transmiss. Distribution*, vol. 12, no. 8, pp. 1738–1746, 2018.

[103] E. Castillo, A. J. Conejo, P. Pedregal, R. Garcia, and N. Alguacil, *Building and Solving Mathematical Programming Models in Engineering and Science*. New York, NY, USA: Wiley, 2001.

[104] C. Grigg *et al.*, "The IEEE Reliability Test System-1996. A report prepared by the reliability test system task force of the application of probability methods subcommittee," *IEEE Trans. Power Syst.*, vol. 14, no. 3, pp. 1010–1020, Aug. 1999.

[105] D. Pozo, J. Contreras, and E. E. Sauma, "Unit commitment with ideal and generic energy storage units," *IEEE Trans. Power Syst.*, vol. 29, no. 6, pp. 2974–2984, Nov. 2014.

[106] S. Pineda and J. M. Morales, "Solving linear bilevel problems using big-Ms: Not all that glitters is gold," *IEEE Trans. Power Syst.*, vol. 34, no. 3, pp. 2469–2471, May 2019.

[107] H. Alharbi and K. Bhattacharya, "Energy storage and ancillary services markets in North America," in *Proc. CIGRE Canada Conference*, Montreal, QC, 2019, pp. 1–5.

[108] ——, "Stochastic optimal planning of battery energy storage systems for isolated microgrids," *IEEE Trans. Sustain. Energy*, vol. 9, no. 1, pp. 211–227, 2018.

[109] ——, "An optimal investment model for battery energy storage systems in isolated microgrids," in *Advances in Energy System Optimization*. Springer Publishing, 2017, pp. 105–121.

[110] ——, "A goal programming approach to sizing and timing of third party investments in storage system for microgrids," in *Proc. IEEE Electrical Power and Energy Conference*, Toronto, ON, 2018, pp. 1–6.

[111] ——, "Participation of pumped hydro storage in energy and performance-based regulation markets," *IEEE Trans. Power Syst.*, pp. 1–1, 2020.